A MATRIX ISOLATION STUDY OF THE SOLVATION OF LITHIUM NITRATE ION PAIRS WITH BENZENE, PYRIDINE, BIPYRIDINE, AND 1,10-PHENANTHROLINE USING INFRARED SPECTROSCOPY

By

KEITH ALAN CONSANI

Bachelor of Science

Kansas State University

Manhattan, Kansas

1977

Submitted to the Faculty of the Graduate College
of Oklahoma State University
in partial fulfillment of the requirements
the Degree of
Doctor of Philosophy
July, 1983

A MATRIX ISOLATION STUDY OF THE SOLVATION OF LITHIUM NITRATE ION PAIRS WITH BENZENE, PYRIDINE, BIPYRIDINE, AND 1,10-PHENANTHROLINE USING INFRARED SPECTROSCOPY

Thesis Approved:

J. Paul Devlin
Thesis Adviser

Larry E. Halliburton

Clarence M. Cunningham

Norman N. Durham
Dean of the Graduate College

ACKNOWLEDGMENTS

I would like to thank J. Paul Devlin for advice and assistance rendered during the course of this work.

The assistance of glass blower Wayne Adkins, Research Associate Gary Ritzhaupt, Mr. Brewer and Ms. Struble of the Physical Sciences Section of the library, and of the machine shop personnel is acknowledged.

The financial support of the National Science Foundation, the Johnston Fund, and the Phillips Petroleum Company is gratefully acknowledged.

Finally, the encouragement and support of my family, especially that of my mother, was essential to my success.

TABLE OF CONTENTS

LIST OF TABLES

LIST OF FIGURES

CHAPTER I

INTRODUCTION

Matrix isolation is a technique used to isolate a molecule (or ion) from the influence of other like molecules (or ions). This is commonly done by co-condensing the species of interest with an inert gas on a cold substrate where it may be inspected at leisure, using any number of spectroscopic tools. Matrix isolation developed in the mid-ninteen fifties, and rapidly became a popular, useful, and unique way to study species which could be difficult to study otherwise. As several good books exist on the topic,[1a,b,c,d,e] a description of the technique will not be given.

Matrix isolation was used, in 1971, to obtain the mid-IR spectra of certain metal nitrates monomers and multimers.[2] That work, and the one that followed it in 1972 on aggregates and glassy thin films,[3] principally sought to firmly establish that such ion pair monomers could easily be obtained from the molten salts, repeatedly, and without significant decomposition products within the sample. The mode of coordination of the metal ion was unclear at the time, but later ab initio work for $LiNO_3$,[4a,b,c] matrix isolation/nitrogen isotope work for KNO_3,[5a,b,c] and electron diffraction studies on $CsNO_3$,[5d] and $RbNO_3$,[5e] strongly support a C_{2v} bidentate structure for the alkali nitrates.

What eventually developed to be of interest were two vibrational

modes, which are best described as the modes resulting from the lifting of the degeneracy of the antisymmetric doubly degenerate stretch ν_3 of the isolated nitrate ion, by coordinating it with M^+. Therefore, when one isolates a lithium nitrate contact ion pair (from the influence of other ion pairs) in an inert gas, the result of this coordination is that the single ν_3 absorption peak becomes two peaks (arbitrarily labeled ν_{3a}, and ν_{3b}), roughly centered near the original absorption. As was shown in the two earlier papers,[2,3] the degree of separation of these peaks is a rough measure of the ability of M^+ to interact with NO_3^-; the stronger the interaction, the greater the separation. Hence, $\Delta\nu_3^{LiNO_3} > \Delta\nu_3^{NaNO_3} > \Delta\nu_3^{KNO_3} > \Delta\nu_3^{CsNO_3}$, where $\Delta\nu_3^{MNO_3} = \nu_4(B_2) - \nu_1(A_1) = \nu_{3b} - \nu_{3a}$.

At this level of understanding (in the matrix isolation of ion pairs) it became possible for one to consider the use of this technique for the benefit of solution physics, for it was then possible to isolate the ion pair, not in an inert gas, but in a solvent. In this way, one alters the interaction of M^+ and NO_3^- in the contact ion pair by feeding electron density into the metal ion part of the ion pair via a base (i.e. electron donor) and, hence, alters the nitrate end's vibrational modes. Therefore by totally replacing the inert gas with water (or, alternatively, ammonia), Smyrl and Devlin were able to obtain the first mid-IR spectra for completely solvated MNO_3 ion pairs.[6a,b]

The importance of this was (and still is) that this technique allows the isolation of solvated and non-solvated ion pairs from the influence of other solvated and non-solvated ion pairs, where dipole coupling effects of the vibrations of the nitrates could otherwise contribute to the spectra. Also, in the case of "ionizing" solvents,

matrix isolation is possibly the only way to obtain the infra-red spectrum for the solvated contact ion pairs separated from the infra-red spectra due to the solvated nitrate ion. Both of these points have ramifications for concentrated solution work and molten salt work, and have been discussed and stressed in the early publications of this technique.[6,7]

After the spectra of the completely solvated ion pairs were obtained, the next (obvious) step was to variably hydrate (or ammoniate) the MNO_3 monomer by contaminating the argon with a known amount of H_2O (or NH_3).[7a,b] Theoretically one could isolate $(H_2O_2)_xMNO_3$ or $(H_3N)_yMNO_3$ where x and y could be experimentally predetermined to be a desired integer (in reality, however, one isolates a mixture of the solvates, say, x, x+1, and x-1, for example).

In general, one expects that since x+1 molecules of solvent will donate more electron density to MNO_3 than x molecules one would observe $\Delta\nu_3^{SMNO_3} > \Delta\nu_3^{S_2MNO_3} > \Delta\nu_3^{S_3MNO_3}$, etc. where S = solvent. Further, for any solvent, S, which is a better electron donor than solvent, T, then $\Delta\nu_3^{S_xMNO_3} < \Delta\nu_3^{T_xMNO_3}$, for any integer x.

These trends were observed using the common solvents water and ammonia,[7a,b] and the results were in general agreement with values calculated using ab initio methods.[4a,b] Although this (and later) work would seem to demonstrate (somewhat conclusively) that one may have to take into account the contribution of differently solvated contact ion pairs to the spectra of $LiNO_3$ dissolved in aprotic and protic solvents, solution chemists continue to insist that only the totally solvated nitrate and totally solvated ion pairs are contribu-

tors of intensity to the ν_3 region, unreasonably clinging to arbitrary curve resolution methods (see, for example, ref. 8, and references therein).

Because of the unwanted hydrogen bonding interactions between the protic solvents and the oxygens of the MNO_3 ion pair which excessively broadened the ν_3 bands, the above "variable solvation" matrix isolation experiments were repeated using $LiNO_3$ and only aprotic solvents.[9a,b] These studies involved the solvents Acetonitrile (ACN), Tetrahydrofuran (THF), Dimethylsulfoxide (DMSO), and Dimethylformamide (DMF). Although the assignment for peak positions of $\nu_{3a}^{n=1,2,3,etc}$, and $\nu_{3b}^{n=1,2,3,etc.}$ for these solvents were made, it seems now that these assignments are not correct.

First of all, even as a small contaminant in the aprotic solvent, water can cause peaks due to $(H_2O)_xLiNO_3$ (which were not correctly assigned in the above work), and peaks due to mixed solvates with both the solvent and water binding to the ion pair $LiNO_3$ are also problems. Further, "hydrogen bonding" of the water to the nitrate ion part of the ion pair MNO_3 can be expected to be quite substantial (ref. 4, for example, calculates $\cong$ 17 kcal/mole). That peak or broadness problems are even apparent at what has to be very low concentrations of water indicates that the combination of flow/condensation/temperature used in the investigations allows substantial wandering of the small water molecule during the initial stages of formation of the rigid lattice of the matrix.

Secondly, as noted before, one isolates not only the n^{th} solvate (e.g. S_nLiNO_3), but also the $(n-1)^{th}$ and $(n+1)^{th}$ solvates, and sometimes the $(n-2)^{th}$ and $(n+2)^{th}$ solvates. This sometimes results in a

great deal of confusing overlap (we further assume, for the sake of simplification, that the absorption coefficients of the solvates are comparable). In regard to this problem it should be noted that (in this particular apparatus) the flowing mixture of $LiNO_3$ and argon/contaminant does not have time to reach equilibrium, and one should not expect the population of solvates condensing on the substrate to be representative of the gas phase statistics.[10] This is seen not only by the fact that "warm-up" experiments make more solvent available to S_xLiNO_3, and by the fact that one might see $(H_2O)_xS_yLiNO_3$ even when S is a stronger base than H_2O, but is also seen in the fact that $LiNO_3$ ion pairs can actually be isolated in solvents in which they would normally (at room temperature) dissociate.

Thirdly, band assignments are difficult because at high solvation numbers steric hindrance could cause formation of an unsymmetrically distorted bidentate nitrate, or the coordination of the nitrate ion to the lithium ion could "go" monodentate. The energy difference between the mono and bidentate forms of $LiNO_3 \cdot 3H_2O$ is calculated to be be only 11.5 kcals/mole,[4] for example, and given this as an order of magnitude value for ligands, concern about possible steric problems for larger ligands is not unreasonable. Under these circumstances the splitting $\Delta\nu_3=\nu_{3a} - \nu_{3b}$ would no longer be the useful probe of the environment it once was.

Finally, it should be remarked that distortion of absorption peaks by matrix effects is possible (apparently, particularly when argon is used), and because of the nature and number of variables, it is not immediately obvious when this problem would be important, nor what it's magnitude would be if it did arise. Matrix effects are a

bothersome possibility, but they are generally small (less than 2 cm^{-1}) and will presumably become of less importance as the number of ligands added to the ion pair increases. Clearly, however, the band analysis is not always straightforward.

Having carefully delineated the pitfalls of matrix isolation for this type of work in the last few paragraphs, it seems only fair to re-emphasize its place in the overall scheme of things. As any observer may note, the solvation of ions and ion pairs in solution has a very rich history.[11] A voluminous amount of literature exists, much more than can adequately be covered here, and many tools have been used in the attempt to understand solution physics. Looking back on this work, one can see that even though they began in a very macroscopic, thermodynamic way, solution chemists have developed (with the advent of advanced theory and modern instrumentation) a distinctly microscopic outlook. However, even with modern tools solution physics can be complicated, as many times there are too many variables at work to be able to unambiguously observe that which is of interest.

Many of these "modern tools" cannot selectively determine the properties of the n^{th} solvate, in a mixture of all the other solvates. Infrared, Raman, X-ray, EXAFS, NMR, and so on, are all techniques which give average information. So, if any of these techniques are to be used unambiguously, a method of producing a sample of known solvate must be used ... the observation of the molecule properties of $S_x \cdot LiNO_3$ in an inert media is a first step to understanding the nature of the bulk solvent via it's individual constituents.

Even where experimental difficulties do not easily permit the 100% production of the n^{th} solvate, free of the $(n-1)^{th}$ and $(n+1)^{th}$

solvate, matrix isolation is sometimes the only practical alternative (gas phase techniques are plagued with similar production problems, too, though additional information is sometimes available in the gas phase). The use of matrix isolation as a necessary tool to study solvation has never been fully appreciated by solution chemists in general, as there are only a handful of papers on this application compared to the thousands of papers on the study of molecules in solutions via solution "group body" properties.

As the above mentioned aprotic matrix isolation work was being finished, a Russian group published the infra-red spectra of $LiNO_3$ (and $Ca(NO_3)_2$) dissolved in pyridine,[12a] which was in a vein of work similar to their previous studies (and which they subsequently extended to other nitrate salts in other solvents[12b,c]). Through concentration and temperature variation studies they came to the conclusion that two species were present in solution. Presuming the coordination number of the lithium ion to be four, they assigned a set of bands at 1330 and 1410 cm^{-1} for ν_{3a} and ν_{3b} of $(pyridine)_3Li\text{-}O\text{-}N\lesssim^{O}_{O}$, and a set of bands at 1354 and 1440 cm^{-1} for the bridging nitrate triplets $((pyridine)_3Li)_2NO_3^+$, and $(pyridine)_2Li(NO_3)_2^-$ - the triplet bands reportedly increase with concentration of $LiNO_3$ and solution temperature.

As no account was taken of the bidentate coordination possibility, or the effect of the varying number of pyridines, it was felt that the complimentary matrix isolation/dilution work for the lithium nitrate/pyridine pair would be appropriate; and, because pyridine has only a partial "window" in the ν_3 region of $LiNO_3$, the work was also extended to include deuterated pyridine. It was further believed that the use of phenanthroline as a solvent would be of particular value. As a

bidentate nitrogen ligand it would have approximately twice the effect of pyridine at the same "molarity", and further help to justify and substantiate the assignments of ν_{3a} and ν_{3b} for the pyridine/$LiNO_3$ case. The bidentate solvent bipyridine was also investigated. Unfortunately bipyridine had a tendency to only "half chelate" under the deposit conditions, chelating fully only when the matrix was warmed, so work on this compound never progressed further than the isolation and solvation of $LiNO_3$ in a glassy deposit of bipyridine. These three amines were also of particular interest in light of scattered evidence in the literature concerning stable compounds between themselves and the alkali metal ions, the lithium ion in particular.[13]

Another solvent of interest was benzene. This compound was quite naturally suggested from work that has investigated the extent and nature of the interactions between alkali ions and alkene or aromatic compounds. For example, simple ab initio calculations on the interaction between a sodium ion and a benzene molecule have yielded $\Delta E = -78$ kJ/mole.[14b] And, in a rather thorough mass spectrometric study, the $(benzene)_n \cdot K^+$ interaction was found to vary between 54 and 80 kJ/mole for n between 1 and about 4.[14b] Such a complete study as the last one does not seem to have been done for a lithium ion/benzene complex, though ICR determinations have given $D(benzene \cdot Li^+) = 155$ kJ/mole (± 8.4 kJ/mole),[14c] and 196 kJ/mole (± 8.4 kJ/mole).[14d]

In light of these facts, and in light of the fact that most workers have considered the interactions between alkali ions and benzene as minor (at best),[15] it seemed of interest to investigate the interaction of benzene and the lithium ion part of the ion pair,

using the $\Delta\nu_3$ as an indicator; as the lithium ion of the ion pair has only 0.34 positive charge[4a] it might be expected to differ from a bare lithium ion in interesting ways. Work on benzene, however, did not progress further than the isolation of the ion pair in the pure solvent (benzene).

Having obtained the $\Delta\nu_3$ values for various solvents, it could prove interesting to compare the $\Delta\nu_3$ of a solvate of $LiNO_3$ with the thermodynamic data (ΔH_{rxn}, ΔS_{rxn}, etc.) for formation of that solvate. Unfortunately, these numbers are not currently available. The best prospect for obtaining them in the future appears to be some type of flowing afterglow mass spectrometric experiment. Until then, however, we must look to other sources for these thermodynamic values.

As noted previously, quantum mechanics has been used to calculate energy values for small molecules (e.g. H_2O and NH_3) attached to $LiNO_3$; however, because of the sizes of our molecules, and because of the time needed to compute and optimize geometries, other methods were sought. In a less rigorous manner, one could search for possible connections between the electron donor/acceptor properties of solvents[16] and the corresponding $\Delta\nu_3$'s they produce. Specifically, the single scale donicity model of Gutman[17] was used to qualitatively propose a connection between the "donor number" of the solvent and the $\Delta\nu_3$ it produces.[9a,b] Upon closer inspection, however, this model has several problems associated with it that make it unsuitable for application in this instance. In particular, it is an LFER single scale model (requiring $\Delta H^{LiNO_3} = a\Delta H^{SbCl_5 \cdot C} + b$),[16,18] it is temperature dependent,[16] and, in addition there are several other minor flaws that have been discussed quite well by Drago[18] and will not be

reviewed here (it should also be noted that the so-called "Gutman pile-up effect" is not observed using the STO-3G calculation mentioned earlier[4,17]).

Drago has proposed an empirical "E and C" model to replace the donor and acceptor numbers of Gutamn.[18] Using empirically determined parameters ("E" and "C") for compounds, he proposes an equation to calculate the ΔH of their reaction (which might usefully be related in some ways to the spectroscopic values of $\Delta\nu_3$ that we observe). Since this model has been thoroughly discussed in the literature, including how to apply it to spectroscopic problems,[18] discussion in this thesis will center around its application to the particular problem of ion pair solvation.

CHAPTER II

EXPERIMENTAL

Equipment and Related Techniques

For the production and observation of samples, two cryogenic vacuum cells were used in this work. For the partial solvation experiments (i.e. those involving argon), a cryostat built around a CS-202 Displex^{TM} closed cycle cooler (Air Products) was used. This cryostat, and it's ancillary equipment, has been described in detail in a previous thesis,[2b,3b,6b] and it's description will therefore be omitted here (these thesis should be consulted for a clearer understanding of this experimental section).

The other cryostat was originally constructed for work unrelated to this thesis, and it has not been described elsewhere. It's design is very typical of cold cells used in this type of work, and it's description will be omitted except to say that it was made of a nickel plated brass rotatable shroud (identical to the one that fits on the CS-202 unit), which fits onto a stainless steel dewar (similar to a model LC-1-110 Air Products liquid nitrogen insert dewar equipped with a cryotip substrate holder). This cell was cooled with liquid nitrogen, and was used for the collection of the solvation/isolation spectra of lithium nitrate in pure pyridine, deuterated pyridine, benzene, and 2,2'-bipyridyl.

The temperature of the copper substrate holder in the CS-202

cryostat cell was measured with an iron-doped gold vs chromel thermocouple, while the temperature of the holder in the stainless steel cell was measured with an iron constantin thermocouple. Neither of these thermocouples was carefully calibrated, particularly the iron-doped gold vs chromel thermocouple, and were only used for rough determinations (to provide for internal consistancy from run to run). Thermal contacts between the substrate holders (which were simple screw clamps), and the substrate, were provided by indium wire gaskets.

Cesium iodide was used as the material for the windows and substrate for both cells. They were freshly polished after each run with ethanol, rouge, and kleenex (chamois and ethanol came to be preferred later).

Near vacuum connections likely to be warm, Apiezon T grease was used, while Apiezon N grease was used for all other connections.

A Hastings vacuum gauge was used to determine approximate pressures in the system connected to the cell. The minimum pressure that could be read on this instrument was 1 micron.

Because of the non-volatile nature of two of the solvents in this study, it was necessary to design and construct two new oven ports especially for their use. The 2,2'-bipyridyl was volatilized at room temperature through a small opening in a modified oven port (Figure 1). When deposition of 2,2'-bipyridyl was desired, the rota-flow valve was opened, and volatilization of the 2,2'-bipyridyl occurred at a convenient rate at room temperature (e.g. a rate which could isolate the lithium nitrate effusing from the knudsen cell when co-depositions were attempted).

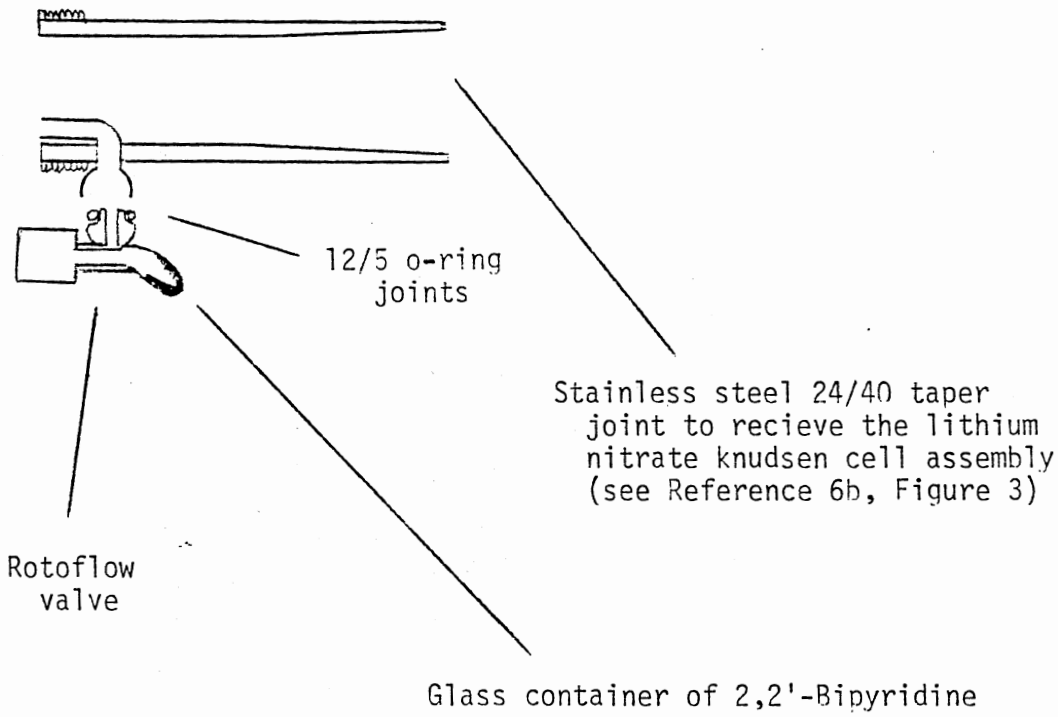

Figure 1. Stainless Steel Oven Port and Sample Vial

Since 1,10-phenathroline was not sufficiently volatile to use the oven port constructed for 2,2'-bipyridyl, an entirely different type of oven port was constructed especially for the 1,10-phenanthroline/lithium nitrate couple. It was fabricated from glass (Figure 2), and utilized a double knudsen cell arrangement; one cell for 1,10-phenanthroline, and one for lithium nitrate. This module was connected to the rotatable shroud using an o-ring clamp arrangement.

A small (#20) o-ring attachment to the vacuum system, which would fit either oven port, was used for keeping the material(s) of the knudsen cell(s) of the oven port dry while the cell was being cleaned between experiments. The material in a knudsen cell might be used three or four times before various circumstances dictated a

new charge of material be placed in the cell; the re-use of material was most convenient.

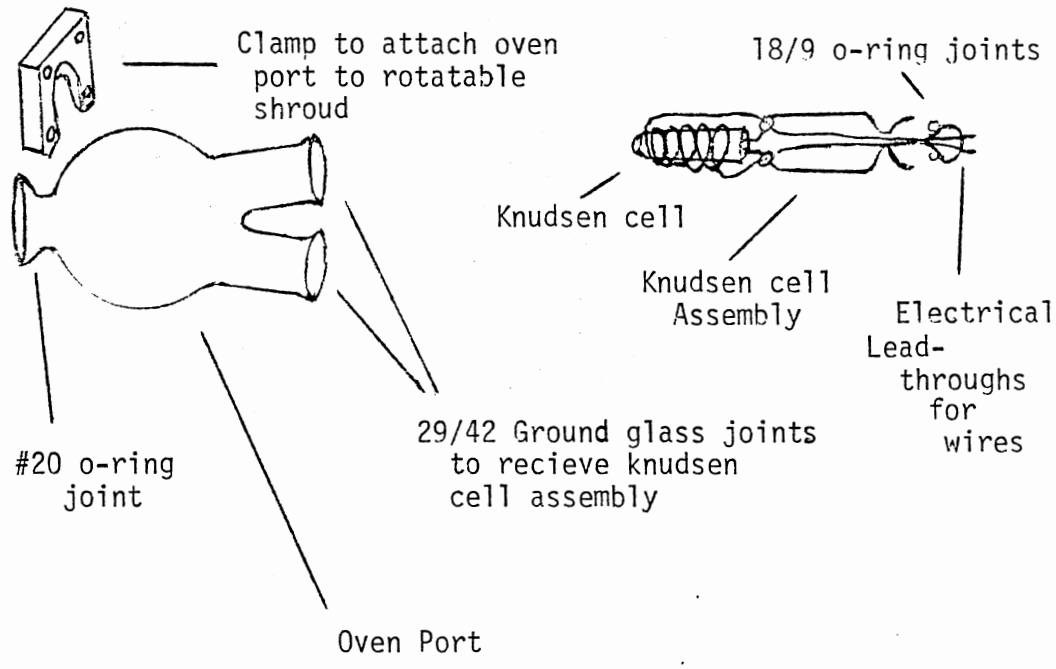

Figure. 2. Glass Oven Port and Accessories

During depositions, the outside of the oven port being used was cooled with a small fan to avoid possible problems arising from volatilization of Apiezon grease or it's possible impurities; grease needed to be especially abundant on the connections of the glass oven port to avoid leakage.

The temperature in the knudsen cells was controlled, as before, by regulating a voltage supplied to a nichrome wire wrapped around the pyrex knudsen cell. Although the correct temperatures needed

to produce a molecular beam useful for this particular cell arrangement were established by trial and error, some thermocouple measurements of the temperatures in the knudsen cells were made. This was not a particularly useful practice. In most cases, the temperature of the knudsen cell varied within the cell itself, due to the inhomogeneous heater windings, or to the particular configuration of various "shields" which were devised to reflect the intense heat from the nichrome wires into the knudsen cells (or, more properly, in the case of the glass oven port, away from the more volatile 1,10-phenanthroline being gently heated in it's own knudson cell close by).

The temperature of the lithium nitrate knudsen cell was believed to have been kept less than $30^{o}C$ above the melting point of lithium nitrate. The temperature of the 1,10-phenanthroline knudsen cell was estimated to be around $70^{o}C$ (the melting point of the anhydrous compound at STP is, for comparison, $117^{o}C$, while the monhydrate melting point range is near $100^{o}C \pm 2^{o}C$).

After molten lithium nitrate has been in contact with a pyrex knudsen cell for a while, small fissures develop in the knudsen cell; this fracturing becomes worse the longer the cell is used, leading to a variety of problems. The phenomena has been attributed to the exchange of the sodium ion (in the glass) for lithium ion.[19] This problem may be alleviated by carefully heating a thoroughly clean "cracked" cell with a hot flame. The fissures can be slowly "annealed" out, giving a knudsen cell with more resistance to molten lithium nitrate and, of coures, more resistance to mechanical shock.

Metering gas flow rates was accomplished using an FP-1/16-08-G-5

glass flow meter (Lab Crest Catalog number 448-001-0116). Both sapphire and glass floats were used. A teflon needle valve (Lab Crest Catalog number 795-500) was used to regulate the gas flow on the CS-202 unit, while a stainless steel valve (Nupro "Fine Metering Valve" catalog number SS-4SG) was used for the stainless steel cell.

To obtain gas mixtures, two glass flow meters were used simultaneously, the volatile solvent being combined with argon after both had been metered, meeting far enough from the cell to be assured that they would be thoroughly mixed before their deposition. Occasionally, mixing the argon with the solvent prior to the experiment provided better accuracy or convenience, and in those cases only one flow meter was required.

The pyrex containers used for solvents (c.a. 5 ml volume), argon (c.a. 1 l volume), and mixture of the two (c.a. 1 to 2 l volume) were equipped with 18/7 joints and rotaflow or o-ring valves. These features allowed procedures which assured dry solvents, or gas mixtures, that could repeatedly be used, once properly prepared. In the first few runs, molecular sieves (which had been thoroughly degassed by heating them in a vacuum) were used as drying agents in the containers holding liquid solvents. Since this practice was found to be unnecessary due to the features described above, it was discontinued.

The infrared spectrometer used was a Digilab FTSIR-20S model. It was found that if the CS202 cryostat was supported by the bench of the FTIR interferometer, the vibrations of the cryostat upset the interferometer, resulting in intolerable signal to noise ratios. The solution was found to be a bracket attached to the wall and ceiling of the laboratory which allowed the cryostat to hang in the optical

path, without any physical contact between the cryostat and interferometer. For convenience, rather than necessity, the stainless steel cell cooled by liquid nitrogen was also hung from the bracket.

The parameter for the resolution of the instrument was set to 2 cm^{-1}. In the data manipulation a triangular apodization option was used (where the apex of the triangle was twice the distance of the interferogram center burst), and this effectively reduced the resolution to 3 cm^{-1}.

Alignment signals for samples were generally 5 to 9, averaging about 7, on a sensitivity magnification factor of 1 (i.e. no magnification). This is to be compared with an alignment signal of 8 to 12 for a cell with no sample, and an alignment signal of about 21 for an unobstructed beam. Occasionally, for thick samples, a magnification factor of 4 was necessary. The co-deposits of lithium nitrate and solvents benzene, pyridine, deuterated pyridine, and 2,2'-bipyridyl were sampled at a gain ranging parameter of 0 (that is, no gain ranging was performed on these spectra, and they were all collected at the sensitivity magnification factor specified). Later, for the argon "isolation" experiments, a gain ranging factor of 40 was used, which is a value promoted by Digilab. Care was always taken to compute the reference (cell with no deposit), and the sample (cell with deposit) using the same gain ranging value.

The initial spectra were composed of 500 interferograms, which were co-added every 10 scans. Other spectra (e.g. the warm-up spectra described later), were composed of 100 interferograms. A fast Fourier transform was used to calculate the "normal" spectrum from the interferogram. All operations in collection and computation were handled

in the "double precision" mode.

Chemicals and Their Purification

All chemicals were purified, to various extents, beyond their "as received" condition.

Argon (Union Carbide 99.98%, or MG Scientific 99.9999%) was bled into a previously evacuated bulb through an acetone slush trap to eliminate possible condensibles. No changes were evident in the infrared spectra of samples when the more pure argon was substituted for the less pure (most of this work was done with the higher purity argon).

The benzenes (d^6 Stohler isotopes 99.5% d; h^6 Sargent-Welch Industrial, distilled twice) were dried with sodium or, in later experiments, with calcium hydride. After several hours of contact with the drying agent, the middle third of the solvent was transferred to a scrupulously dried container via ordinary vacuum rack techniques. When calcium hydride was used as the drying agent, this transfer was made more difficult by hydrogen formation. The benzenes were the further purified by freezing about ninety-five percent of the sample in it's container, and pumping off the remaining liquid; this was generally repeated several times.

Pyridine (Aldrich "Spectrophotometric" grade) was dried[20] and purified by transferring (via vacuum rack techniques) the middle one-third of pyridine which had been standing in contact with calcium hydride for five to eight hours. Due to the high cost of deuterated pyridine (Stohler Isotopes 99.5%, lot 1325), it was transferred wholly by vacuum rack techniques, after drying with calcium hydride for five

to eight hours.

The 2,2'-bipyridyl (99+% Aldrich) and the 1,10-phenanthroline monohydrate (4,5-diazaphenanthrene monohydrate, "Baker Analyzed" Reagent) were purified (and dried in the latter case[21]) by sublimation under an active vacuum at least twice. The sublimate side of the sublimation apparatus was cooled with an acetone slush for 2,2-bipyridyl, and with ice in the case of 1,10-phenanthroline.

Lithium nitrate ("Certified", Fischer Scientific) was recrystallized from hot water at least once, and generally twice. The compound, as it came from the filter frit, was moist, but would dry out after a few hours in a tightly closed bottle. This implies that there is some question which hydrate one gets, depending upon the temperature of the filtrate solution, and this has been noted before.[22] Whichever hydrate it was, it was initially dried in it's knudsen cell, while the oven port was connected to the vacuum rack via an o-ring joint. One could slowly raise the temperature of the knudsen cell to the melting point of lithium nitrate over a period of hours, while monitoring the dehydration (in a crude way) with the pressure gauge.

General Procedure for Depositions

To illustrate the procedures, a typical experiment with the CS-202 unit and a glass oven port will be described. Other experiments were similar, and will not be described in detail.

After the substrate was attached to it's holder, and it's heat shield put in place, the rotatable shroud of the CS-202 unit was slipped over the cooling tip and positioned properly. The glass oven

port was then disconnected from the vacuum line (where the compounds were being dried) and attached to the rotatable shroud with the clamp, as in Figure 2. The CS-202 cryostat cell was then slowly evacuated (to avoid "whirl winds" which would draw materials out of the knudsen cells and into the main body of the cryostat).

The "angle of attack" of the rotatable shroud was set so that molecular beams issuing from the knudsen cells would strike the "heat shield" of the substrate, rather than the substrate itself. In this position the materials of the knudsen cells were further dried. Specifically, the lithium nitrate was melted and cooled once more; as it was previously dried while it was on the vacuum rack, one melting process was generally enough to assure dryness of the salt. The knudsen cell containing the 1,10-phenanthroline was heated to it's deposition temperature for a few minutes, and then cooled.

If a gas inlet connection was desired, the rotatable shroud was turned so that the gas inlet was facing the substrate (which, of course, meant that the knudsen cells were also facing the substrate). In this position, the necessary glass connections, flowmeters, valves, and bulbs, were attached to the cell. The inlet valve was then opened, and the inlet system exposed to the active vacuum of the cell. The entire apparatus, cell and inlet system, was then pumped upon using a 3-stage oil diffusion pump (Dow Corning 702 silicon oil) backed with a model 1402 Welch Scientific forepump for at least five hours.

Approximately an hour before deposition was desired, the Air Products cooler was turned on. During this "cool down" period, the temperatures of the knudsen cells were slowly raised so that they would be at their "working" temperatures at about the same time as

the substrate reached the lowest temperature available from the cooler (c.a. 8 to 12 K). The gas flow was started about this time.

The total time for a deposition was generally around two hours. After a sufficient enough sample was deposited, the main valve to the gas inlet system was closed, and the inlet system disconnected from the cell. The wires connecting the reostat and the knudsen cell feedthroughs were removed, and the rotatable shroud was turned to make further deposition on the substrate impossible. After waiting a few minutes for the lithium nitrate in the knudsen cell to solidify, the cell was disconnected from the vacuum line and transported to the spectrometer.

After taking the initial spectra, it was sometimes illuminating to warm the sample up, to allow diffusion of the molecules in the sample. This was accomplished in the closed cycle cooler with an electrical "heater tape" which was wrapped around the end of the cooling tip (the substrate holder is mounted on the cooling tip). With experience, raising the temperature of the substrate slowly was possible, and steady temperatures between 10 and 30 K were easily achieved (warming the other cell consisted of draining it of coolant, and letting the substrate slowly warm to room temperature; this took about one hour, and spectra were taken "on the fly", a typical spectra consisting of a collection of 100 interferograms at a resolution of 2 cm^{-1} took three to four minutes).

The argon matrices could have been made more stable with an overcoat of xenon, as has been recently demonstrated,[23] but this was not investigated. Upon warm-up of the solvent/lithium nitrate deposits, all solvents, except for 1,10-phenanthroline, quickly

volatilized off the substrate.

After the substrate had warmed to room temperature, the cryostat was dismantled and the cell surfaces cleaned of lithium nitrate and 1,10-phenanthroline. The substrate and the two windows in the optical path were then polished. During this clean-up time, the oven port was attached to the vacuum line to assure that the chemicals in the knudsen cell(s) were kept as dry as possible.

CHAPTER III

EXPERIMENTAL RESULTS AND DISCUSSION

Matrix Isolated Lithium Nitrate

The Data

As a prelude to the work on the solvation of lithium nitrate isolated in argon, the isolation of lithium nitrate in argon was re-investigated. Figure 3 is the full range mid-infrared spectra of a sample of lithium nitrate isolated in argon; Figure 4 is an expanded region of the spectrum for the same sample.

For the determination of site effects, and diffusion effects, the spectra of matrices which have been warmed are convenient. These are shown in Figure 5.

As the ratio of lithium nitrate to argon is raised, one might be able to observe some kind of multimers in the sample. Though the spectra of multimers was not specifically sought after, the pursuit of a satisfactory spectrum of isolated lithium nitrate yielded certain samples which apparently contained multimers. The spectra of three such samples are shown in Figure 6.

The Discussion

While more powerful instrumentation, and better drying techniques, allowed some clarification of the infrared spectrum for lithium nitrate

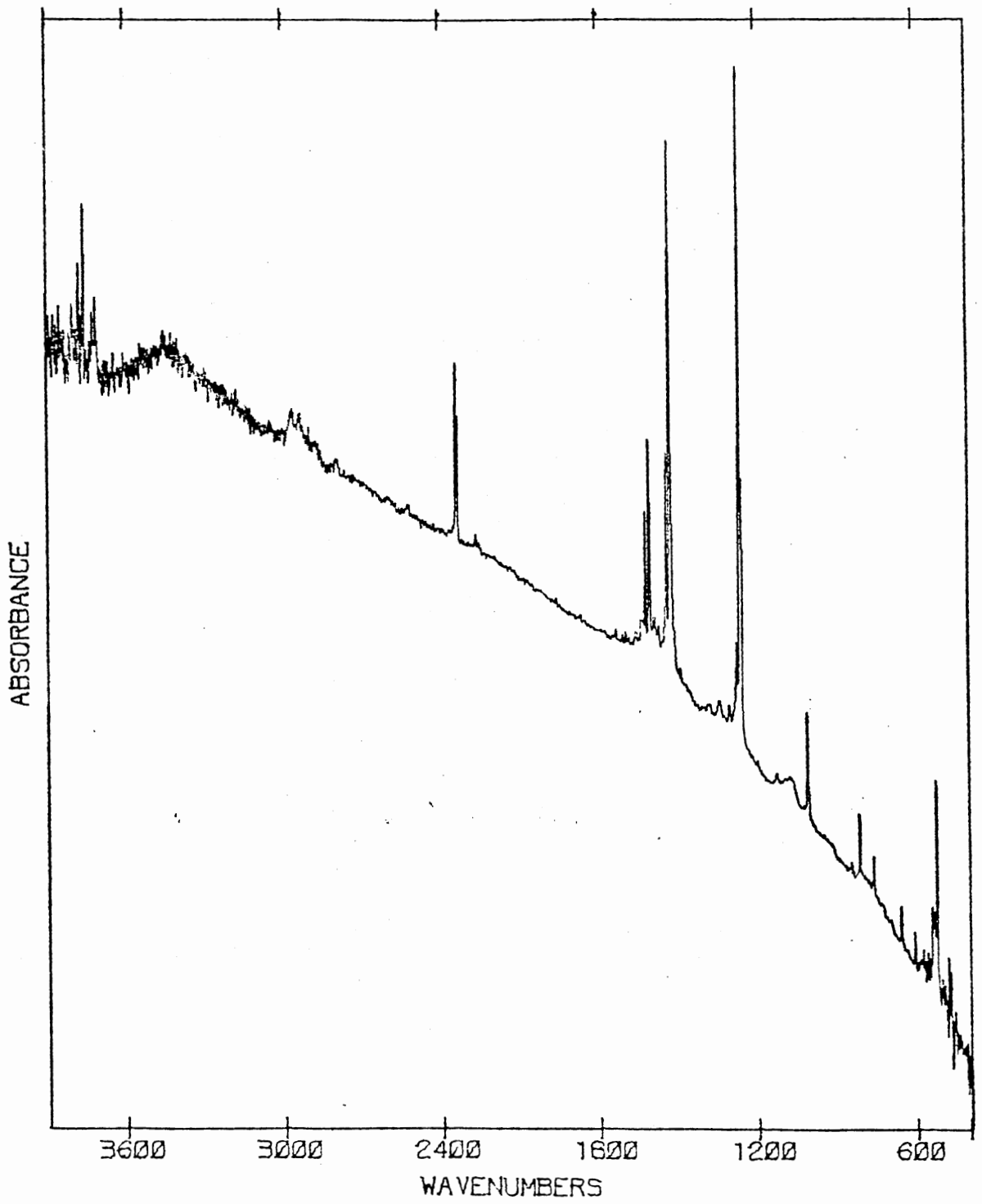

Figure 3. Infrared Spectrum of Lithium Nitrate Isolated in Argon at 10-15 K

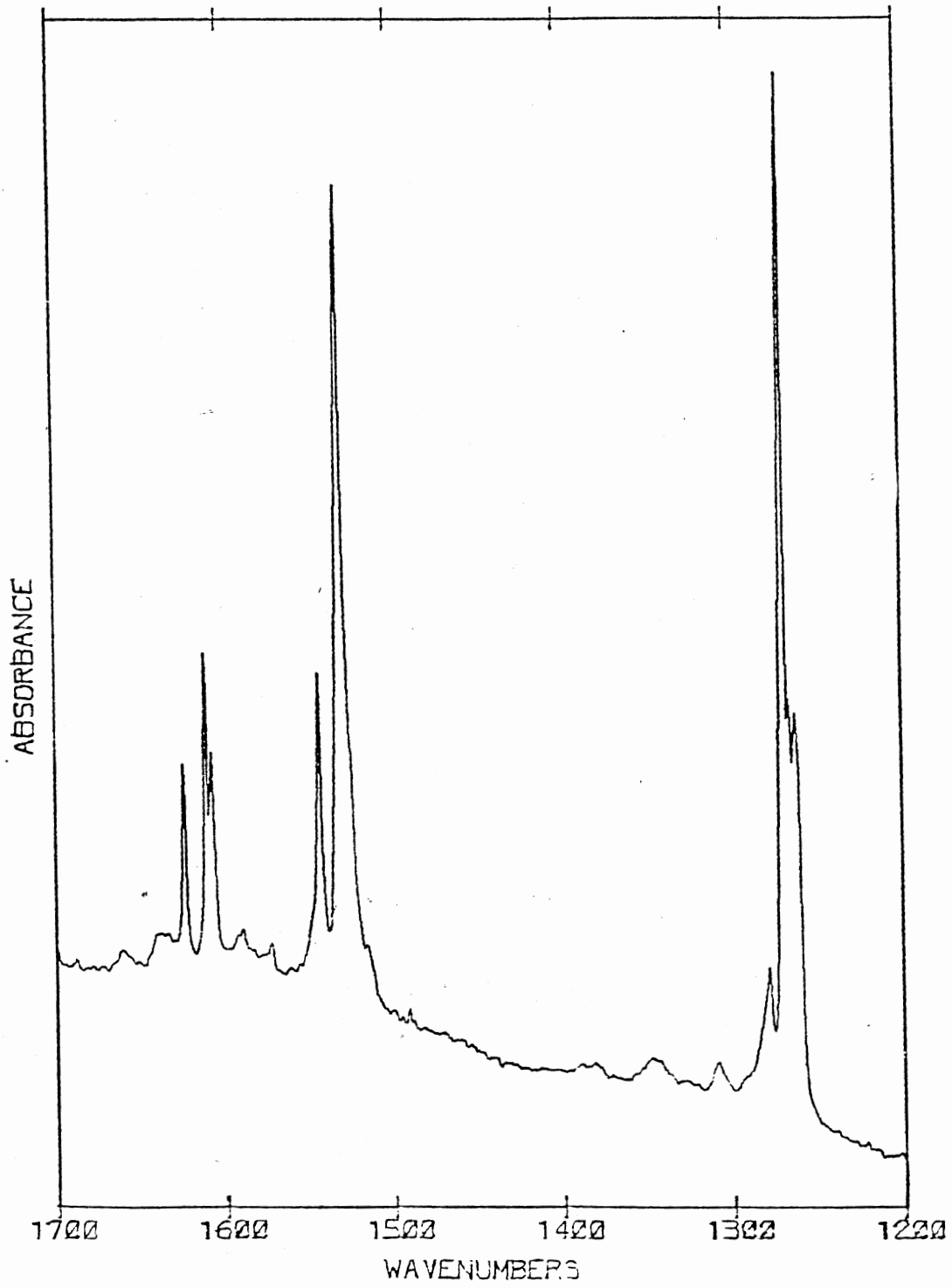

Figure 4. Infrared Spectrum of Lithium Nitrate Isolated in Argon at 10-15 K Showing the $\nu_4(B_2)$ and $\nu_1(A_1)$ Modes

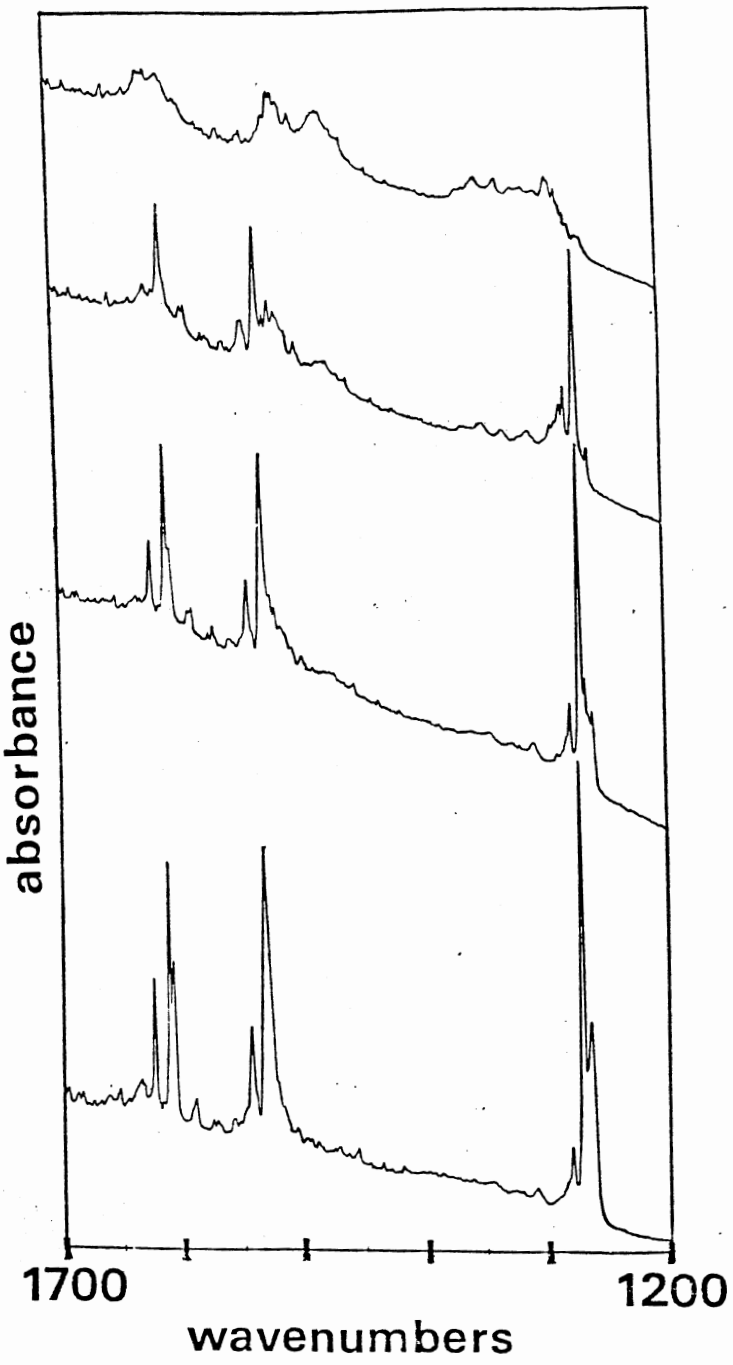

Figure 5. Spectra Showing the Annealing Effect for a Sample of Lithium Nitrate Isolated in Argon: Lower Curve is the Original Sample at 10-15 K, and Each Succeeding Upper Curve is the Sample at a Higher Temperature

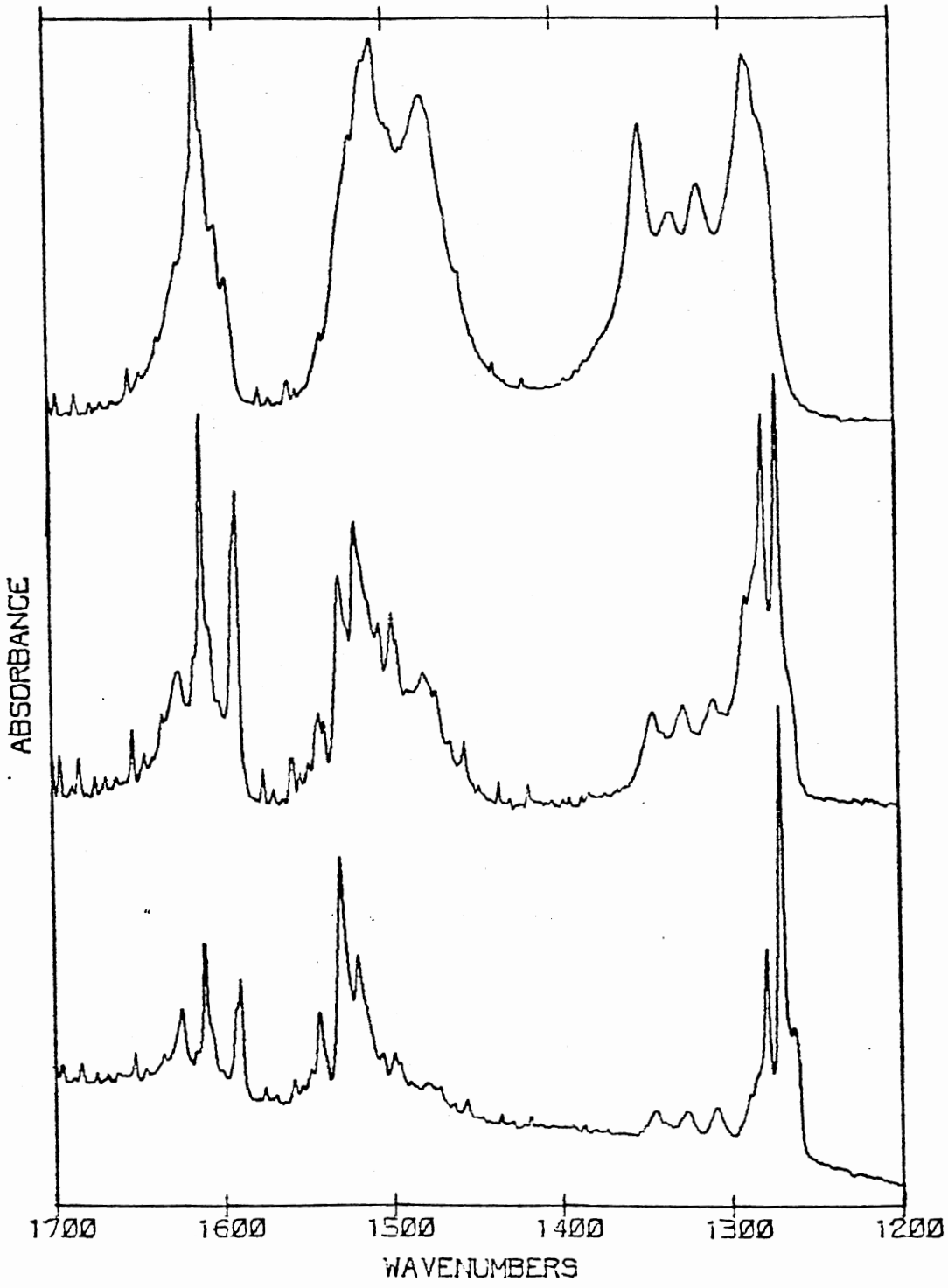

Figure 6. Spectra of Multimers of Lithium Nitrate Isolated in Argon at 10-15 K: Lower Curves are Spectra of Samples More Isolated than Upper Curves

isolated in argon, the results are not basically different from that previously reported.[2,6,9b] Table I summarizes the major results of this study, compared against previous work.

TABLE I

VIBRATIONAL FREQUENCIES FOR MATRIX ISOLATED LITHIUM NITRATE

Mode	$\nu(cm^{-1})$ [6a]	$\nu(cm^{-1})$ [9b]	$\nu(cm^{-1})$ this work
ν_1	1011		1015
ν_2	817		820
ν_{3a}	1264	1268	1269
ν_{3b}	1524	1530	1531
ν_{4a}	736		(not observed)
ν_{4b}	765		768
ν_{M-O}	528		528

Figure 3 is a fairly typical result for a spectrum of lithium nitrate matrix isolated in argon. Small amounts of the impurities water (bands above 3000 cm^{-1}, and near 1600 cm^{-1}), and carbon dioxide (bands near 2300 cm^{-1} and 663 cm^{-1}) are observed. The source of the carbon dioxide is presumably the decomposition of lithium carbonate impurities in the lithium nitrate.[24]

From inspection of the many spectra of samples that were produced

before samples as dry as those used for Figures 3 and 4 were produced, it can be stated with some certainty that the two peaks at 1520 cm^{-1} and 1279 cm^{-1} which are present in previously published spectra[2] are due to the ν_3 splitting of nitrate, for the complex $H_2O \cdot LiNO_3$. The two bands grow and fall in concert, depending upon the amount of water in the sample (as judged by water vibrational mode bands above 3000 cm^{-1}, and near 1600 cm^{-1}).

Because we attempted to obtain the driest samples possible, we have little reliable information to report on what values for ν_{3a} and ν_{3b} of $(H_2O)_n \cdot LiNO_3$, where $n > 1$, though 1289 cm^{-1} and 1506 cm^{-1} are suggested values for $(H_2O)_2 \cdot LiNO_3$. These values of $\Delta\nu_3$ for isolated lithium nitrate (262 cm^{-1}), for $(H_2O)LiNO_3$ (241 cm^{-1}), and $(H_2O)_2LiNO_3$ (217 cm^{-1}), should be compared with Moore's calculated values[4] for these substances, 245 cm^{-1}, 220 cm^{-1}, and 190 cm^{-1}, respectively.

In connection with the perturbation of the bands of lithium nitrate by water, it is natural to inquire if these same samples can provide information on any possible changes of water upon it's interaction with lithium nitrate. It is a long established fact that the dissolution of an alkali salt in water can change the intensities or positions of water mode bands, though the peak frequencies are not generally sensitive.[25] For example, recent ab initio work on the stretching mode intensity increase and frequency change for $LiHOH(OH_2)^+$ vs H_2O,[26] and the stretching and bonding mode intensity increase and frequency shift for $Li(OH_2)^+$ vs H_2O, agrees with this observation.[27]

Unfortunately, a comparison of our sample spectra in the 1600 cm^{-1} region, and the 3000-3700 cm^{-1} region (which did not always have good signal to noise ratios), with the spectrum of isolated water[28]

reveals no unusual occurances. The fact that we can detect no peculiarities in the water vibrations, but can easily detect them in the nitrate vibrations, we feel, testifies only to the largeness of the nitrate absorption coefficient compared to those of the water vibrations, and to the relatively large amounts of water in the matrix which is not associated with the ion pair. Presumably a similar line of reasoning underlies why the four new bands proposed for the intramolecular H-bonded H_2O/alkali halide complex[29] are not also seen here.

The origin of the bands at 1262 cm^{-1} and 1265 cm^{-1} in Figure 4 appears to be a site effect. This can be seen most clearly in Figure 5. The bottom curve of this figure is a spectrum of a sample which, although less dry than the sample of Figure 4, has been prepared at a slower deposition rate. Notably, it has only a single band at 1262 cm^{-1} in place of the two bands in Figure 4. However, upon annealing the sample (upper curves of Figure 5), the band at 1262 cm^{-1} splits into the two bands mentioned above.

The source of the band at 1543 cm^{-1} in Figure 4 is unknown. It does not disappear upon annealing the samples; that is, it does not disappear any faster than the primary lithium nitrate monomer bands do. It has appeared in all spectra to date.

The multimer spectra of Figure 6 qualitatively corroborates data obtained earlier on aggregates.[3] The previous samples contained at least as much water as the present samples, and perhaps more (the water regions of those spectra were omitted for clarity). In any event, the results of Figure 5 indicate that the bands at 1308, 1326, 1345, 1479, 1498, and possibly 1456 cm^{-1}, are multimer connected. The bands at 1308, 1326, and 1345 cm^{-1} are easily seen, even in "high dilution"

samples.

With the paucity of data collected on the aggregates, assignments for these bands cannot be established. Some general observations can be made, however. The number of bands indicates the presence of at least two different multimers, as the dimer is the species first expected upon increasing the ion pair concentration in the matrix, and it would have a maximum of only four ν_3 bands.

The multimer bands have little apparent sensitivity to amounts of solvent (H_2O, pyridine, etc.) present, in contrast to their reported sensitivity to "inert" gas matrices as expressed on page 28 of reference 3b. It should be noted that gas phase studies indicate the dimer formation enthalpy is quite high (255-to 280 kJ/mole),[30] so presumably some large reduction in the polarity of the molecule is occurring which would reduce the sensitivity to the presence of polar solvent molecules. In this vein it should be noted that an increasing amount of research is indicating that aggregates exist in liquid solutions of only moderate concentrations (for example, see reference 31). With respect to this, the author knows of no report of these multimer bands appearing in the spectrum of solutions, although they could be shifted some under conditions of total solvation.

Lastly, we note that as the higher aggregates become more predominant in the matrix the high frequency bands mentioned above seem to move down in frequency by about 5 cm^{-1}, while the low frequency bands move up by about the same amount.

Solvation Studies, Pyridine

The Data

Shown in Figure 7 is the spectrum of a deposit of pure pyridine (bottom curve), and a spectrum of a codeposit of pyridine and lithium nitrate (top curve). Spectra demonstrating the changes that occur upon annealing a codeposit of pyridine and lithium nitrate are shown in Figure 8 on an expanded scale. For comparison, the changes when a sample of pyridine alone is annealed is shown in Figure 9; the bottom curve is a spectrum of a glassy deposit of pyridine, while the upper curve is a spectrum of a polycrystalline film of the same sample.

The bottom curve of Figure 10 is the spectrum of a deposit of pure deuterated pyridine, while the top curve is the spectrum of a codeposit of deuterated pyridine and lithium nitrate. No annealing of the deuterated deposits was performed.

The spectra for the matrix isolated deposits of pyridine, and pyridine/argon codeposits, are shown in Figures 11 (.5% Py), 12 (1% Py), 13 (5% Py), 14 (10% Py), 15 (42% Py), 16 (50% Py), 17 (5% Pyd_5), 18 (10% Pyd_5), and 19 (42% Pyd_5). Figures 20, 21, 22, 23, and 24 are expanded scale spectra for the samples of, respectively, Figures 13 (5% Py), 14 (10% Py), 17 (5% Pyd_5), 18 (10% Pyd_5), and 19 (42% Pyd_5), in various stages of being annealed.

The curves shown in Figure 25 correspond to the same samples as those of Figure 13; the bottom curve is the spectrum of a 5% pyridine/argon mixture, while the upper curve is for a codeposition of lithium nitrate with a 5% pyridine/argon gas mixture.

The bottom curve of Figure 26 is the spectrum of a deposit of very

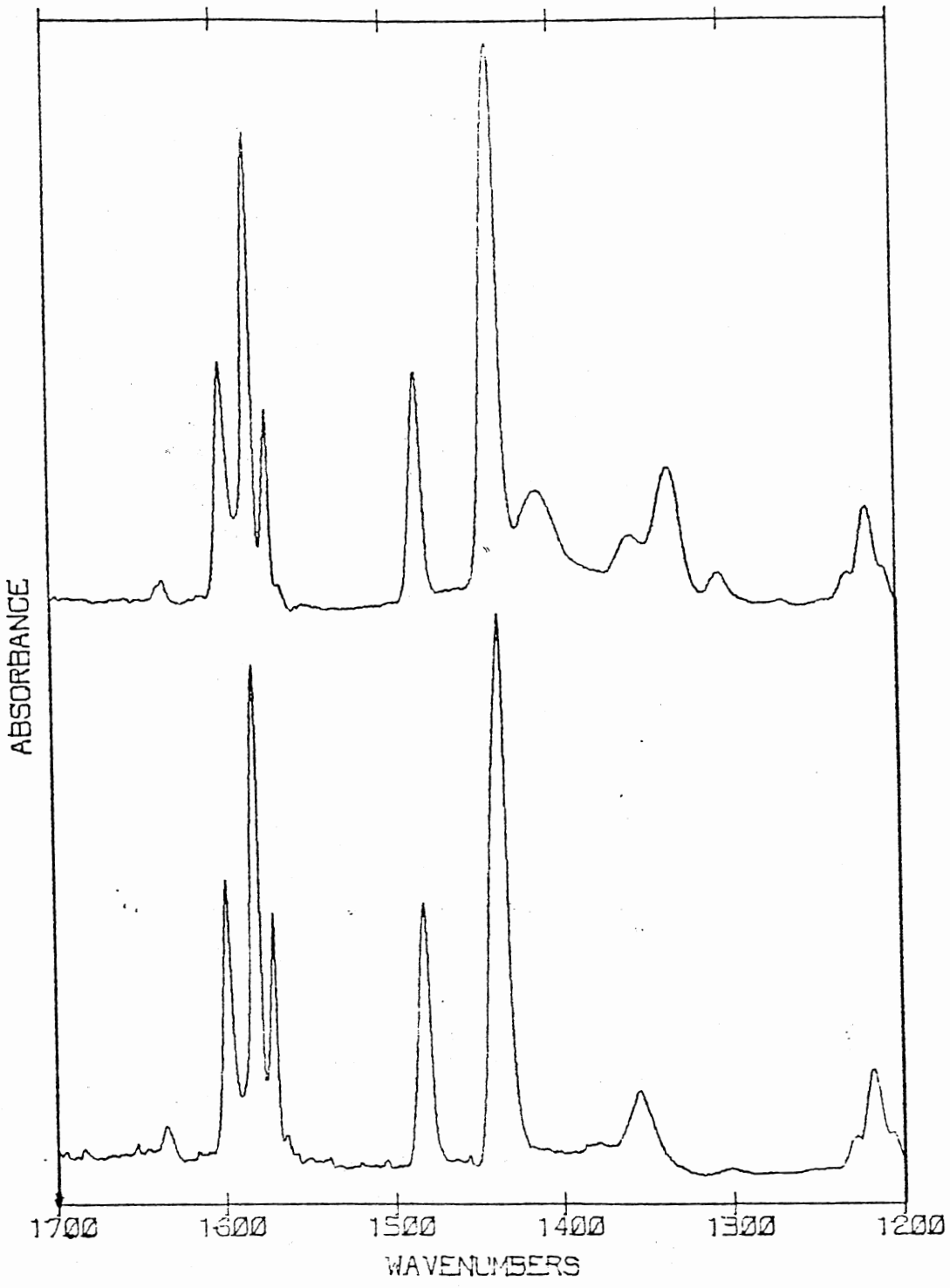

Figure 7. Spectra of "Glassy" Pyridine (Lower Curve), and Codeposit of Pyridine and Lithium Nitrate (Upper Curve), at 77 K

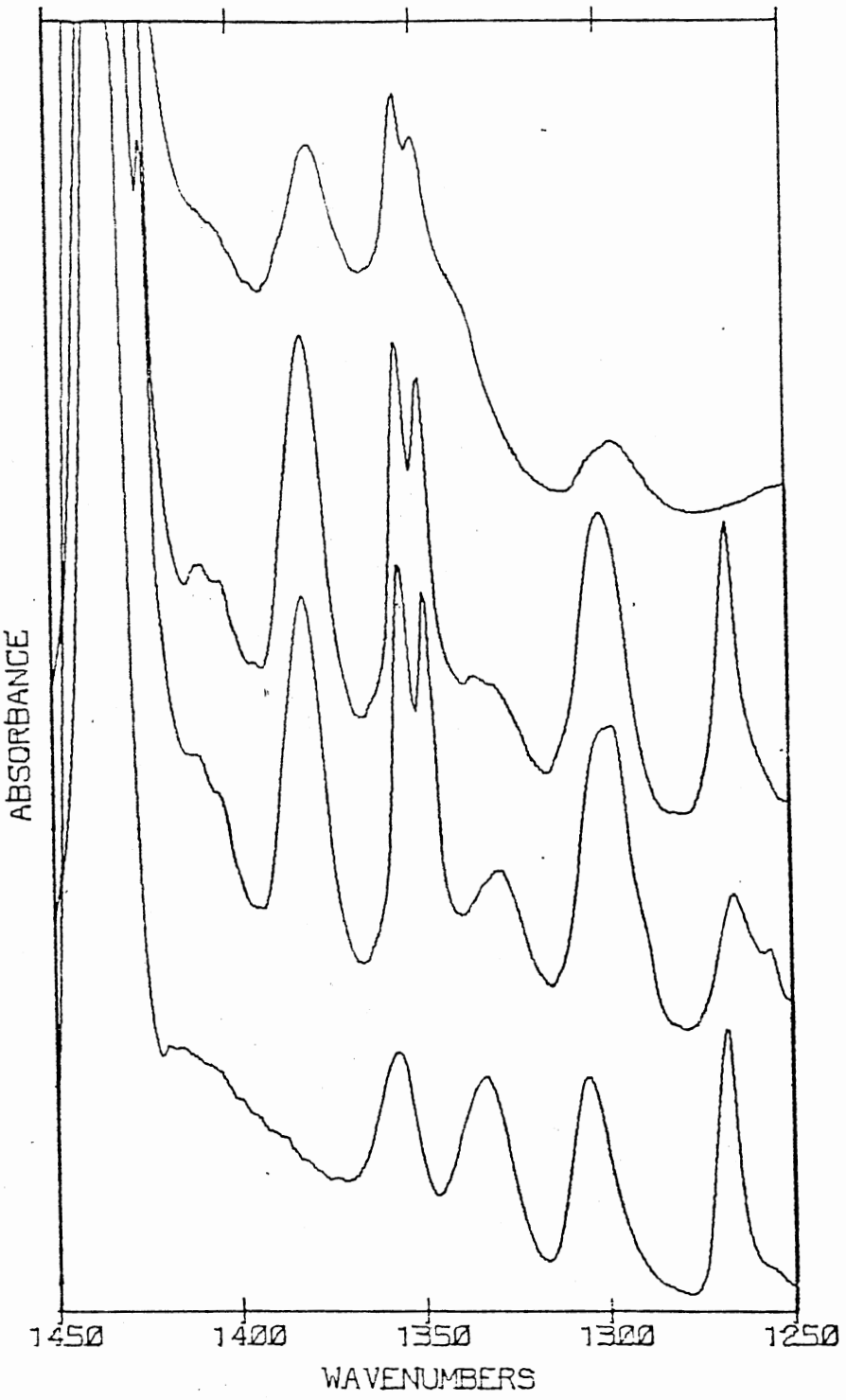

Figure 8. Spectra Showing the Annealing Effect for a Codeposit of Lithium Nitrate and Pyridine: Lower Curve is the Original Sample at 77 K, and each Succeeding Upper Curve is the Sample at a Higher Temperature

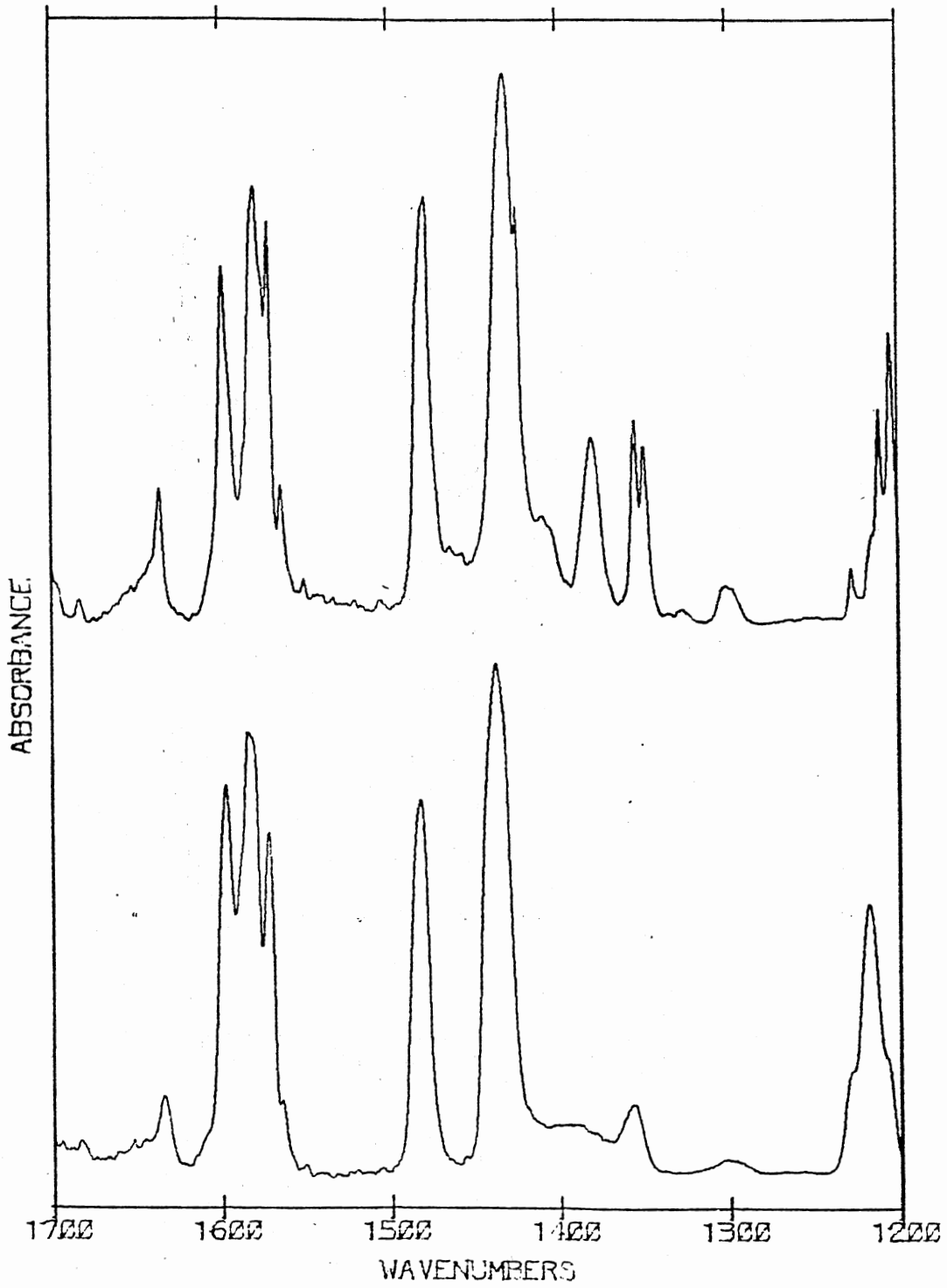

Figure 9. Spectra of "Glassy" Pyridine at 77 K (Lower Curve), and of Polycrystalline Film Obtained from Warming the Sample (Upper Curve)

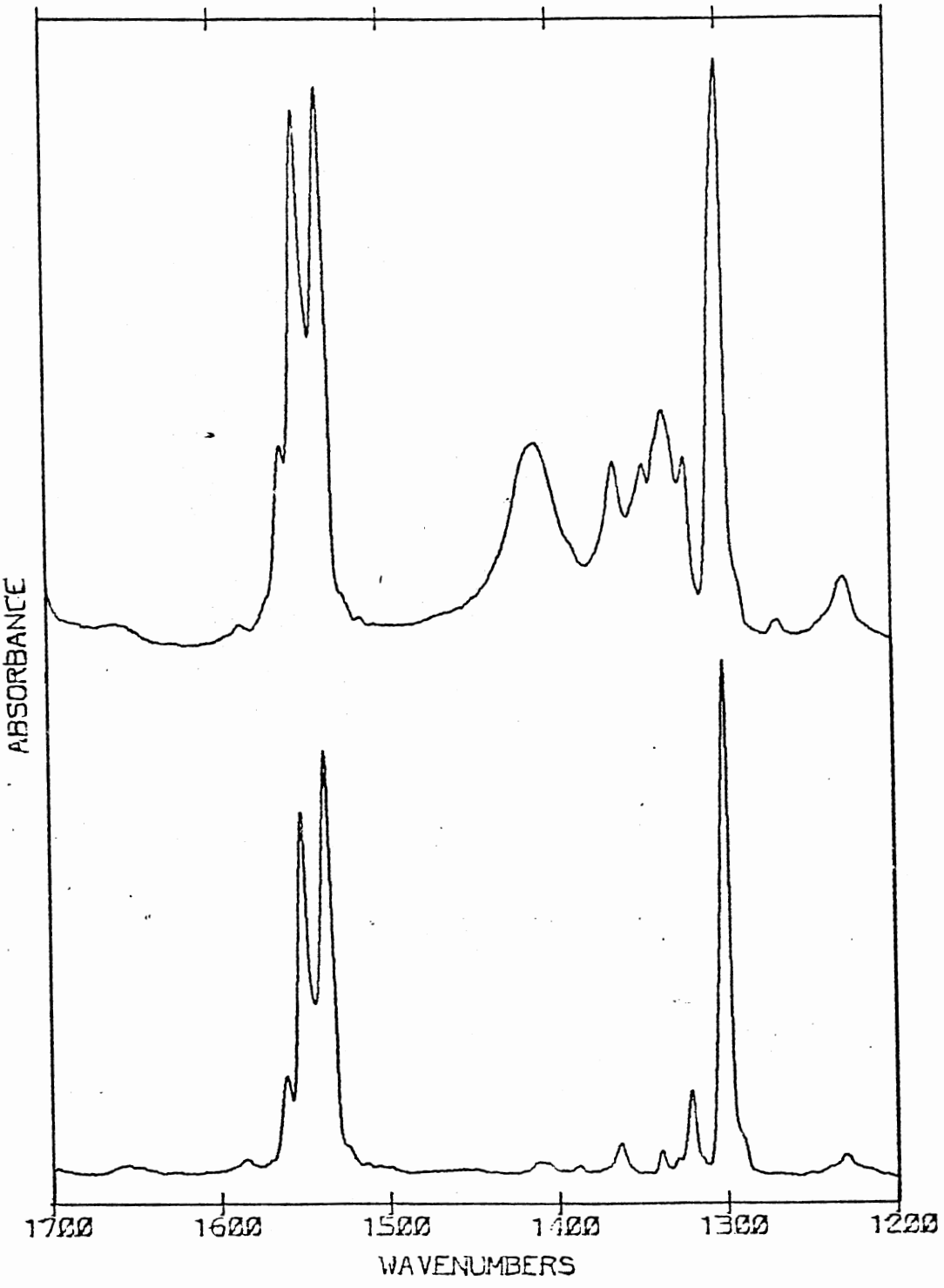

Figure 10. Spectra of "Glassy" Deuterated Pyridine (Lower Curve), and of a Codeposit of Lithium Nitrate and Deuterated Pyridine (Upper Curve), at 77 K

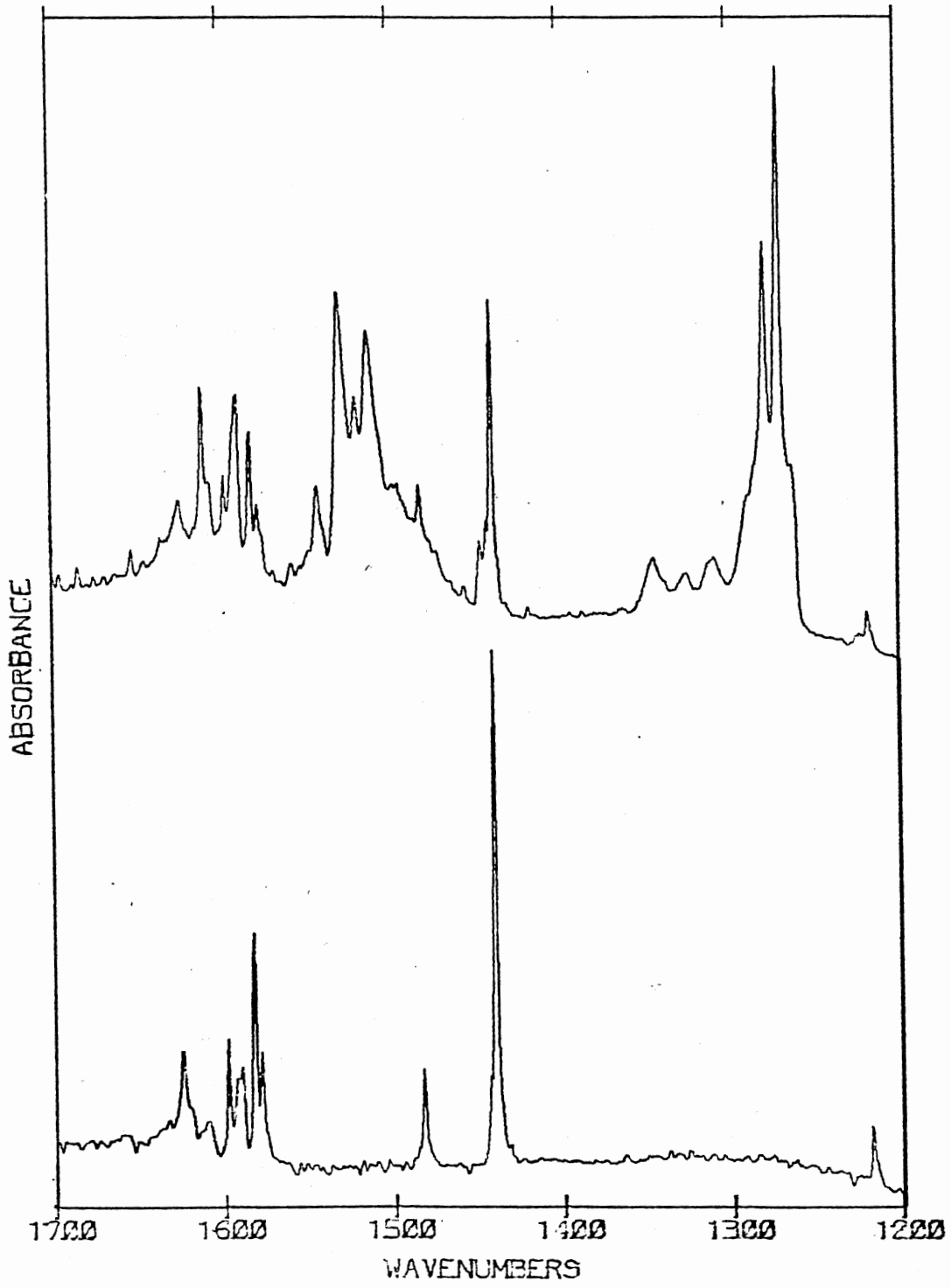

Figure 11. Spectra of .5% Pyridine in Argon (Lower Curve), and of a Codeposit of Lithium Nitrate with this Gas Mixture (Upper Curve), at 10-15 K

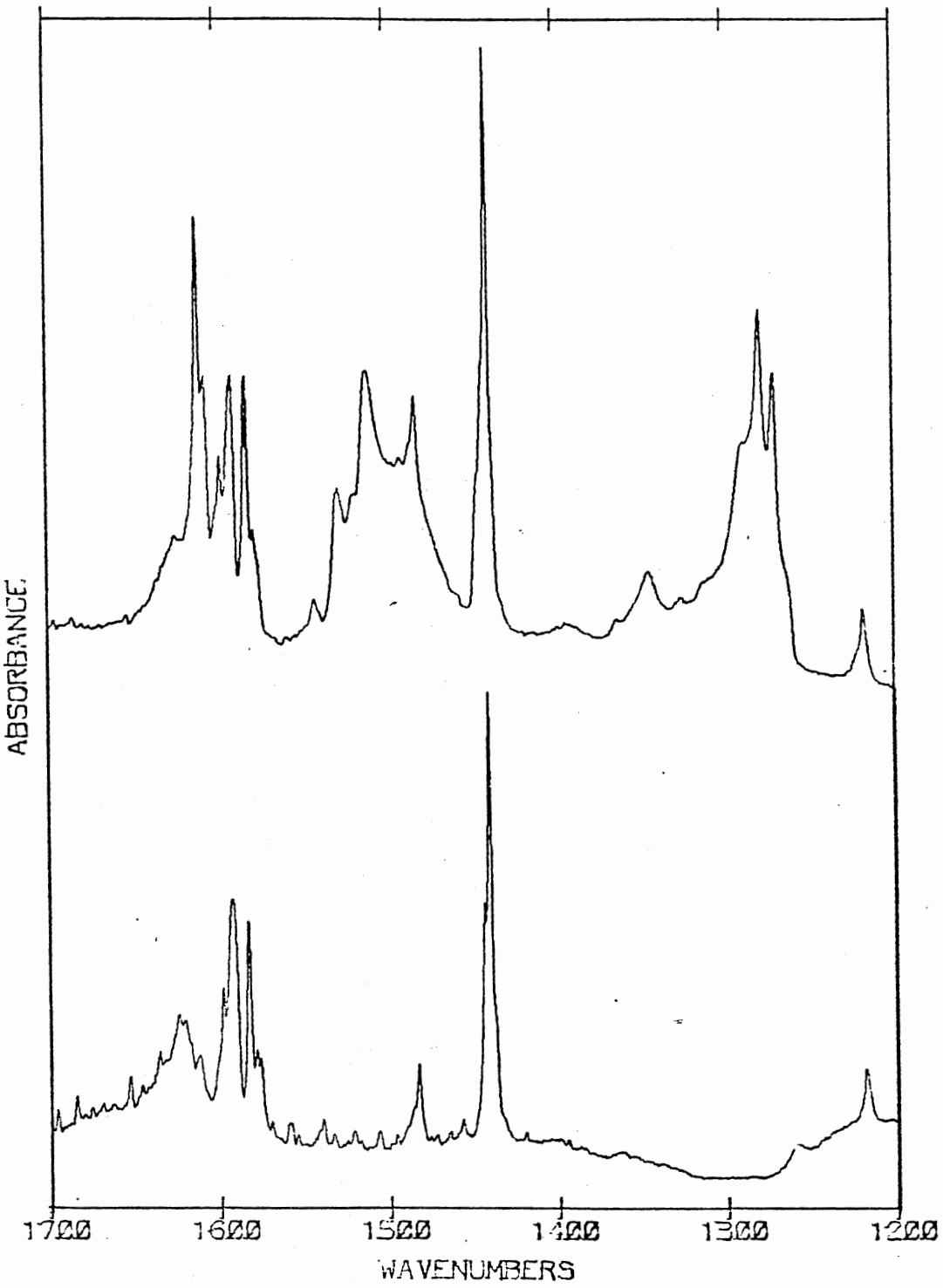

Figure 12. Spectra of 1% Pyridine in Argon (Lower Curve), and of a Codeposit of Lithium Nitrate with this Gas Mixture (Upper Curve), at 10-15 K

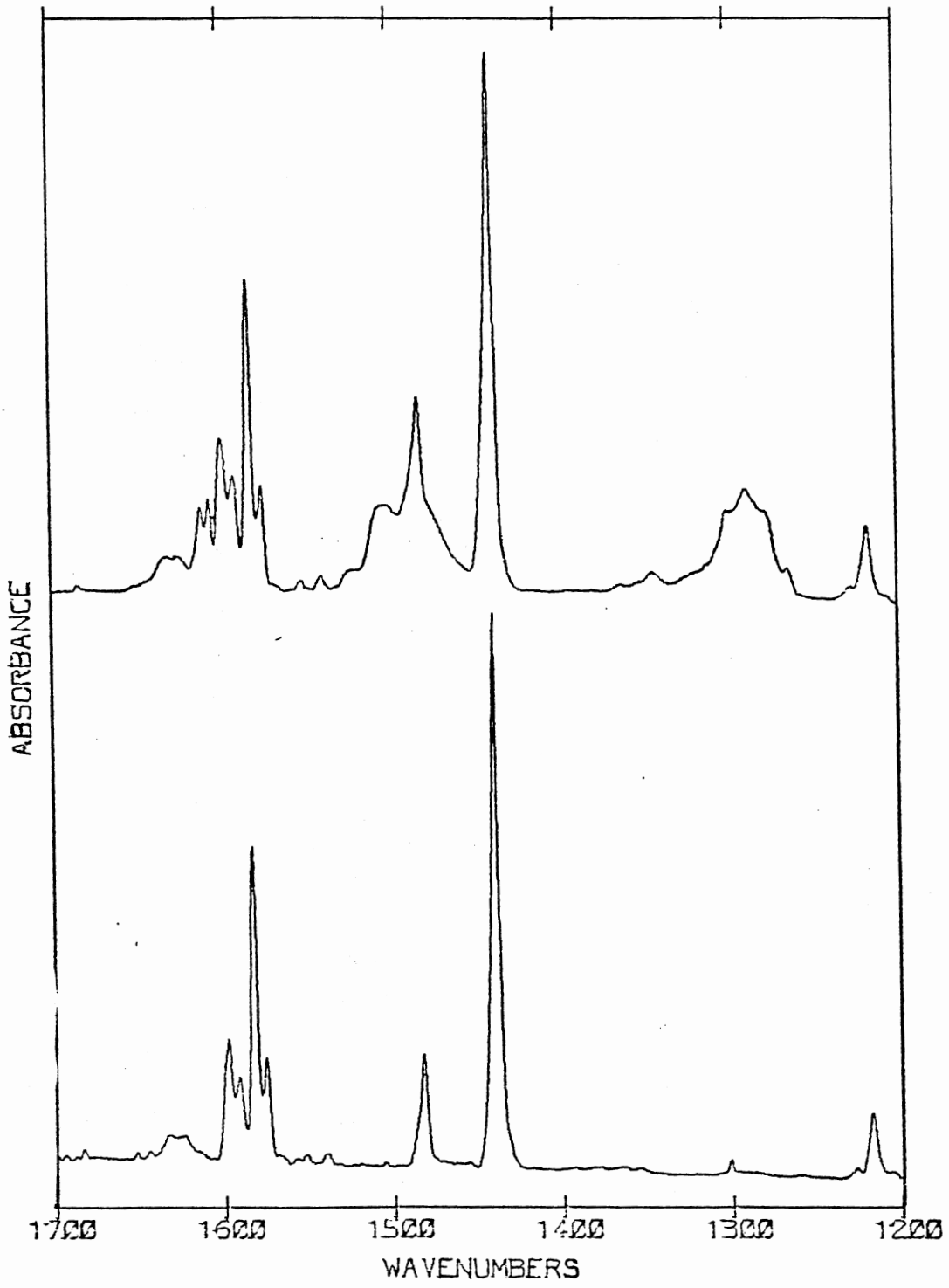

Figure 13. Spectra of 5% Pyridine in Argon (Lower Curve), and of a Codeposit of Lithium Nitrate with this Gas Mixture (Upper Curve), at 10-15 K

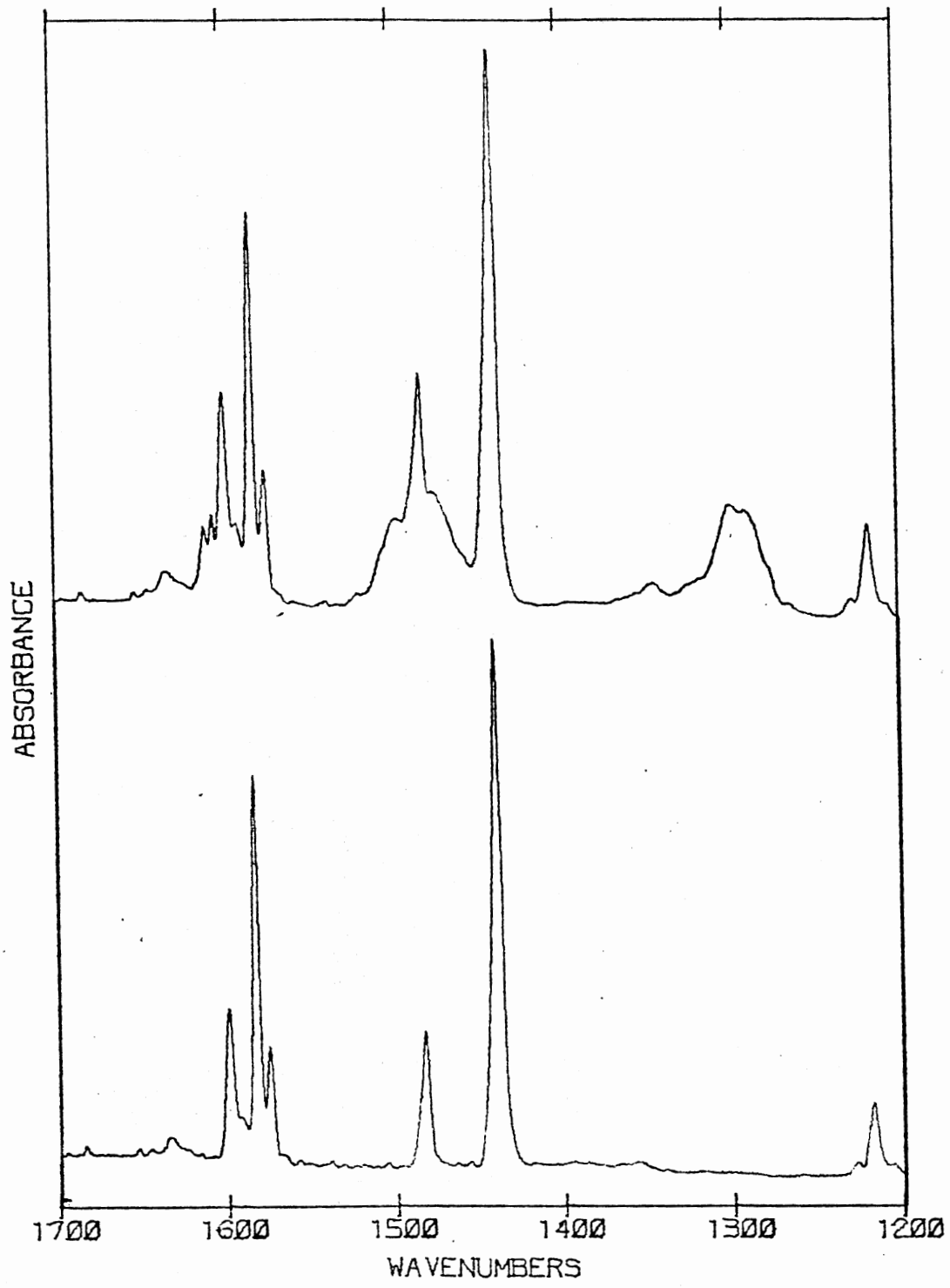

Figure 14. Spectra of 10% Pyridine in Argon (Lower Curve), and of a Codeposit of Lithium Nitrate with this Gas Mixture (Upper Curve), at 10-15 K

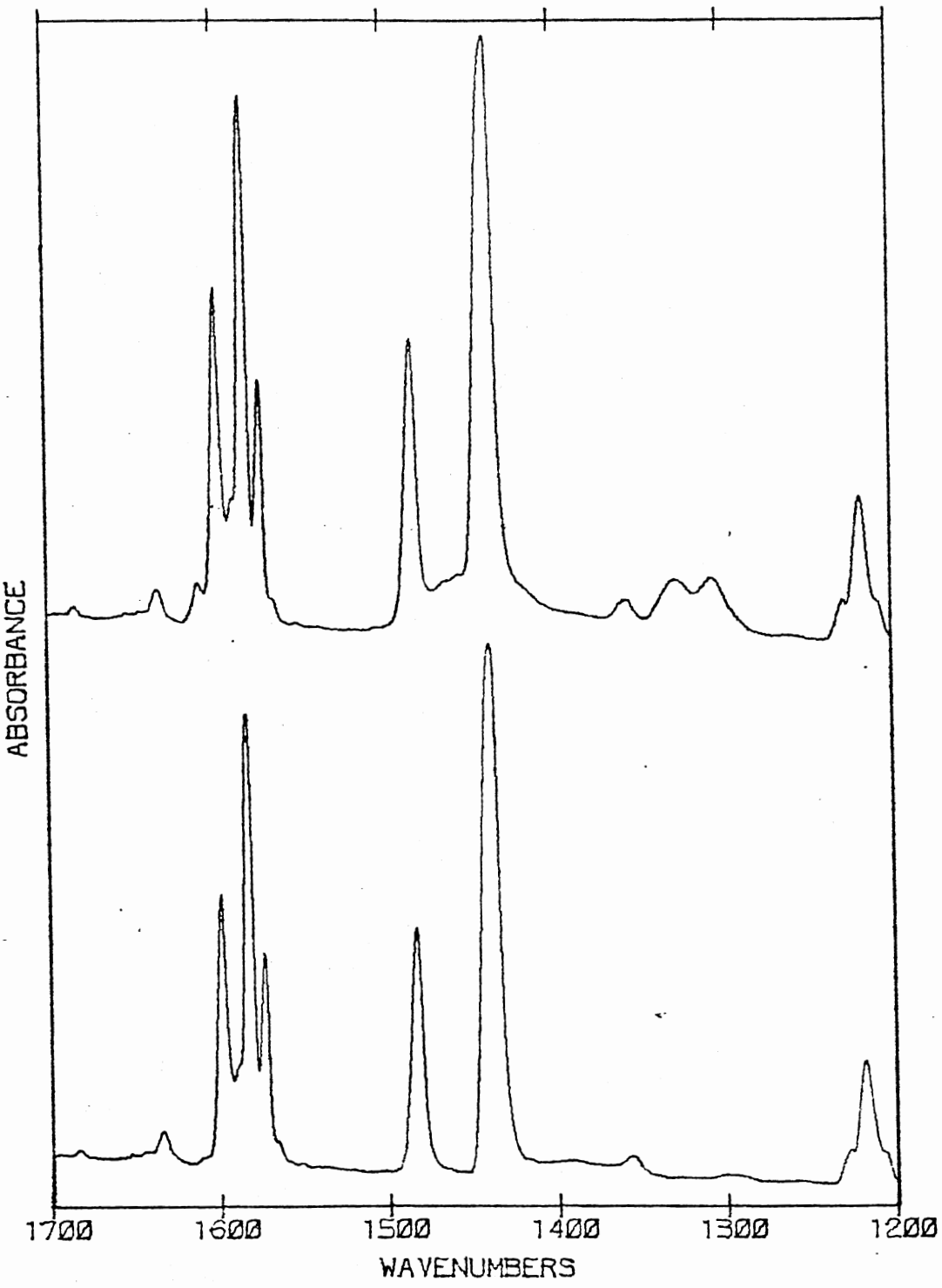

Figure 15. Spectra of 42% Pyridine in Argon (Lower Curve), and of a Codeposit of Lithium Nitrate with this Gas Mixture (Upper Curve), at 10-15 K

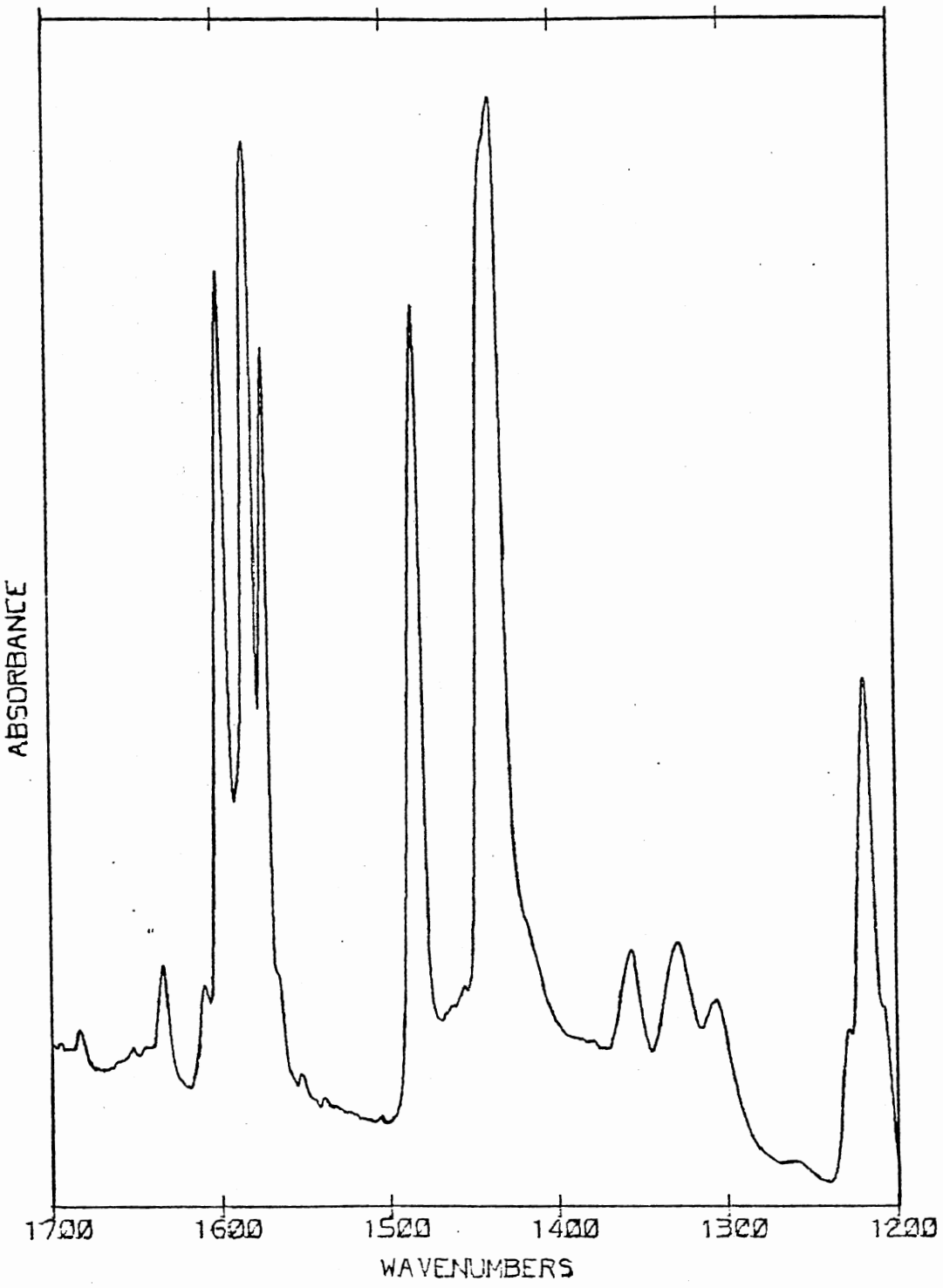

Figure 16. Spectrum of a Codeposit of Lithium Nitrate with a Gas Mixture of 50% Pyridine in Argon, at 10-15 K

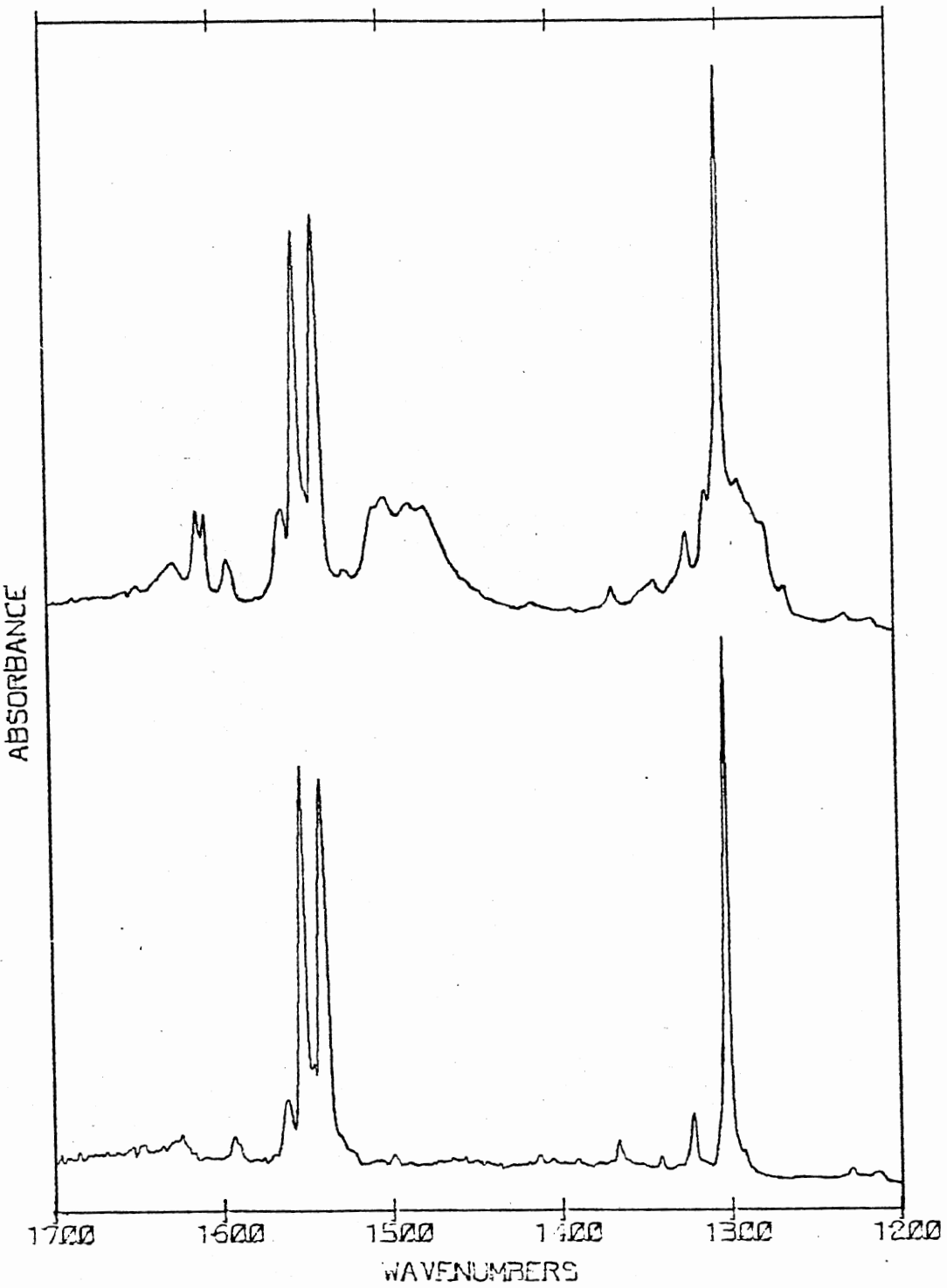

Figure 17. Spectra of 5% Deuterated Pyridine in Argon (Lower Curve), and of a Codeposit of Lithium Nitrate with this Gas Mixture,(Lower Curve), at 10-15 K

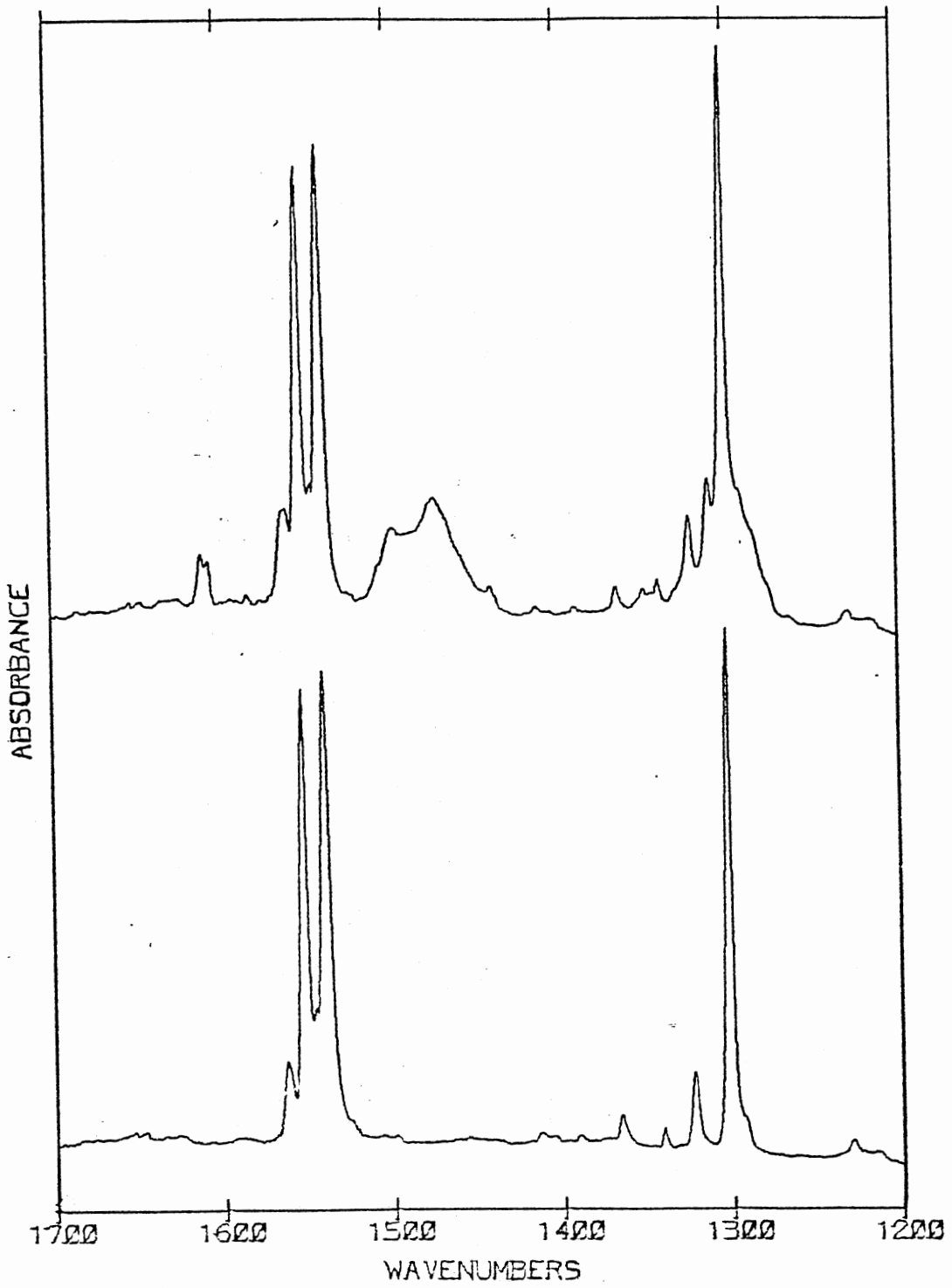

Figure 18. Spectra of 10% Deuterated Pyridine in Argon (Lower Curve), and of a Codeposit of Lithium Nitrate with this Gas Mixture (Upper Curve, at 10-15 K

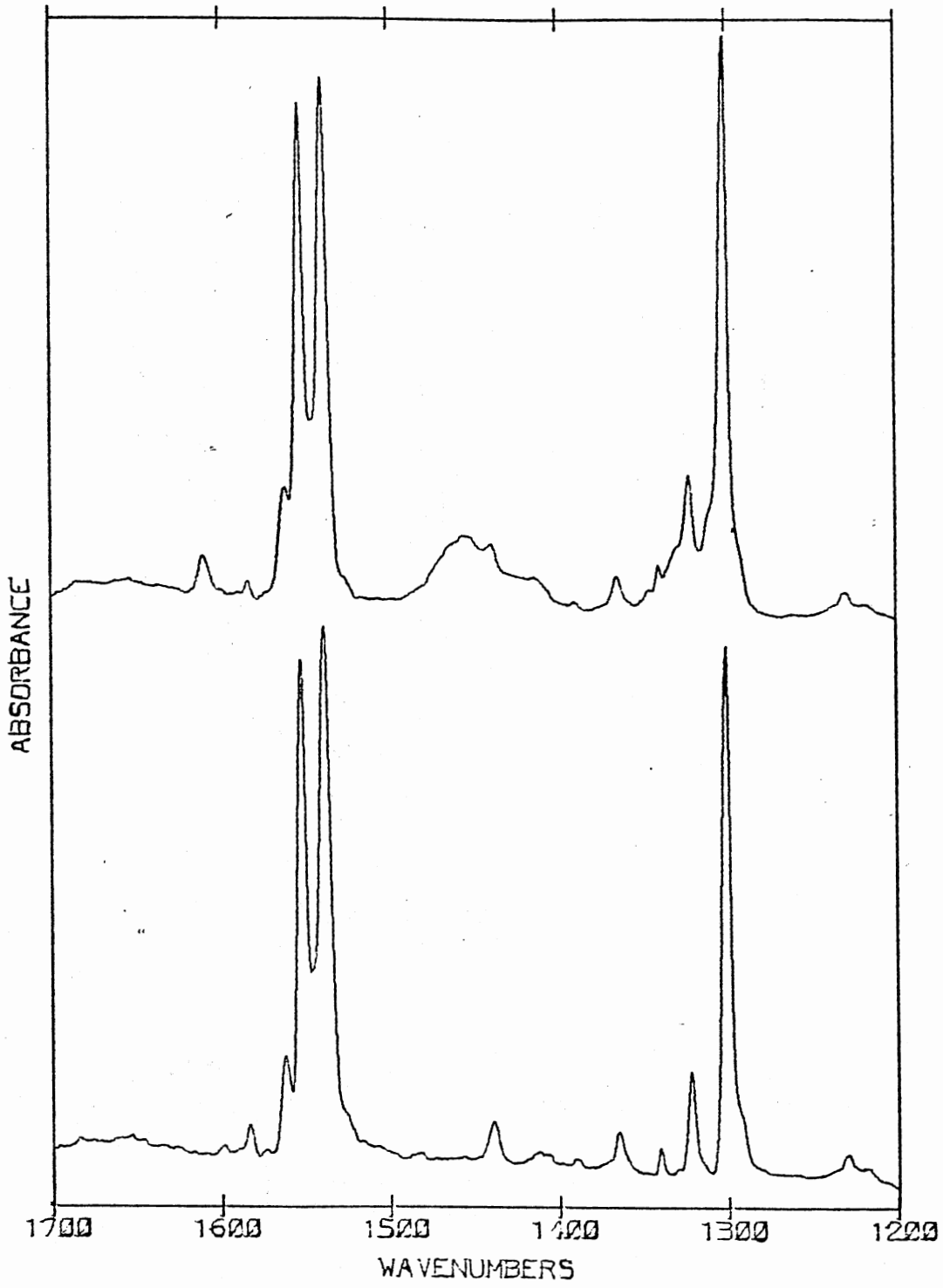

Figure 19. Spectra of 42% Deuterated Pyridine in Argon (Lower Curve), and of a Codeposit of Lithium Nitrate with this Gas Mixture, at 10-15 K

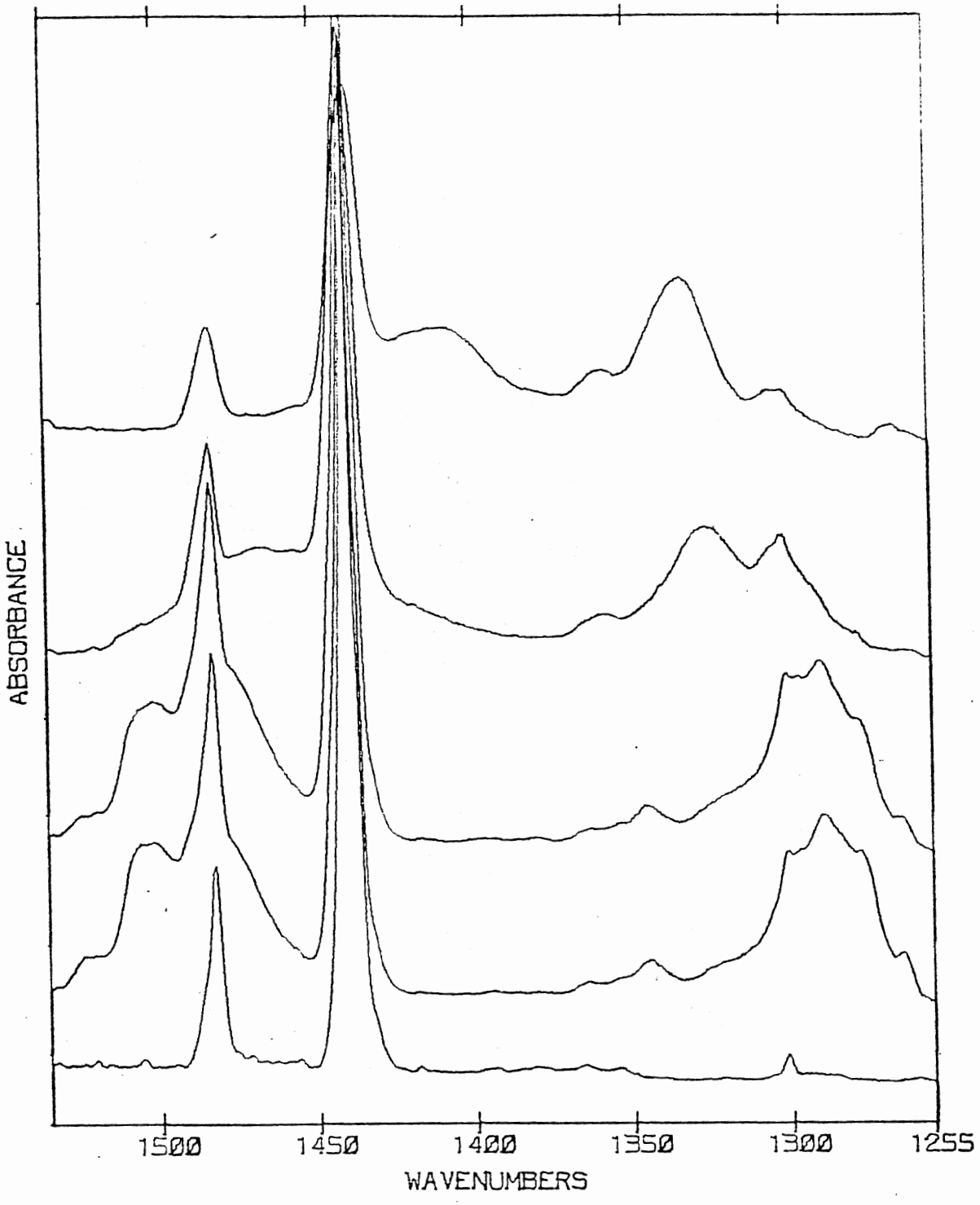

Figure 20. Spectra Showing the Annealing Effect for a Codeposit of Lithium Nitrate with a Gaseous Mixture of 5% Pyridine in Argon: the Bottom Two Curves are Identical to those of Figure 13, and each Succeeding Curve of the Upper Three Curves is the Spectrum for the Sample at Increasingly Higher Temperatures

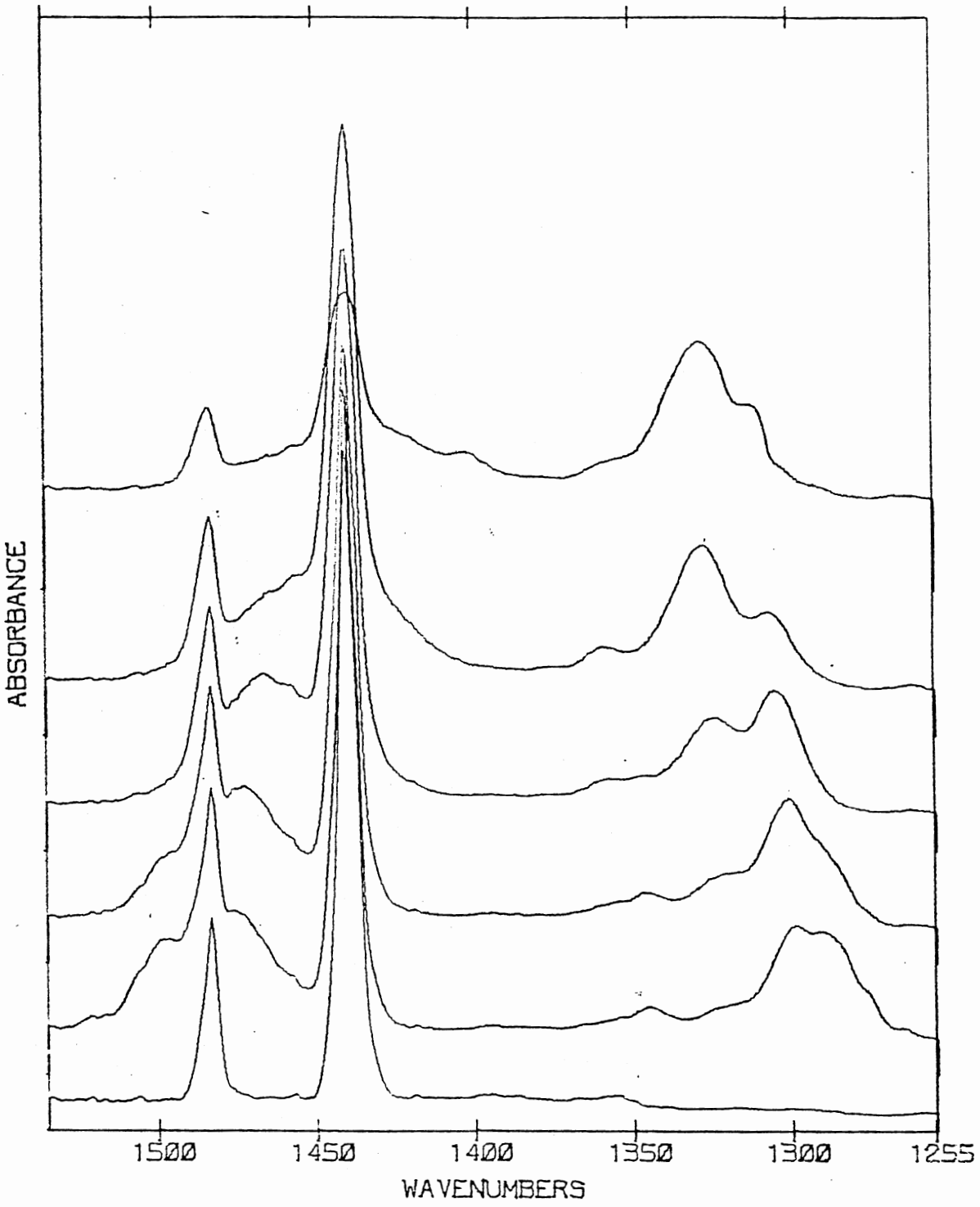

Figure 21. Spectra Showing the Annealing Effect for a Codeposit of Lithium Nitrate with a Gaseous Mixture of 10% Pyridine in Argon: the Bottom Two Curves are Identical to those of Figure 14, and each Succeeding Curve of the Upper Three Curves is the Spectrum for the Sample at Increasingly Higher Temperatures

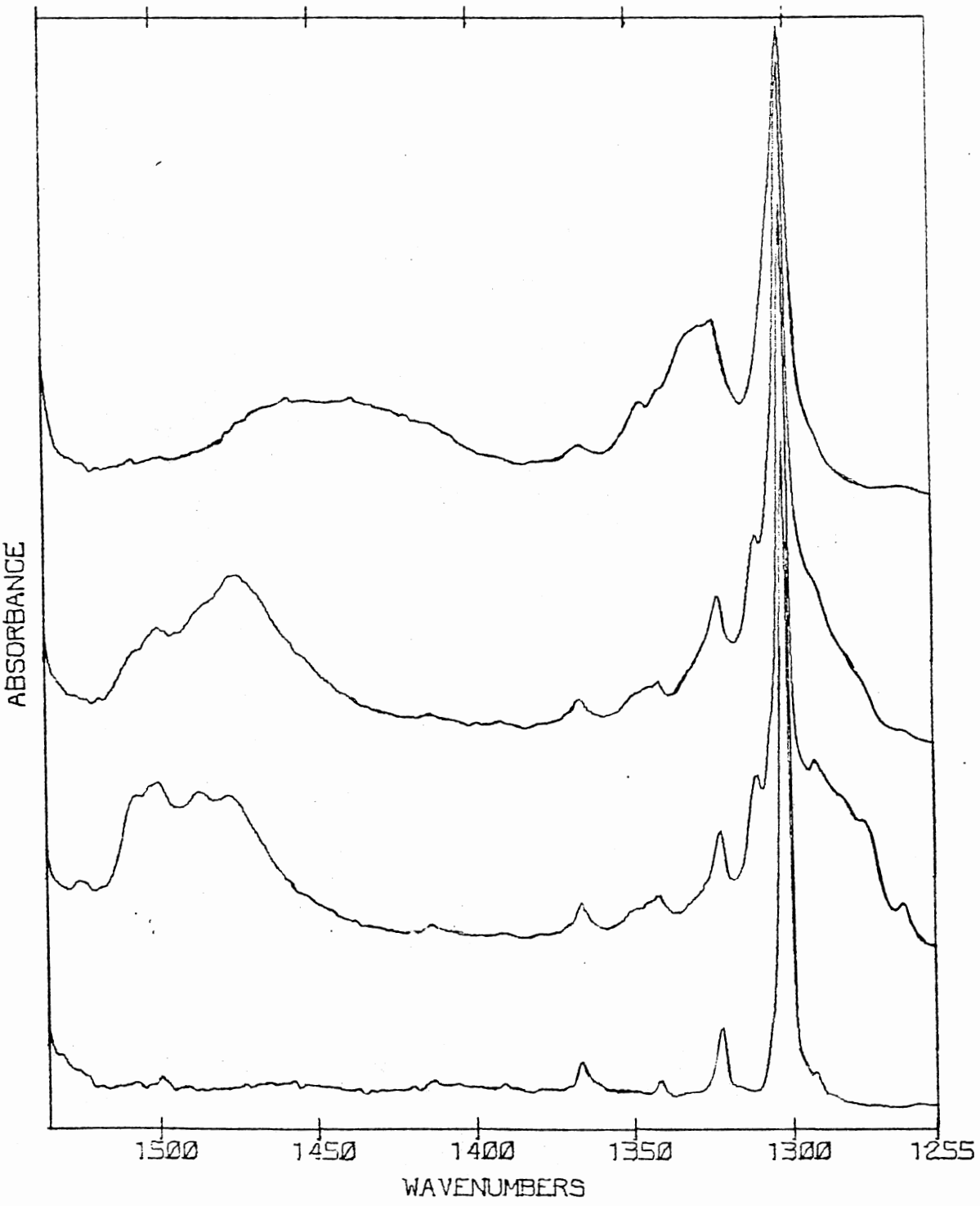

Figure 22. Spectra Showing the Annealing Effect for a Codeposit of Lithium Nitrate with a Gaseous Mixture of 5% Deuterated Pyridine in Argon: the Bottom Two Curves are Identical to those of Figure 17, and each Succeeding Curve of the Upper Two Curves is the Spectrum for the Codeposit Sample at Increasingly Higher Temperatures

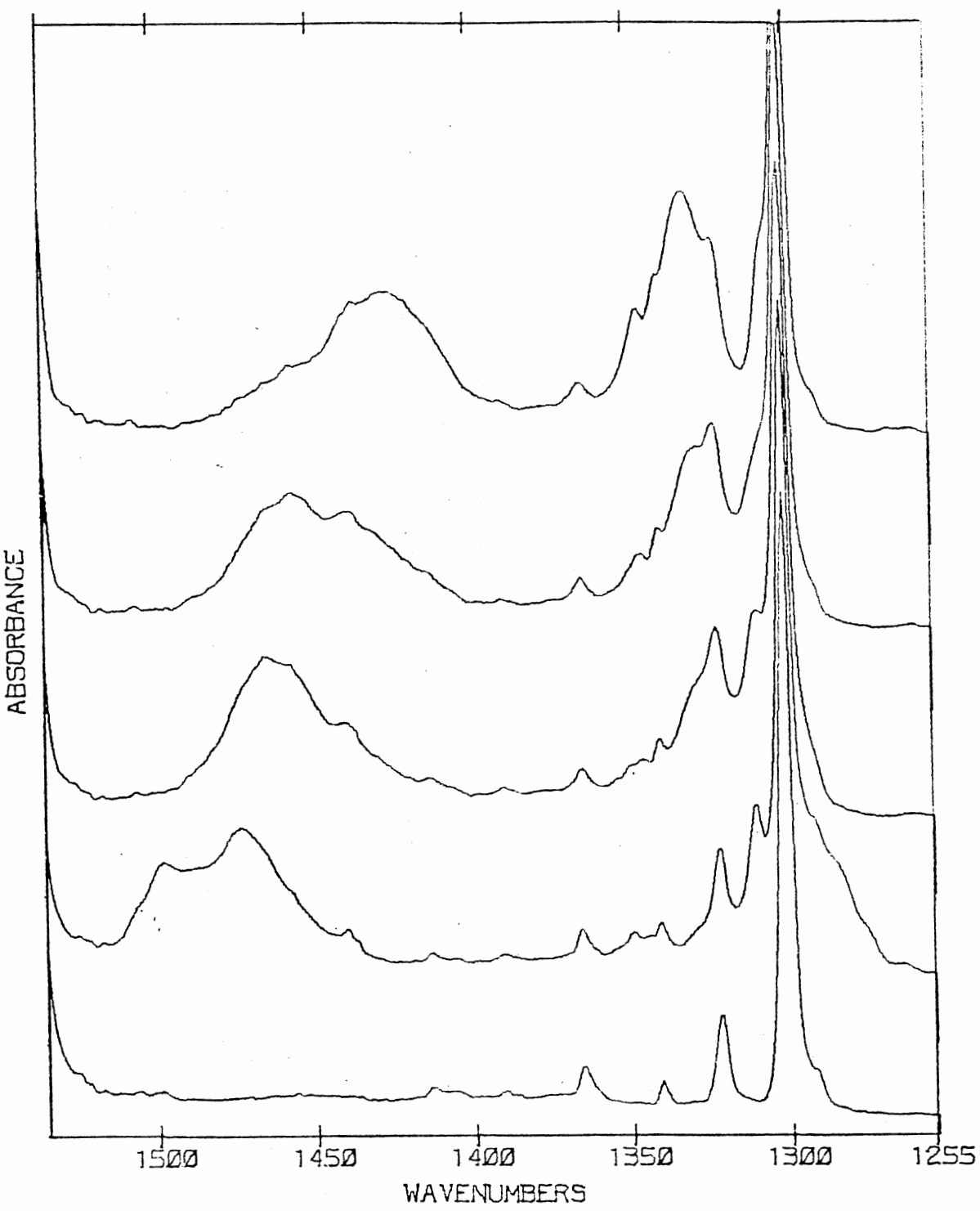

Figure 23. Spectra Showing the Annealing Effect for a Codeposit of Lithium Nitrate with a Gaseous Mixture of 10% Deuterated Pyridine in Argon: the Bottom Two Curves are Identical to those of Figure 18, and each Succeeding Curve of the Upper Three Curves is the Spectrum for the Codeposit Sample at Increasingly Higher Temperatures

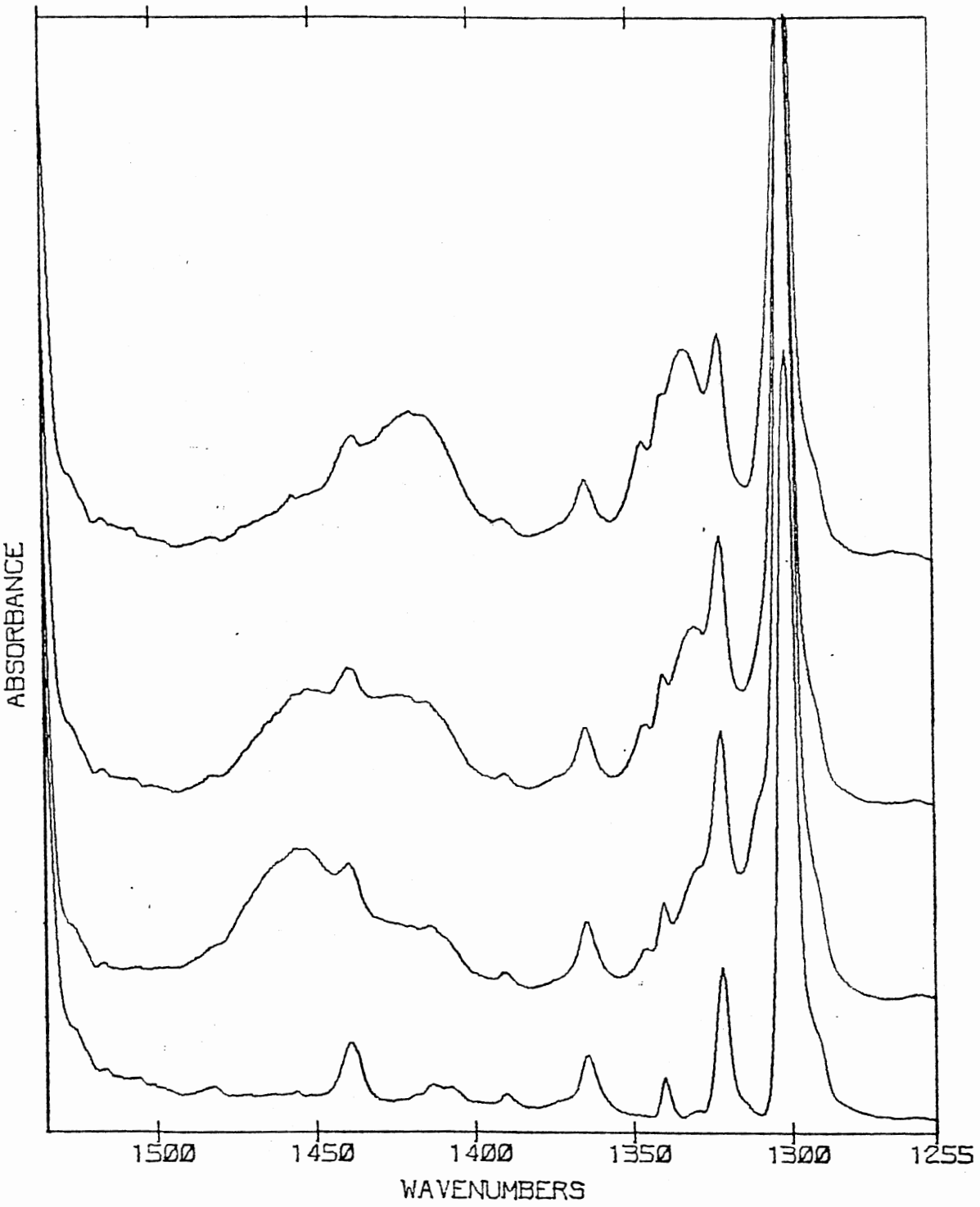

Figure 24. Spectra Showing the Annealing Effect for a Codeposit of Lithium Nitrate with a Gaseous Mixture of 42% Deuterated Pyridine in Argon: the Bottom Two Curves are Identical to those of Figure 19, and each Succeeding Curve of the Upper Two Curves is the Spectrum for the Codeposit Sample at Increasingly Higher Temperatures

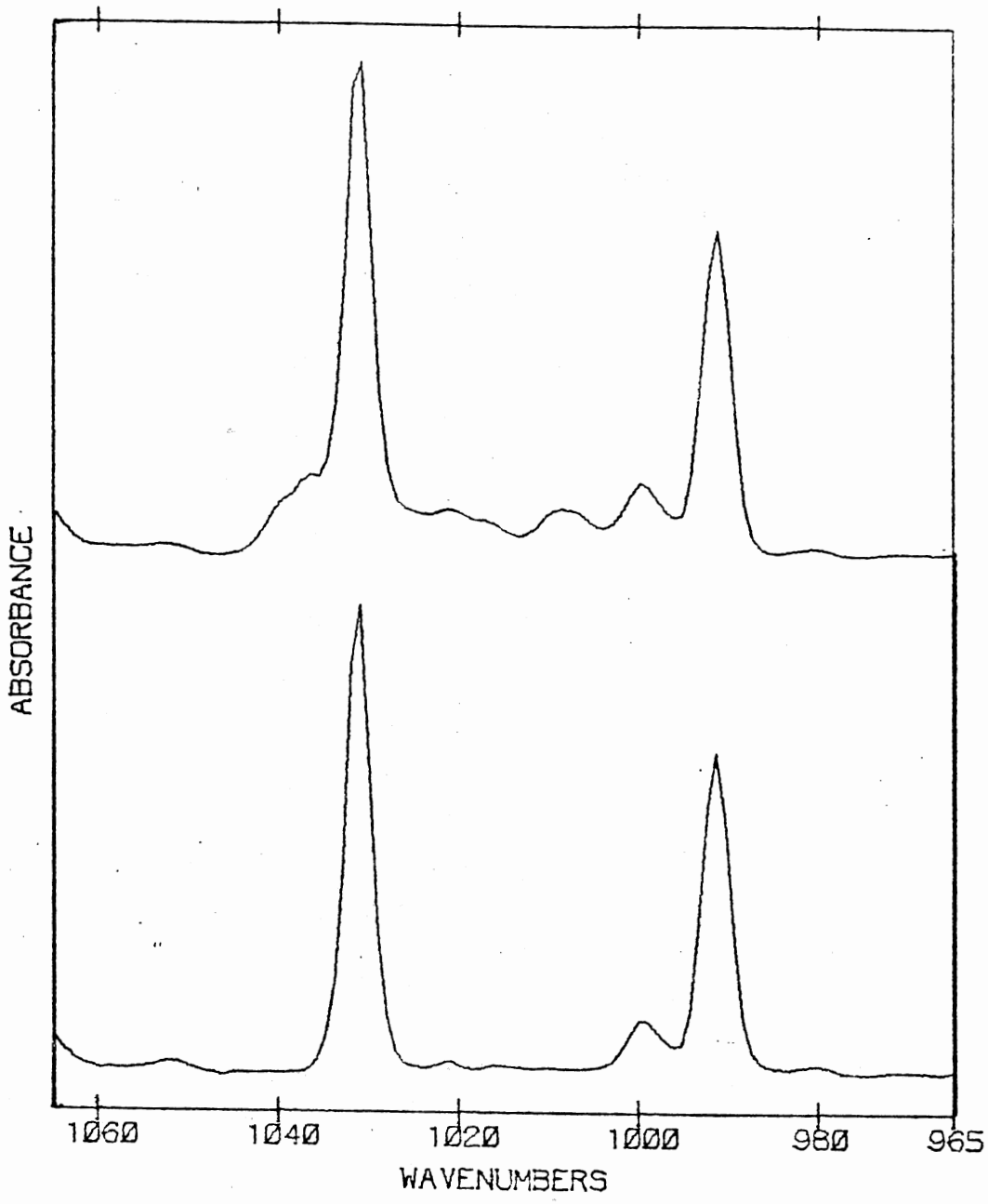

Figure 25. A Selected Region of the Spectra of 5% Pyridine in Argon (Lower Curve), and of a Codeposit of Lithium Nitrate with this Gaseous Mixture (Upper Curve), at 10-15 K

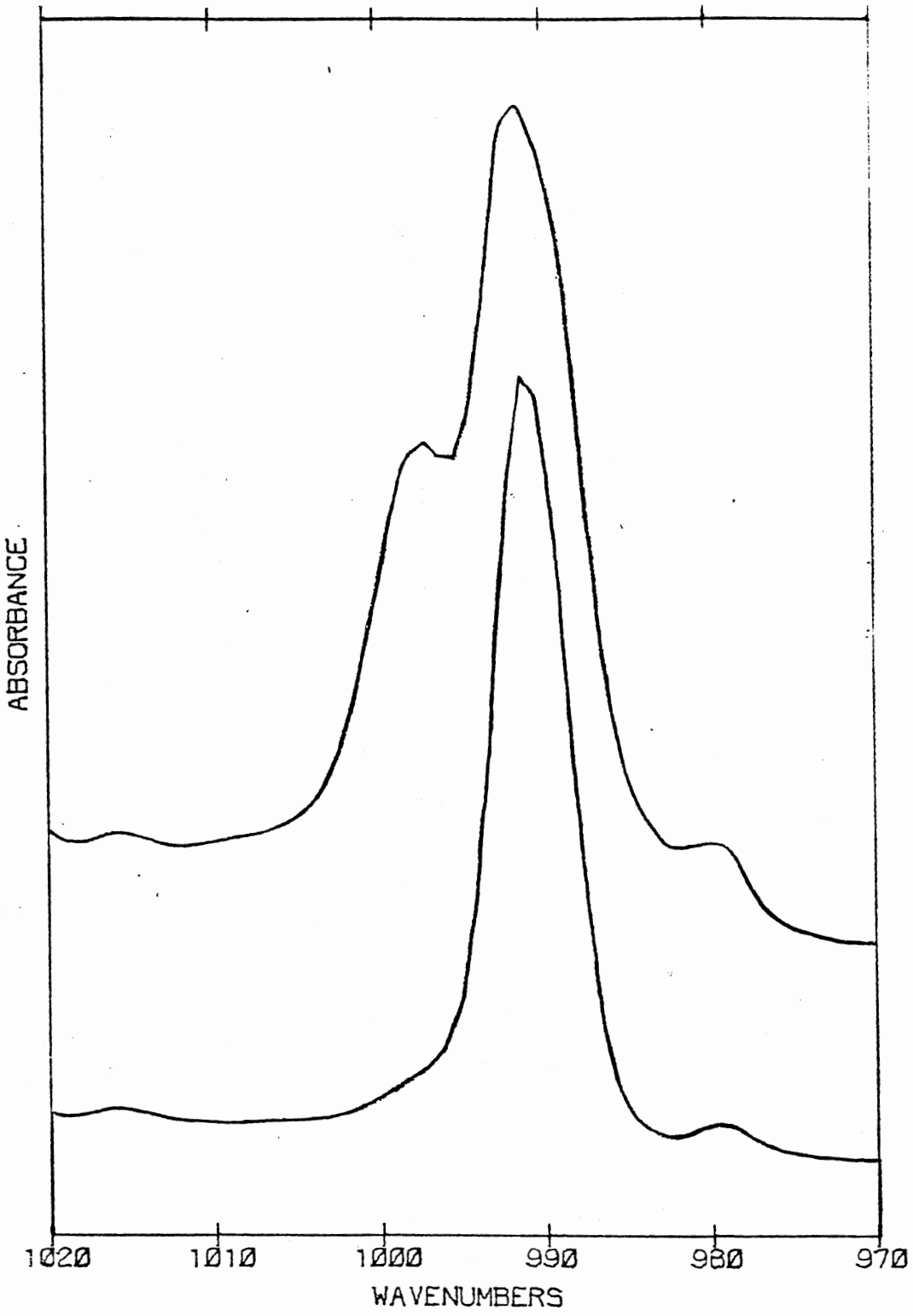

Figure 26. A selected Region of the Spectra of Pyridine (Lower Curve), and of Pyridine Contaminated with Water (Upper Curve), at 77 K

dry, 100%, pyridine, while the upper curve is the spectrum of a sample of pyridine deliberately contaminated with water.

Figure 27 shows a region of the infrared spectrum for a sample of pure pyridine (bottom curve), and for a codeposit sample of pyridine and lithium nitrate, both at 77K.

The Discussion: Nitrate Bands

From Figures 7 and 10 it is seen that when the lithium nitrate ion pair is isolated in, and totally solvated by, pyridine, the ν_3 peaks of the complex $(Py)_nLiNO_3$ appear at 1334 cm^{-1} and 1411 cm^{-1}. Both values can be plainly seen in the pyridine/lithium nitrate case of Figure 7, but since pyridine can have a broad absorption near 1400 cm^{-1} (c.f. the bottom curve of Figure 9), it is better to use the deuterated pyridine/lithium nitrate sample (Figure 10) to assign the value 1411 cm^{-1}, as deuterated pyridine has no absorptions in this region. The bandwidth of the upper frequency band is about 1.5 times larger than that of the lower frequency band, reflecting the greater sensitivity of the corresponding ion pair species to it's environment.

Upon annealing a codeposit of lithium nitrate and 100% pyridine (Figure 8), several interesting things occur. Perhaps the most important information, however, is the fact that when the sample crystallizes (second curve up from the bottom in Figure 8), the general ion pair conditions of the initial deposition apparently do not change much, as judged from the minor changes in the ν_3 absorptions. Presumably this implies that when the major constituent pyridine crystallizes, solvated ion pairs somehow still exist in the crystalline sample. With further annealing, the bands due to the totally solvated ion pair gradually

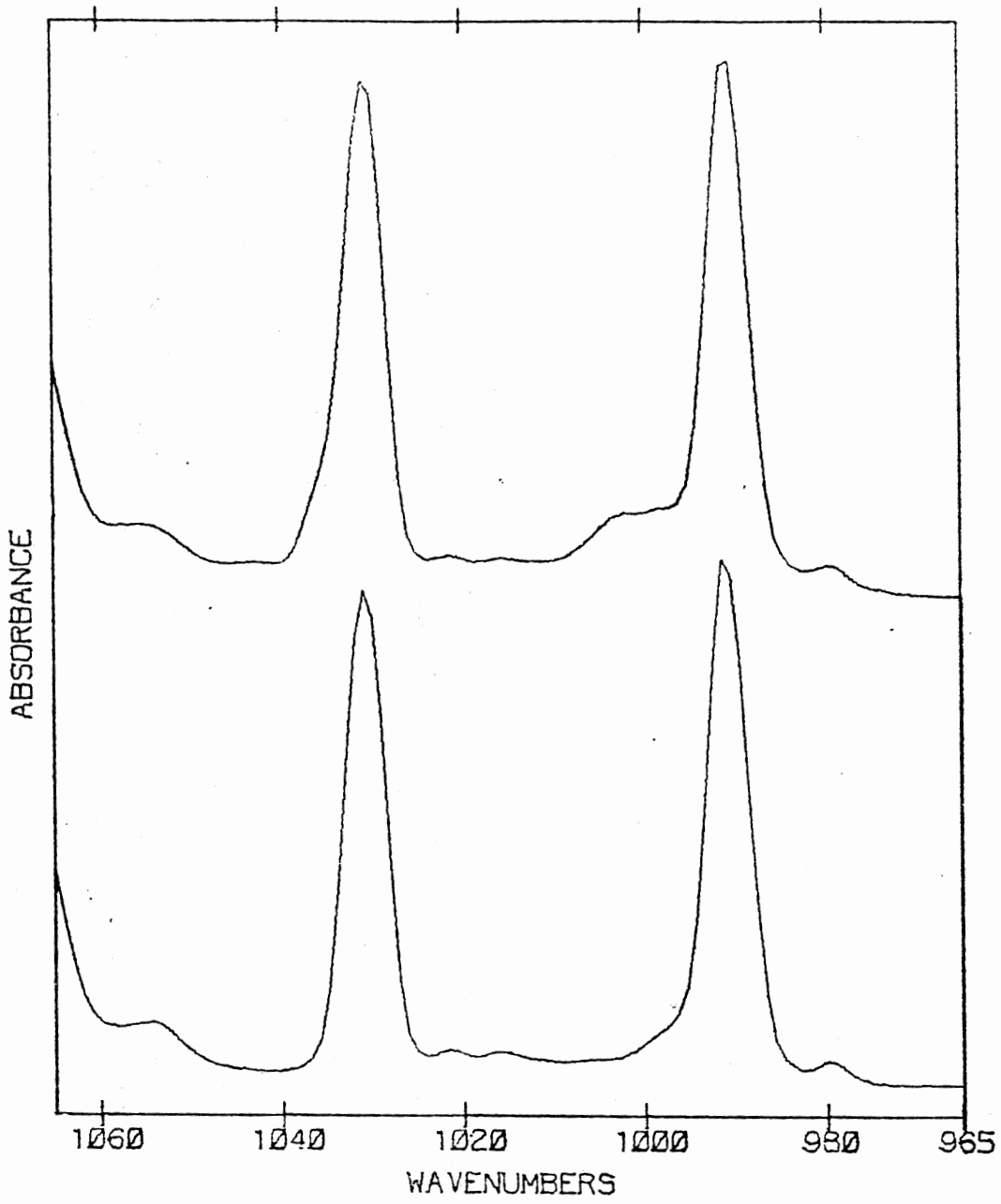

Figure 27. A Selected Region of the spectra of Pyridine (Lower Curve), and of a Codeposit of Lithium Nitrate and Pyridine (Upper Curve), at 77 K

wash out, and appear to ultimately be replaced by bands at c.a. 1340 cm^{-1} and 1360 cm^{-1}, as seen in the top curve of Figure 8. As a point of reference, the nitrogen oxide impurities of the sample, as determined by their absorptions[49] at 1305 cm^{-1}, and 1267 cm^{-1}, do not leave the sample until the destruction of the initial ion pair conditions is nearly complete.

Also it can be seen that, upon crystallization of the codeposit sample of Figure 8, a new band appears at 1381 cm^{-1}. The appearance of this band when a "glassy" deposit of 100% pyridine is crystallized (Figure 9), proves that it is due solely to the pyridine. This band is apparently the one found at 1375 cm^{-1} in the liquid, and described as $\nu_{14}(B_1)$ in references 32 and 40. No mention is made of a 1381 cm^{-1} band in the description of the infrared spectrum of "glassy" pyridine in reference 33, where the $\nu_{14}(B_1)$ mode is assigned to the intense 1437.5 cm^{-1} absorption.

The codepositions of lithium nitrate and pure pyridine, while interesting, provide less unambiguous information than do the isolation experiments utilizing argon. From the spectra for the codepositions of .5% pyridine (Figure 11), and 1% pyridine (Figure 12), with lithium nitrate, it is readily deduced that the bands at 1279 cm^{-1} and 1513 cm^{-1} are due to the ν_3 absorptions of the monosolvate (pyridine)$\cdot LiNO_3$. The bands for the ν_3 absorptions of a small amount of $H_2O\cdot LiNO_3$ are also present for these codeposits (upper curves); the water apparently came from incompletely dried lithium nitrate, as the lower spectra, for pure solvents do not contain any significant amounts of water (as judged by the absence of absorptions near 1600 cm^{-1}, and above 3000 cm^{-1}, which could be assigned to water[28]).

In a tangential comment, it should be noted that although the frequencies of the ν_{3a} (monosolvate) modes for water and pyridine are mathematically identical within experimental error, this does not necessarily imply that the frequencies of the ν_{3b} (monosolvate) modes of water and pyridine will be equal. They are not, and this is due to a general movement of the ν_{3a} and ν_{3b} modes to lower frequencies as the matrix medium polarizability increases with increasing amounts of pyridine in the matrix. Hence the assignments of $\nu_{3b}(H_2O \cdot LiNO_3)$ = 1520 cm^{-1}, and ν_{3b} (pyridine$\cdot LiNO_3$) = 1513 are consistent with this expectation.

Also, from the same two figures, it can be deduced that the band at 1289 cm^{-1} must correspond to ν_{3a} (n = 2) of (pyridine)$_n \cdot LiNO_3$. The corresponding high frequency band, ν_{3b} (n = 2), is difficult to ascertain in these two figures. It is, however, easily assignable in the spectra for the 5 and 10% deuterated pyridine/lithium nitrate codeposits (Figures 17 and 18) as 1497 cm^{-1}.

The band for the ν_{3a} absorption of (pyridine)$_3 \cdot LiNO_3$ is quite easily seen at 1300 cm^{-1} in the spectra of the 5% (Figure 13) and 10% (Figure 14) pyridine/lithium nitrate codeposits. The ν_{3b} absorption of the trisolvate is seen at 1473 cm^{-1} in the corresponding spectra of the 5% (Figure 17) and 10% (Figure 18) deuterated pyridine/lithium nitrate codeposits.

The ν_{3a} band of (pyridine)$_4$ $LiNO_3$ can be seen at 1312 cm^{-1} in the 5% (Figure 13) and 10% (Figure 14) pyridine/lithium nitrate codeposits. It can also be seen in the corresponding spectra of the 5% (Figure 17) and 10% (Figure 18) deuterated pyridine/lithium nitrate deposits. This particular band is difficult to observe unambiguously, as an N_2O_3

absorption, a very weak pyridine absorption, and a very strong deuterated pyridine absorption obscure the region to varying degrees.

The lower frequency ν_{3a} band for $(pyridine)_5 \cdot LiNO_3$ is easily assigned the value of 1327 cm^{-1} by inspection of the spectra for the 42% (Figure 15) and 50% (Figure 16) pyridine/lithium nitrate deposits. The higher frequency ν_{3b} band is much more difficult to determine. Inspection of the spectra for the diffusion experiments of 5% (Figure 22), 10% (Figure 23), and 42% (Figure 24) deuterated pyridine/lithium nitrate deposits, however, yields a value of about 1430 cm^{-1}.

Table II summarizes the results for the solvates.

TABLE II

VIBRATIONAL FREQUENCIES FOR ν_{3a} AND ν_{3b} OF $(PYRIDINE)_n \cdot LiNO_3$

ν_{3a} (cm^{-1})	ν_{3b} (cm^{-1})	Number of Solvent Molecules
1279	1513	n = 1
1289	1497	2
1300	1473	3
1312	1457	4
1327	1430	5
1334	1411	6

The incremental steps that are observed in ν_{3a} and ν_{3b} for

successive pyridine molecules is fairly regular for the first four steps, with about a 10-20 cm^{-1} change between successive ν_3 values. The last two steps have unusual behavior in this regard. For n = 4 to n = 5, the incremental steps of ν_{3a} and ν_{3b} are large compared with those in any of the previous four steps. One rationalization for this unexpected decrease in distortion of the nitrate ion modes when the fifth pyridine molecule is added, is that the addition of the fifth molecule causes the (bidentate) nitrate to switch to a monodentate configuration.

The last step, n = 5 to n = 6, also has peculiar values for the incremental changes in ν_{3a} and ν_{3b}. However, because of the method of sample production, it is reasonable to expect "bulk" effects in the latter stages of solvation - the lack of which made matrix isolation attractive in the first place. Hence, failure to be conclusive about assignments in this concentration range is to be expected, and the assignments in the higher concentration samples must therefore be tentative, and open in interpretation.

Several points may be made regarding previous reports on solutions of lithium nitrate in pyridine.[12a,34a,b] On the basis of the positions and appearance of certain bands in the infrared spectra of lithium salts in pyridine, Popov has proposed that there is no direct contact between ions in dilute solutions of lithium nitrate in pyridine.[34a,b] Other researchers,[12a] however, have reported the mid infrared spectrum for solutions of lithium nitrate in pyridine (at similar concentrations), and a rough comparison of the gross features of this spectrum with the spectra for codeposits of lithium nitrate with pyridine (Figures 29-32) implies the existence of contact ion pairs, if the interpretation given

for the present results is accepted.

Their assignments for the ν_{3a} and ν_{3b} bands of the totally solvated Li-O-N$\lesssim^{O}_{O}$ species, given as 1330 cm^{-1} and 1410 cm^{-1}, compare favorably with the values reported herein for those bands, 1334 cm^{-1} and 1411 cm^{-1}. As the preparative method used in the present work excludes the presence of triplets, no direct comment may be made concerning the absorptions seen at 1354 cm^{-1} and 1440 cm^{-1} in solutions of lithium nitrate and pyridine which have been assigned to the triplets.

Although we cannot refute these latter assignments, it should be noted that the intensity of pyridine bands in this region will make assignments difficult (c.f. Figure 9), particularly near the intense 1439 cm^{-1} band of pyridine. A band is, in fact, seen to grow in intensity at 1358 cm^{-1} when the 5% and 10% pyridine/lithium nitrate samples are annealed (Figures 20 and 21); the annealing spectra of the 5% and 10% pyridine samples (which are not shown) also have a small absorption which grows at 1358 cm^{-1} upon annealing the sample, though not to the same extent as the codeposit samples.

These facts, coupled with the observation that no such bands in this region are visible in the annealing spectra of the 5% and 10% deuterated pyridine samples, leads one to suspect that the bands reported for the triplets at 1354 cm^{-1} and 1440 cm^{-1} are not connected with the nitrate absorption itself, but instead are perturbed or enhanced pyridine bands, linearly related to the lithium nitrate concentration. (Alternatively, the 1354 cm^{-1} band could be caused by crystalline lithium nitrate produced by lower temperatures, and the 1440 cm^{-1} band could be a subtraction artifact, though for the reasons

given above, the former argument is preferred.)

Two difficulties in the reasoning which lead to their assignments should be pointed out. First, they assume that the ν_3 modes for the two ion triplets, $(pyridine)_2Li(NO_3)_2^-$(triplet-1), and $(pyridine)_6Li_2NO_3^+$ (triplet+1), are identical. This seems highly unlikely considering quantum chemical arguments.[4]

Secondly, they assert that the inner sphere solvent molecules can have no effect on the ν_3 modes of the ion pair. The work presented in this thesis, and that of similar previous matrix isolation experiments,[4,7,9] clearly suggests otherwise. In fact this assertion does not seem likely, even considering their own data; with pyridine as solvent they claim the values 1330/1410 cm^{-1} for the unidentate complex of lithium nitrate and the values 1354/1440 cm^{-1} for the bridged triplets, but when acetone is used as a solvent, different values are presented, 1331/1397 cm^{-1} and 1355/1430 cm^{-1}, respectively.

Before leaving the topic of the nitrate bands in pyridine, it is useful to note that the spectra of a solution of tetramethylammonium nitrate in pyridine has a single band for the ν_3 vibration, of half width at half height equal to 39 cm^{-1}.[12a] Since there is no reason to suspect that nitrate will be any more sensitive to distortion by pyridine in low temperature matrices than in room temperature solutions, the distortion of the nitrate by pyridine is probably not significant enough to greatly affect the band assignments presented here.

The Discussion: Pyridine Bands

As only the mid-IR beam splitter of the spectrometer was used, no far-IR spectra of the samples were obtained. As it was, the software

of the computer calculated no spectral points below around 390 cm^{-1}, and the bands near 400 cm^{-1} did not seem especially reliable. We were, therefore, unable to investigate the "cage bands" that have been proposed for totally solvated lithium ions in pyridine, the results of which we are in some disagreement (34a, 34b, 35, and references therein). This was unfortunate, as the advantages that make matrix isolation an attractive tool in the mid-infrared are also operating in the far infrared, namely the production of known samples.

Because of a long waiting time to receive a replacement laser for the interferometer, it was necessary to use a portable He-Ne laser as a substitute, so that work could progress on schedule; this resulted, for some reason, in large noise levels above about 3500 cm^{-1}, and below 750 cm^{-1}, in the spectra taken during that time. The accuracy of bands, and the signal to noise ratios, were all found to be reasonable in the mid-infrared region, however.

The combination of the above factors made analysis of the 750 to 400 cm^{-1} region difficult. Although the bands in this region were not exceptionally consistent, it seems that the upshift reported for the 408 cm^{-1} band of pyridine (to 420 cm^{-1}), and the downshift of the 405 cm^{-1} deuterated pyridine band (to 368 cm^{-1}) seen in solutions with lithium nitrate, is not observed in our samples at the concentrations of pyridine and lithium nitrate used (for typical values of this band see 34a, 36, 37).

As for the shift of the pyridine band at 604 cm^{-1} to about 620 cm^{-1}, seen in solutions,[34c,36] and compounds,[35] with lithium nitrate, this was not observed. However, the presence of water shifts the

pyridine band to 612-613 cm^{-1}, as reported earlier.[38,39]

The upward shift of the 754 cm^{-1} absorption[36] of pyridine, when lithium nitrate is a solute, seemed to be noticeable as a side band in some samples, but this was not especially convincing.

The widely reported upshifted 991 cm^{-1} pyridine band,[34c,36,37] due to the presence of lithium salts in solution, was apparently intense enough[36] to be observed in our samples. If the spectrum of a "glassy" codeposit of lithium nitrate and pyridine is inspected (Figure 27), the upshifted band appears at 1003 cm^{-1}, precisely matching the value reported for solutions (the intensity seen in Figure 27 at 999 cm^{-1} is an upshift of the 991 cm^{-1} pyridine band due to a water/pyridine interaction,[38,39] as demonstrated in Figure 26). It is interesting to compare the "glassy" codeposit value with the value obtained from the spectrum of a 5% pyridine/lithium nitrate deposit, i.e. 1008 cm^{-1}. Also seen in the codeposit curves of Figures 25 and 27 is extra intensity on the high frequency side of the 1031 cm^{-1} band of pyridine — how much of this is due to the ν_1 nitrate mode of the solvated ion pair is not clear.

It has been reported[34c,36,37] that the pyridine band at 1581 cm^{-1} shifts upward, in the presence of lithium salts as solutes, to about 1597 cm^{-1}, and the intensity of the shifted band is apparently quite high.[36] Unfortunately, in the argon isolation experiments, where water contamination is practically an inevitable occurrence, the bands for the H_2O•pyridine interaction (1591 cm^{-1}),[39] and the water monomer and dimer bands ($\sim$1600 cm^{-1}),[28] made unambiguous identification of frequency shifts impossible. In the codepositions of lithium nitrate and 100% pyridine, there was apparently inadequate amounts of ion pair in the

sample to produce a band of sufficient size to see, in competition with the 1599 cm^{-1} band of pyridine. However when the subtraction of the pyridine spectrum from the spectrum of codepositions of lithium nitrate and pyridine was attempted, these attempts invariably failed in such a way as to indicate upshifts of the pyridine 1441 cm^{-1} and 1581 cm^{-1} absorptions.

Lastly it is noted that the spectrum of pyridine in argon is concentration dependent due to the formation of dimers and multimers.[33,39,40] The differences from the monomer spectra are small (e.g. 1 to 3 cm^{-1} shifts), and were not considered important in the analysis of the data.

Solvation Studies, 1,10-Phenanthroline

The Data

Shown in the bottom curve of Figure 28 is the spectrum for a "glassy" deposit of 1,10-phenanthroline at 77K, while the upper curve is the spectrum of the same sample after 12 hours at room temperature. This sample is exceedingly dry as judged by the lack of any bands in any region of the spectrum which could be attributed to water.[28]

Shown in the bottom curve of Figure 29 is the spectrum of a codeposit of phenanthroline and lithium nitrate taken at 77K, while the upper curves are the spectra of this sample as it was annealed at increasing temperatures. An expanded region of the spectra for this sample, with more intermediate temperatures, is given in Figure 30.

A codeposit sample of greater nitrate concentration than that of the sample of Figure 29 is shown in Figure 31. An expanded region of

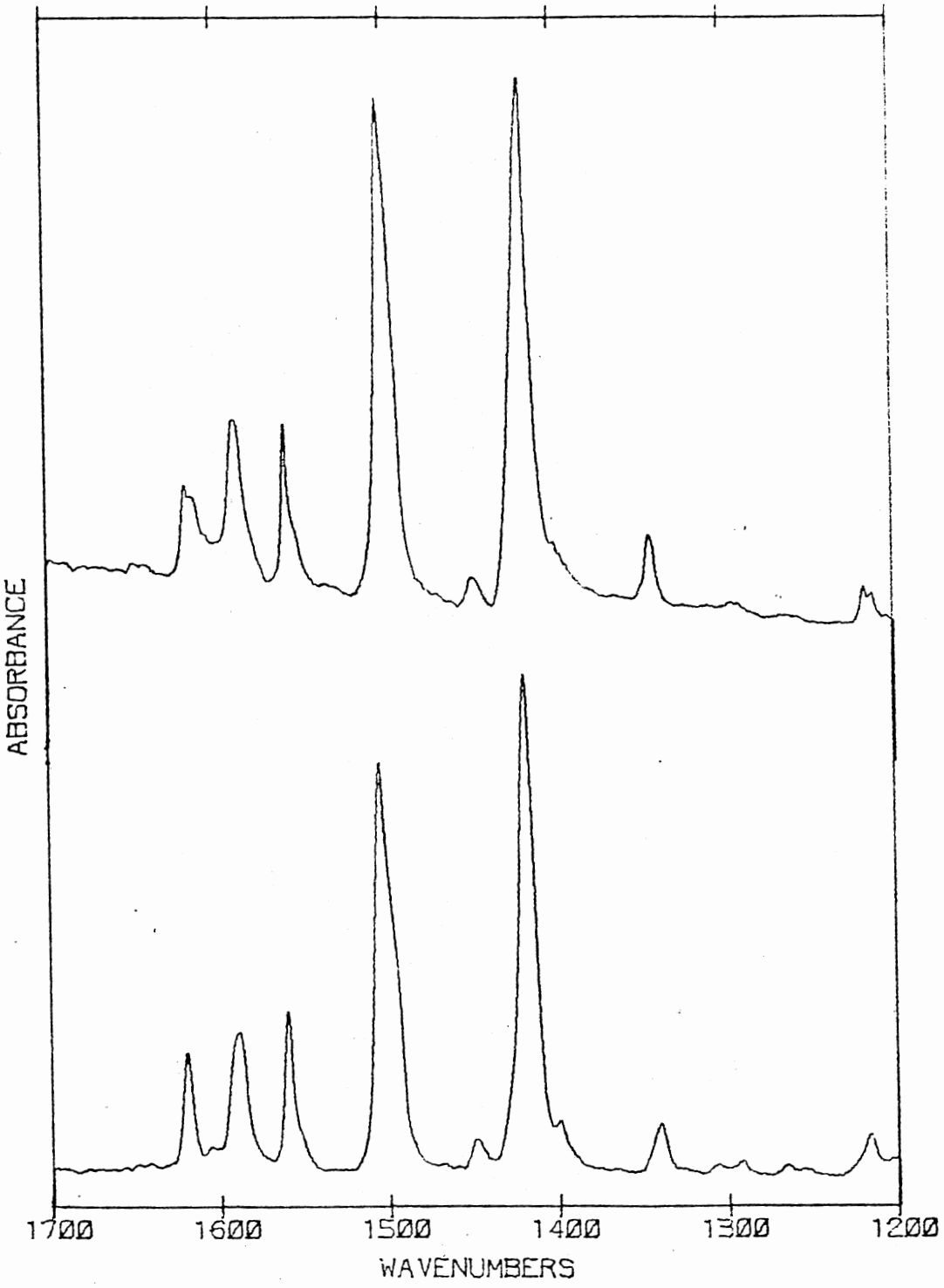

Figure 28. Spectra of "Glassy" 1,10-Phenanthroline (Lower Curve) at 77 K, and of a Polycrystalline Film Obtained from Warming the Sample (Upper Curve)

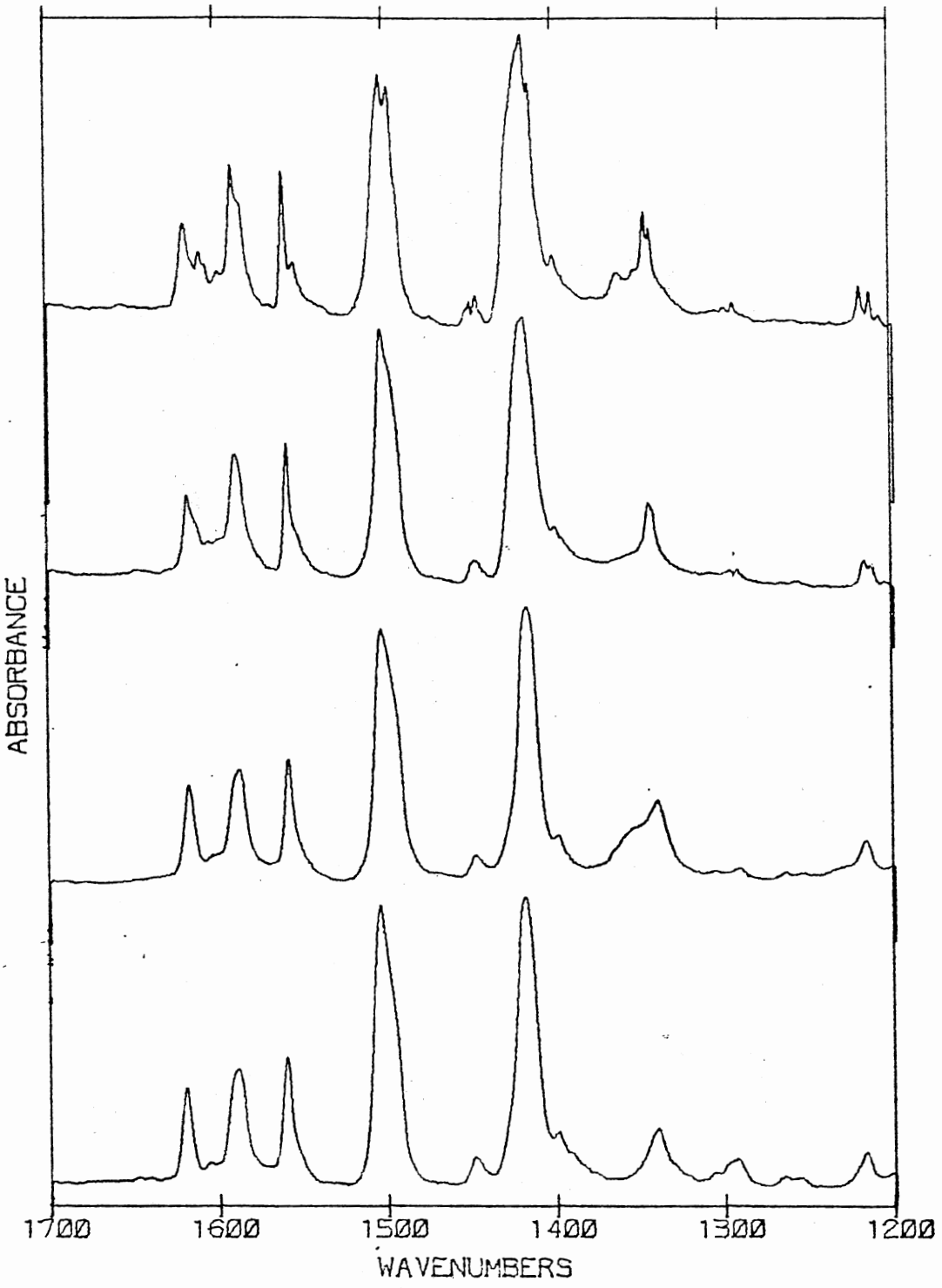

Figure 29. Spectra Showing the Annealing Effect for a Codeposit of Lithium Nitrate and 1,10-Phenanthroline: Lower Curve is the Original Sample at 77 K, and each Succeeding Upper Curve is the Sample at a Higher Temperature

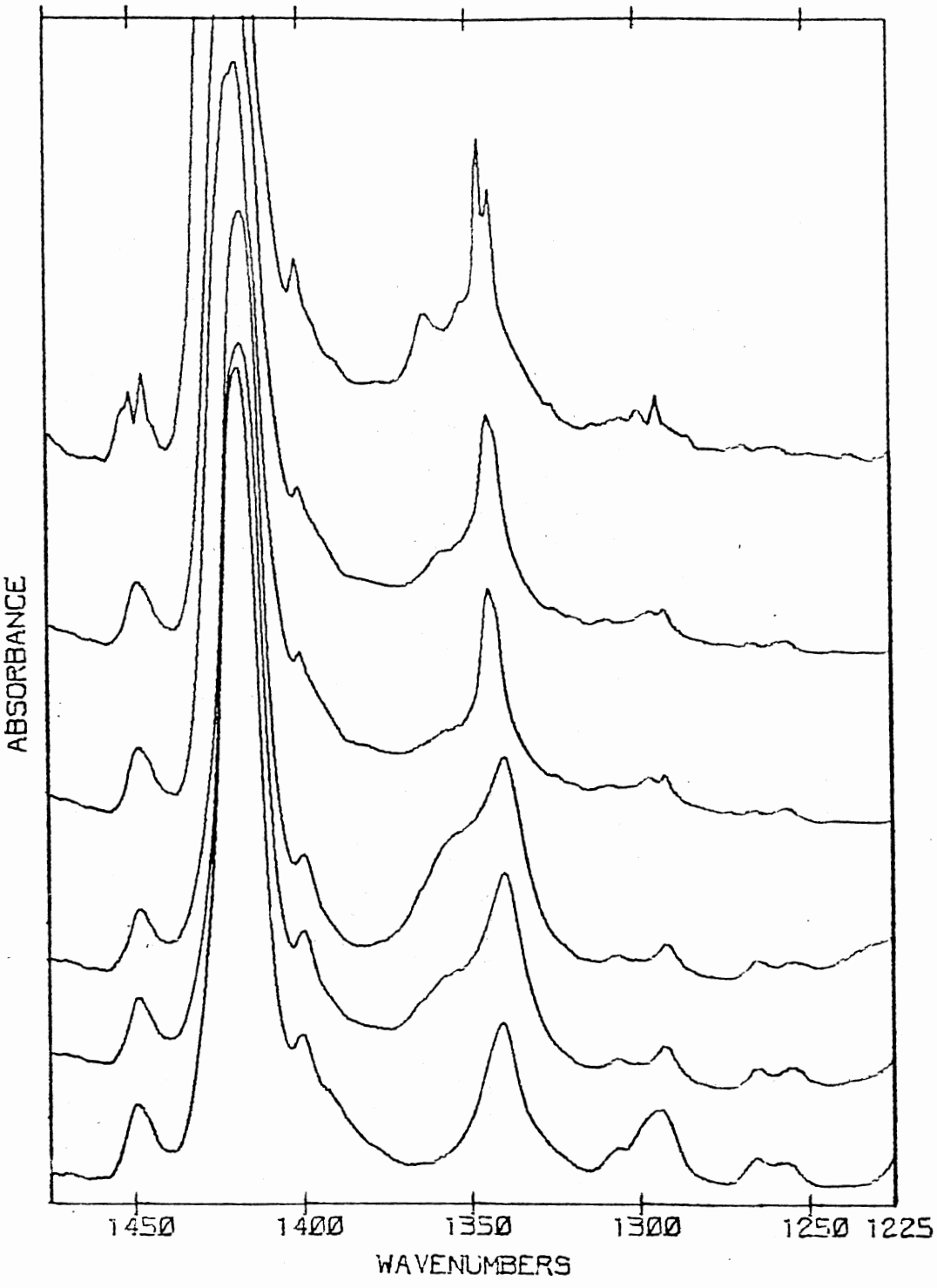

Figure 30. Spectra Showing Greater Detail of the Annealing Effect for a Codeposit of Lithium Nitrate and 1,10-Phenanthroline: Lower Curve is the Original Sample at 77 K, and Each Succeeding Upper Curve is the Sample at Higher Temperatures

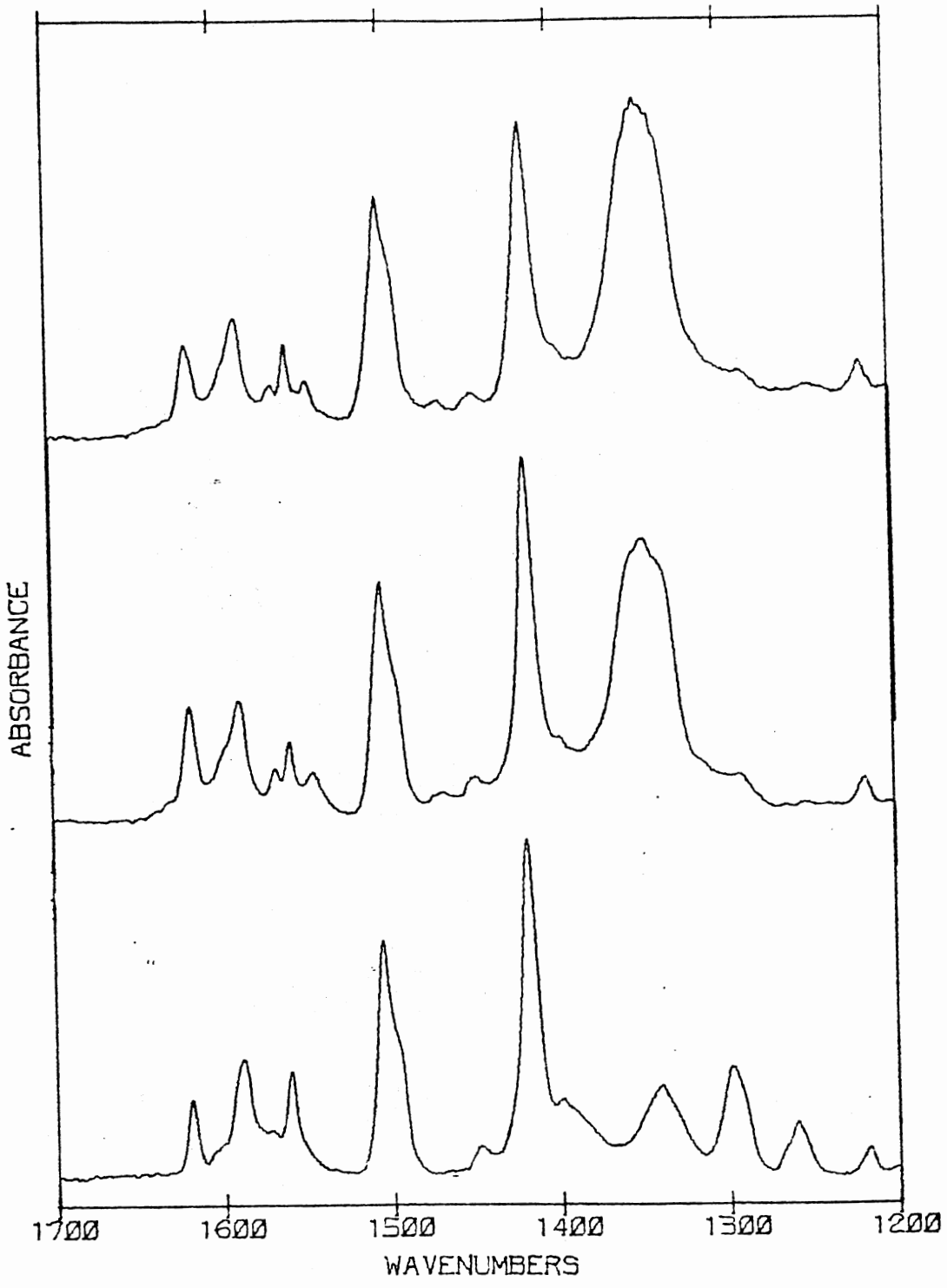

Figure 31. Spectra Showing the Annealing Effect for a Codeposit of 1,10-Phenanthroline and a Large Amount of Lithium Nitrate: Lower Curve is the Original Sample at 77 K, and Each Succeeding Upper Curve is the Sample at Higher Temperatures

the spectra of this sample, with more spectra of intermediate temperatures, is given in Figure 32.

Figures 33 through 37 show the argon isolation experiments with phenanthroline and lithium nitrate. All argon isolation samples were annealed, to permit the study of diffusion effects on the sample. Annealing the lithium nitrate/phenanthroline/argon samples properly was difficult, as the temperature necessary to promote diffusion was close to the vaporization temperature of argon under vacuum conditions.

The Discussion: Nitrate Bands

As may be seen from Figure 28, the spectrum of phenanthroline is similar to that of pyridine, but assignments of bands for the nitrate ν_3 values of solvates will be more difficult, as the deuterated compound was not easily available as was the case for pyridine. From Figure 28 it may also be seen that the infrared spectrum of polycrystalline phenanthroline is much like that of "glassy" phenanthroline in the region of interest, except for a small increase in intensity upon crystallization on the low frequency side of the strong 1419 cm^{-1} band.

In the case of the codeposits of lithium nitrate and phenanthroline (bottom curves of Figures 30 and 32), the high frequency ν_3 band of the totally solvated ion pair is rather difficult to determine accurately, but the lower frequency ν_3 peak can be assigned the value of 1340 cm^{-1} with some degree of confidence. Using this value, and the values for ν_3 in the case of total solvation by pyridine (1334, 1411), one would estimate that the phenanthroline high frequency absorption for ν_3 would be near 1404 cm^{-1}; since the ν_{3b} intensity is difficult to locate any

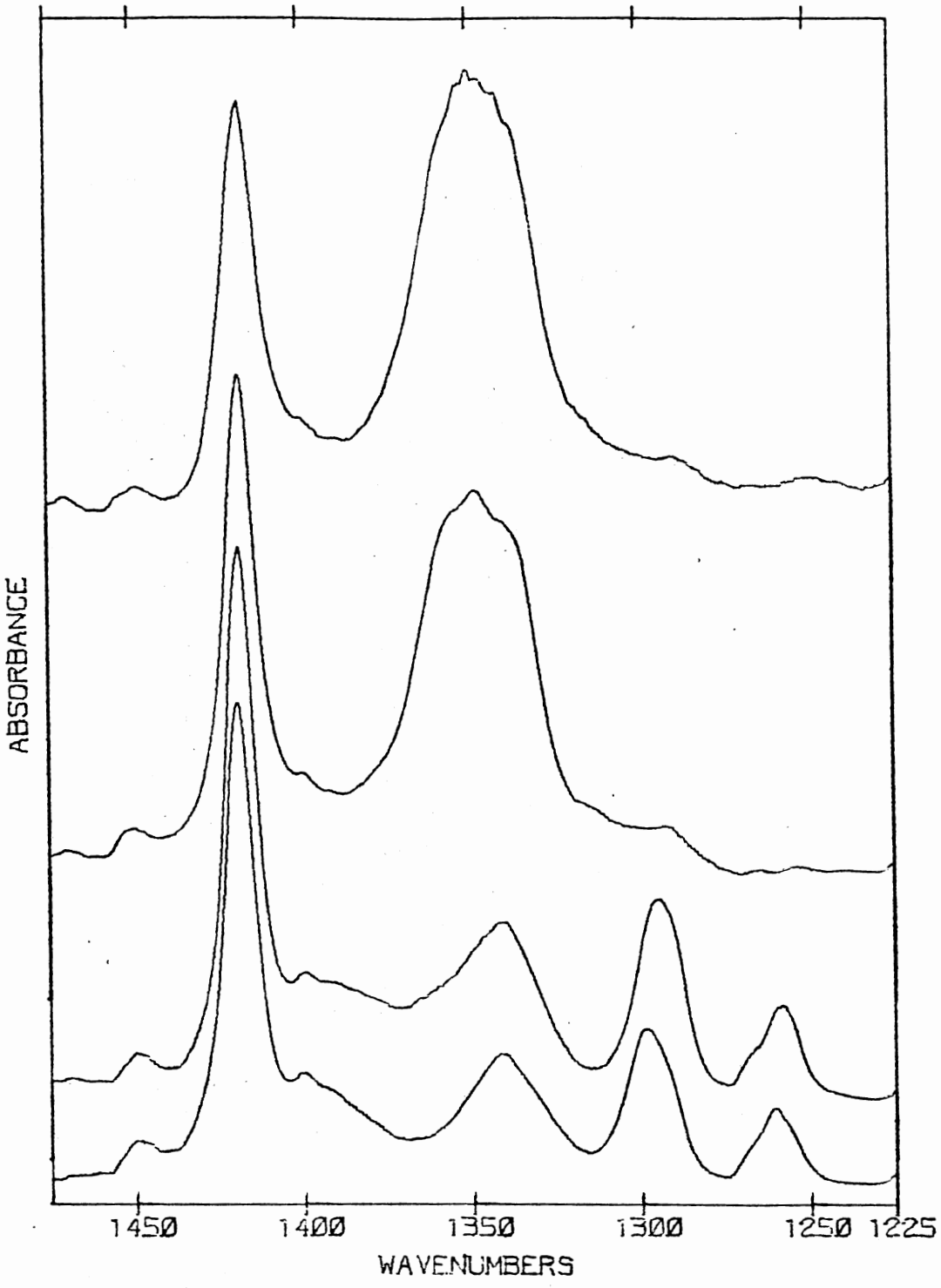

Figure 32. Spectra Showing Greater Detail of the Annealing Effect for a Codeposit of 1,10-Phenanthroline and a Large Amount of Lithium Nitrate: Lower Curve is the Original Sample at 77 K, and Each Succeeding Upper Curve is the Sample at Higher Temperatures

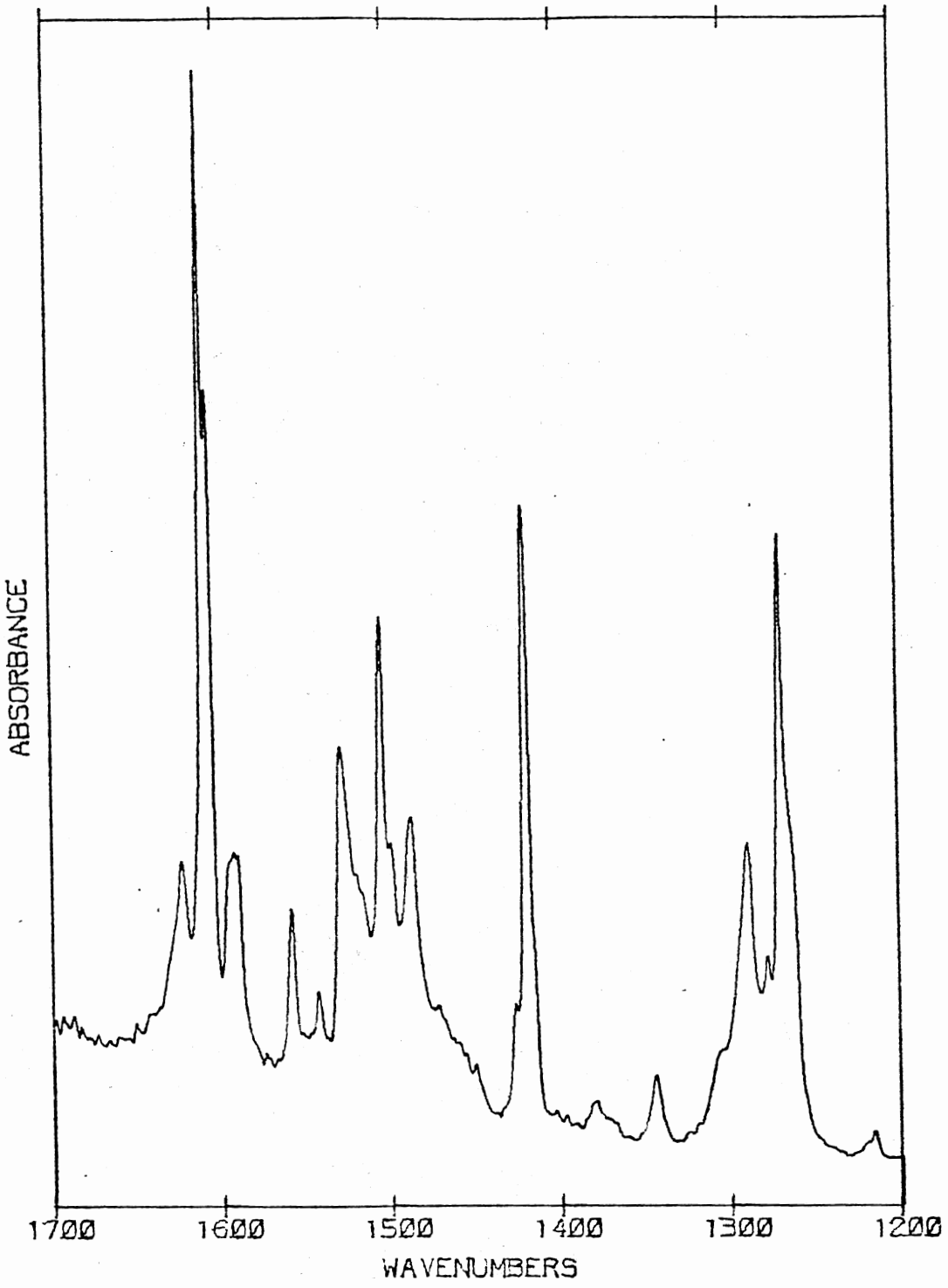

Figure 33. Spectrum of Codeposit of Lithium Nitrate and 1,10-Phenanthroline, and Argon at 10-15 K

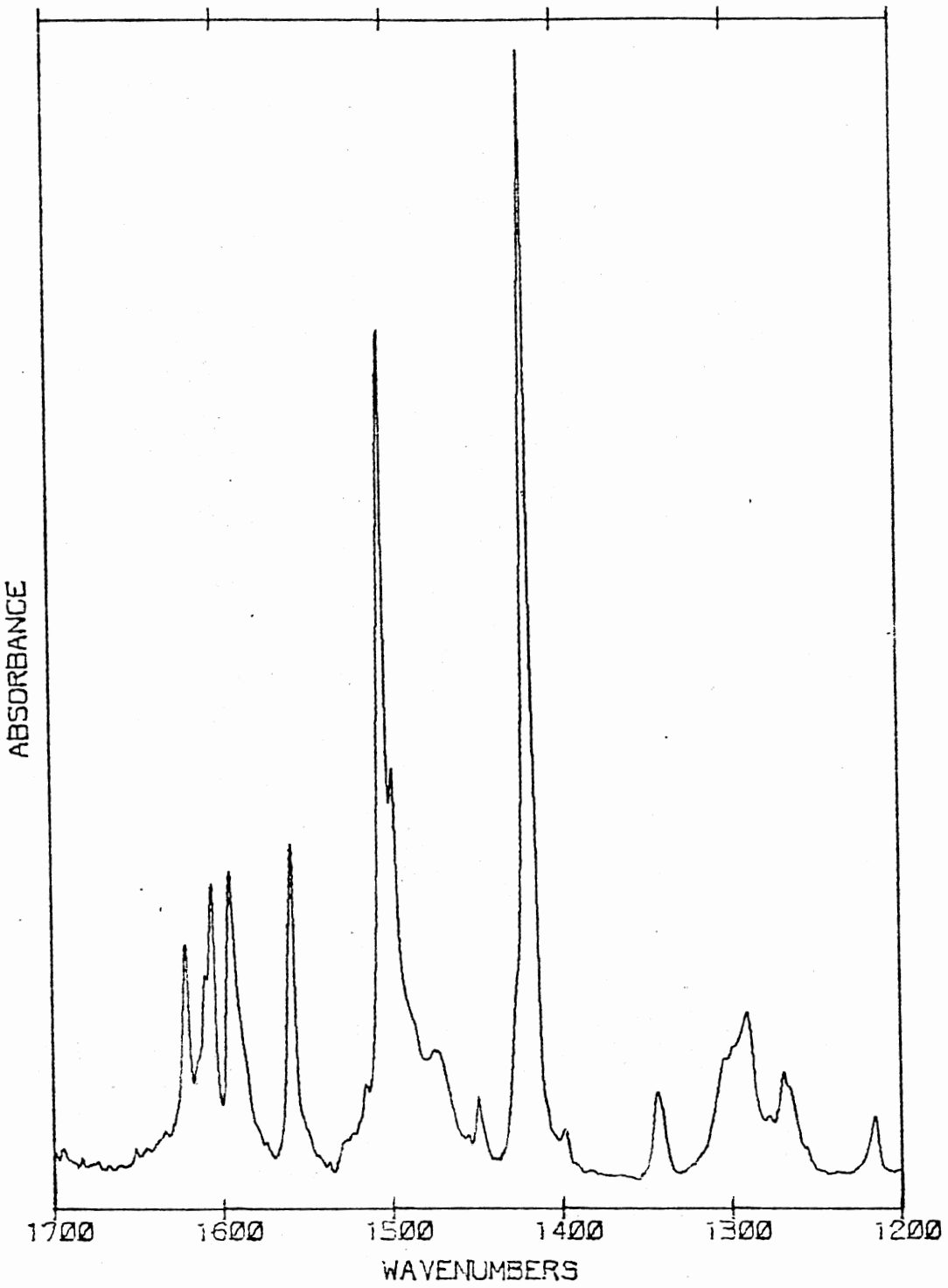

Figure 34. Spectrum of a Codeposit of Lithium Nitrate, 1,10-Phenanthroline, and Argon at 10-15 K

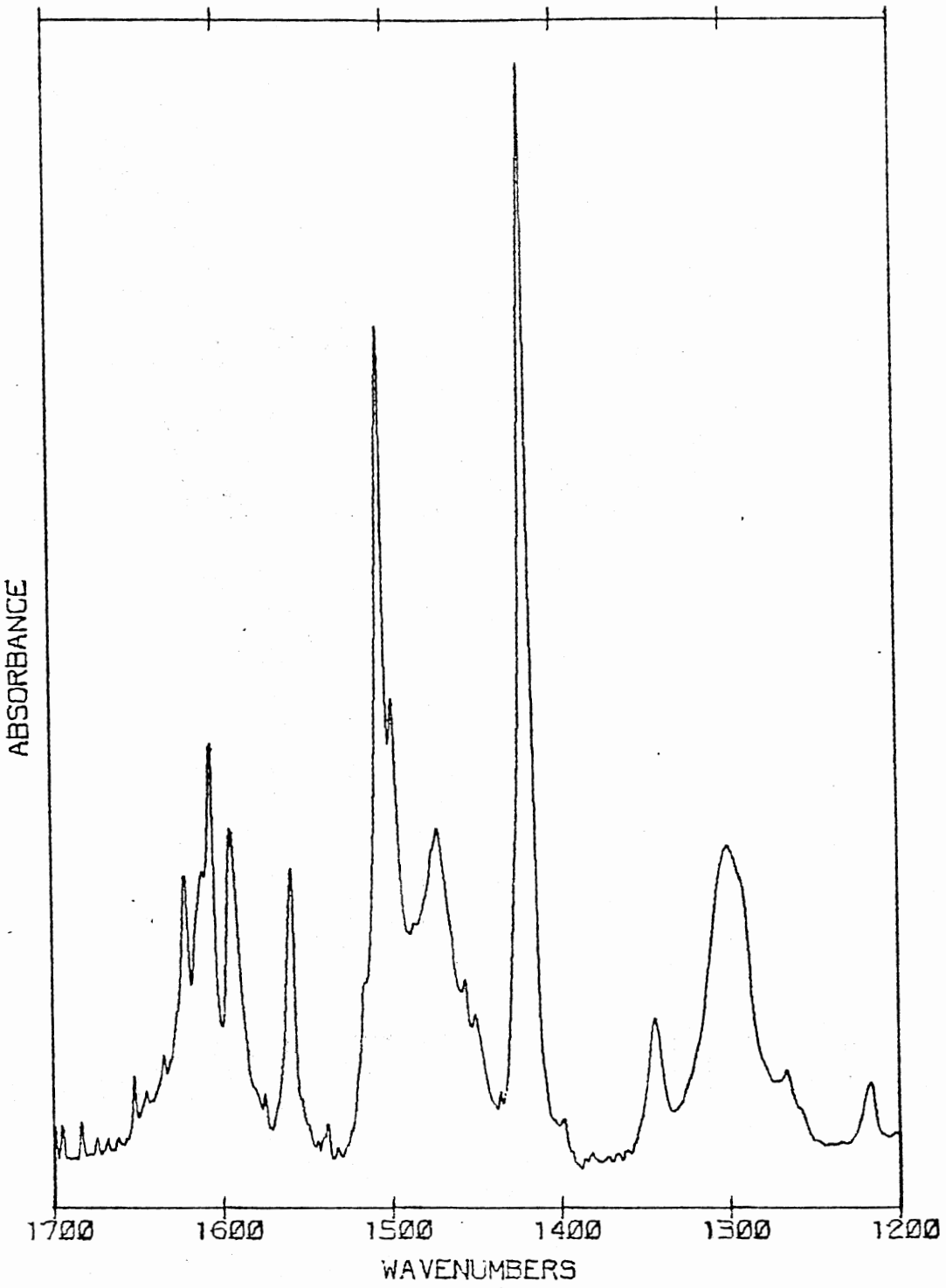

Figure 35. Spectrum of a Codeposit of Lithium Nitrate and 1,10-Phenanthroline, and Argon at 10-15 K

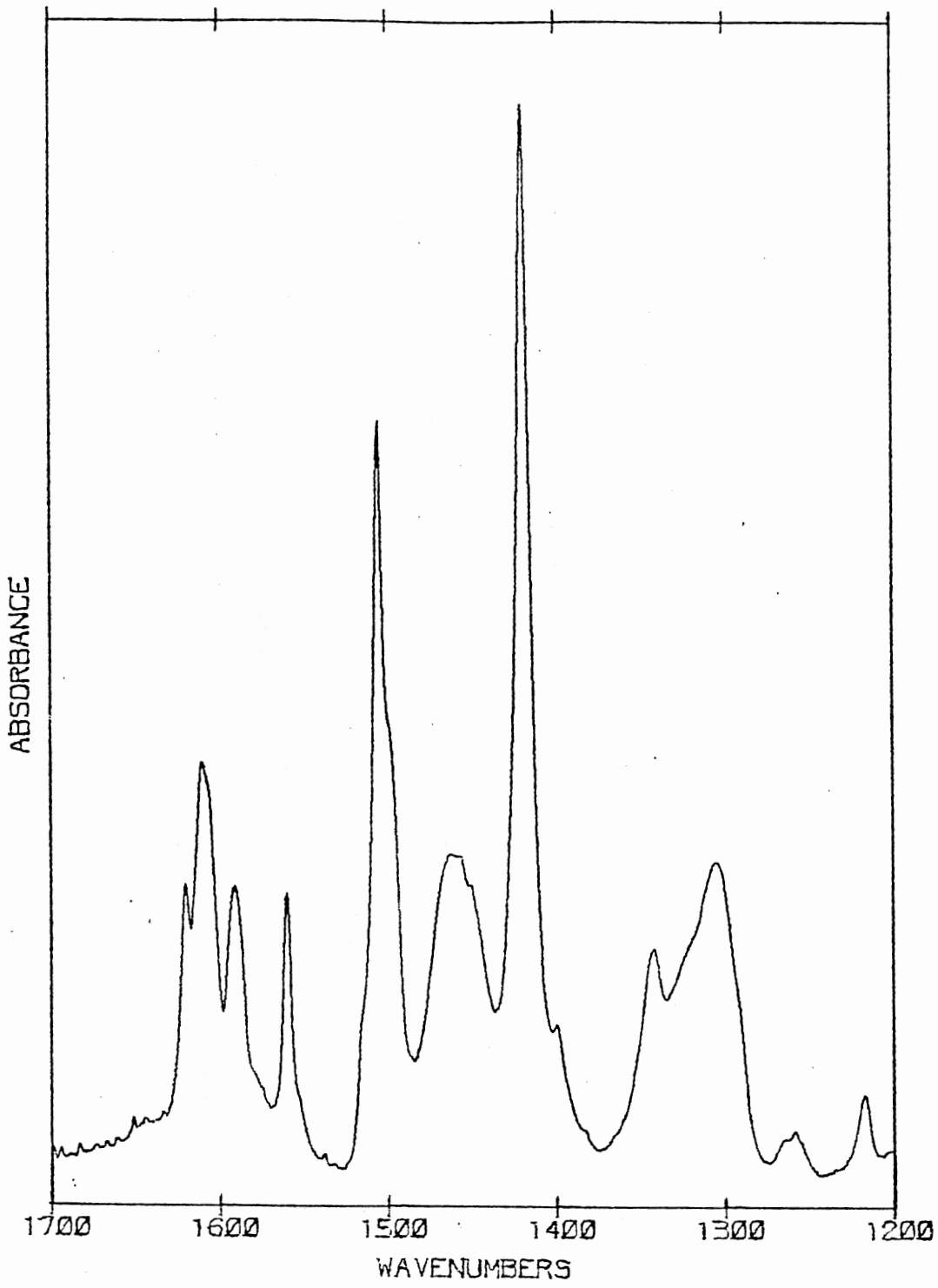

Figure 36. Spectrum of a Codeposit of Lithium Nitrate and 1,10-Phenanthroline, and Argon at 10-15 K

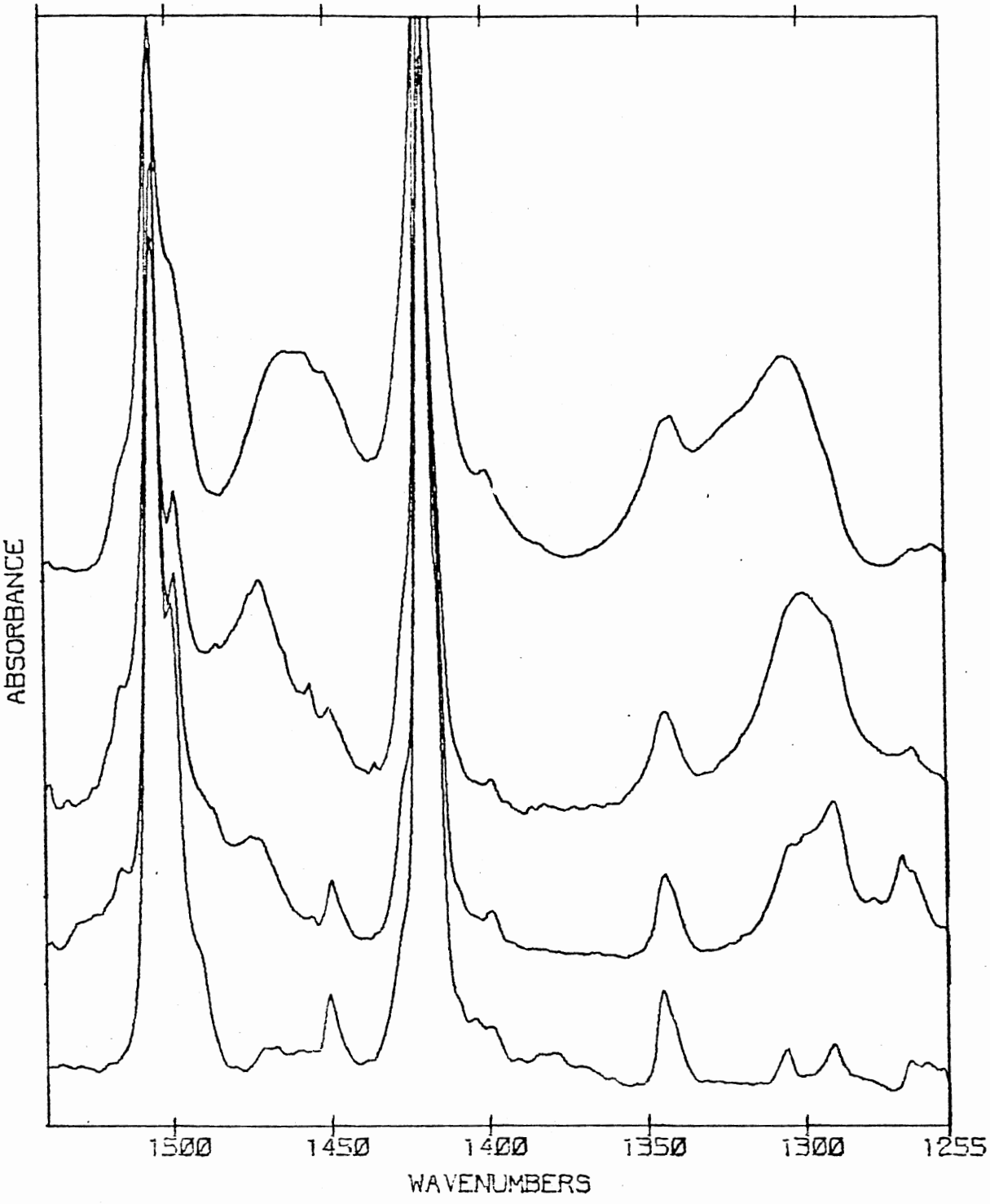

Figure 37. Spectrum of Isolated 1,10-phenanthroline at 10-15 K, and Figures 34-36, on Expanded Scale

more precisely, the value of 1404 cm^{-1} is suggested for ν_{3b}.

The effects of annealing lithium nitrate and phenanthroline codeposits is markedly interesting, and a typical example of the effects is seen in Figure 30. As the sample is warmed, a band of medium intensity grows at 1358 cm^{-1}. Concomitant with this, if such an observation may be trusted, there is a weakening of intensity on the low frequency side of the 1419 cm^{-1} phenanthroline band (i.e. near the ν_{3b} value of 1404 cm^{-1}), so apparently the growth is caused by the nitrate.

The small band near 1300 cm^{-1}, which disappears at about the same time, is caused by N_2O_3.[49] The presence of N_2O_3 does not affect the results for the annealing matrix, as codeposit samples not containing N_2O_3 are seen to give virtually identical spectra to those of Figure 30. The reason spectra for a sample contaminated with N_2O_3 is presented in place of one without N_2O_3 is that an exceptionally large number of intermediate spectra were taken for this particular sample, providing a continuity not available in any one of the other samples.

When the sample crystallizes (fourth curve up from the bottom in Figure 30), the band intensity at 1358 diminishes. At the same time there is a slight increase in the general absorption between 1350 cm^{-1} and 1400 cm^{-1}, though as noted before, this also happens to a small extent when a glassy deposit of pure phenanthroline cryatallizes. When the sample is completely crystallized (top curve of Figure 30) the final band structure near 1350 cm^{-1} suggests there are bands at 1363 cm^{-1}, 1337 cm^{-1}, and 1350 cm^{-1}, as well as the phenanthroline doublet at approximately 1344 cm^{-1}. Evidently there are two sites that nitrate occupies in this crystalline sample; one undisturbed D_{3h} nitrate

(ν_3 = 1350 cm^{-1}), and one distorted nitrate (ν_{3a} = 1337 cm^{-1}, ν_{3b} = 1363 cm^{-1}).

When a sample more concentrated in lithium nitrate is studied, the annealing spectra (Figures 31 and 32) give results complementary to those obtained from Figure 30. The sample did not seem to crystallize at any one single temperature, and changes in bands indicative of crystallization were evident at lower temperatures than those of the samples less concentrated in lithium nitrate. Apparently more isolated conditions than those of concentrated samples are necessary to observe the rapid disappearance of the 1358 cm^{-1} band, as seen in Figure 30.

The matrix isolation data for phenanthroline and lithium nitrate provides fairly strong confirmation of the assigned ν_3 values for pyridine shown in Table II. A priori, one expects that phenanthroline will give values for ν_3 peaks at frequencies similar to the n = 2, 4, and 6 cases of pyridine (Table II). By and large, this appears to be what is observed.

In Figures 33-34 (or 37), for example, the first ν_3 peaks seen for phenanthroline/lithium nitrate/argon mixtures are at 1289 cm^{-1} and 1488 cm^{-1}, which may be compared with the values at 1289 cm^{-1} and 1497 cm^{-1} that were seen in the n = 2 solvate case of pyridine. In both figures very little absorption intensity is seen near the n = 1 values of the pyridine solvate, 1279 cm^{-1} and 1513 cm^{-1}. The small bands that are seen at 1279 cm^{-1} and 1520 cm^{-1} are presumed to be primarily due to the ν_{3a} and ν_{3b} modes of $H_2O{\cdot}LiNO_3$ as it is apparent from the 1600 cm^{-1} region[28] that water is in sufficient abundance to produce hydrates of the ion pair.

To be most consistant with the pyridine solvation work, the curves

of Figures 35-36 (or 37) must be interpreted as having ν_3 peaks for the bis phenanthroline complex at 1308 cm^{-1} and 1457 cm^{-1}, which compares favorably with the ν_3 values of 1312 cm^{-1} and 1457 cm^{-1} seen for the $(pyridine)_4 \cdot LiNO_3$ complex. There is, however, some unexplained intensity near 1300 cm^{-1} and 1474 cm^{-1}, for which no plausible explanation exists, within the context of the correlations expected between the ν_3 peaks for the solvates of pyridine and phenanthroline.

The assignment of these "unexplained" bands to correspond to yet another phenanthroline coordination, is clearly an unattractive alternative from several points of view, and second sphere effects for a phenanthroline complex of a lithium nitrate ion pair do not seem likely considering the charge on the lithium ion and the size of the phenanthroline molecule. If the solvent distortion of the nitrate is disregarded on the basis of the spectra of tetramethylammonium nitrate in pyridine,[12a] one has exhausted all of the less exotic explanations for this unexpected intensity.

Table III summarizes the results of this section, disregarding the unexpected intensity, as is most consistant with the pyridine work.

TABLE III

VIBRATIONAL FREQUENCIES FOR ν_{3a} AND ν_{3b} OF $(PHENANTHROLINE)_n \cdot LiNO_3$

ν_{3a}	ν_{3b}	Number of Solvent Molecules
1289	1488	n = 1
1308	1457	n = 2
1340	1404	n = 3

The Discussion: Phenanthroline Bands

The modes of phenanthroline are sensitive to whether its nitrogens are coordinated in an ion, or molecule, and this is well documented in the case of crystalline compounds.[13b-c,41-48] Analysis of the spectra for "glassy" codeposits of lithium nitrate and phenanthroline indicate that the modes of phenanthroline in "glassy" deposits are not particularly sensitive to the presence of lithium nitrate. There are only minor changes, with the apparent upshifts of the 1551 cm^{-1} and 1589 cm^{-1} bands (Figure 29 and 31), and the appearance of a small band at 715 cm^{-1} being the two most notable.

When the sample crystallized, however, the presence of lithium nitrate had a profound effect upon the bands of phenanthroline. The changes which occurred were dependent upon the amount of lithium nitrate in the sample. In samples of low nitrate concentration there was evidence of upshifts in frequencies of absorptions, or splittings, particularly in, but not confined to, the 700-1000 cm^{-1} region. In samples of higher concentration, most of the bands would broaden, sometimes diminish in intensity, or "wing" on the low frequency side, when the samples crystallized. Of the more noticeable band changes in the concentrated samples was the growth and shift of a band at 716 cm^{-1} to 713 cm^{-1}, the growth of a new band at 628 cm^{-1}, and the growth of an unusual multiplet near 1550 cm^{-1}.

Overall, the changes in the infrared bands of phenanthroline depended upon the concentration of lithium nitrate, and upon the phase of the sample (for example, the 993 cm^{-1} band of phenanthroline which is reported to be sensitive to coordination does not even appear until

crystallization of the sample). These two factors, concentration of the lithium nitrate, and phase of the sample, were interrelated, of course, and this complicated the interpretation of the data.

Solvation Studies, 2,2'-Bipyridine

The Data

Shown in Figure 38 are the spectra for a deposit of bipyridine (bottom curve), and for a codeposit of bipyridine and lithium nitrate (top curve). Figure 39 contains the spectra for a codeposit of lithium nitrate and bipyridine (bottom curve), and for the annealed sample (upper curves). An expanded view of Figure 39 is given in Figure 40. For comparison with these "annealed" sample spectra, in Figure 41 we have the spectra of "glassy" bipyridine (bottom curve), and of the polycrystalline film which results from the same sample. Figure 42 contains the spectrum of pure bipyridine (bottom curve), of a codeposit of bipyridine and lithium nitrate (middle curve), and of another codeposit with a much higher concentration of lithium nitrate than the sample of the middle curve (top curve).

Most of the large absorptions (in the codeposit spectra) near 1300 cm^{-1} is N_2O_3 which is verified by a peak (not shown in any of the spectra) at 1854 cm^{-1}.[49] All of the bipyridine, and codeposit lithium nitrate/bipyridine samples were exceedingly dry, as judged by the lack of any absorptions due to water.[28]

The Discussion: Nitrate Bands

In comparison to the amount of information one is able to derive

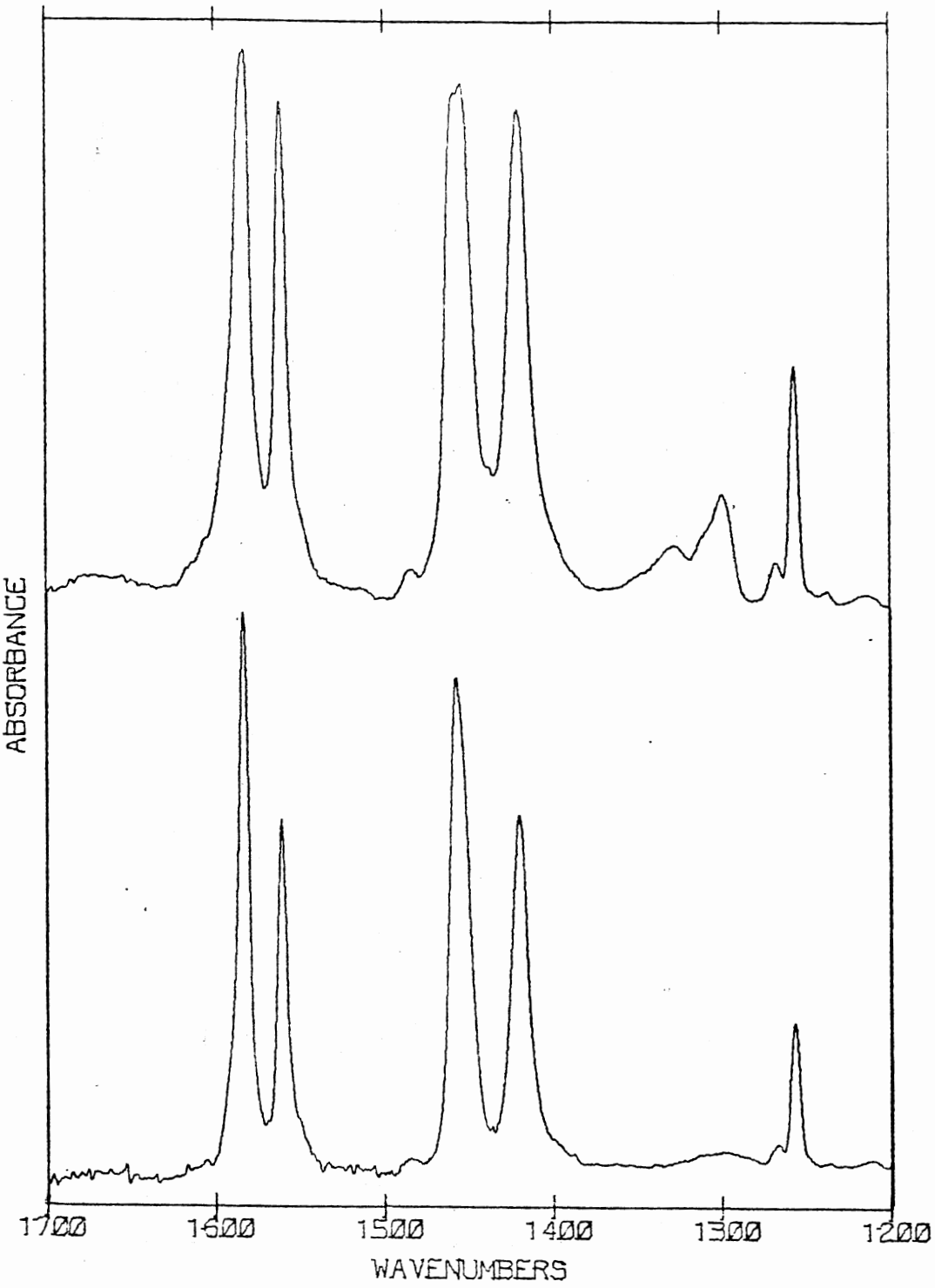

Figure 38. Spectra of "Glassy" Bipyridine (lower Curve), and of a Codeposit of Bipyridine and Lithium Nitrate, at 77 K

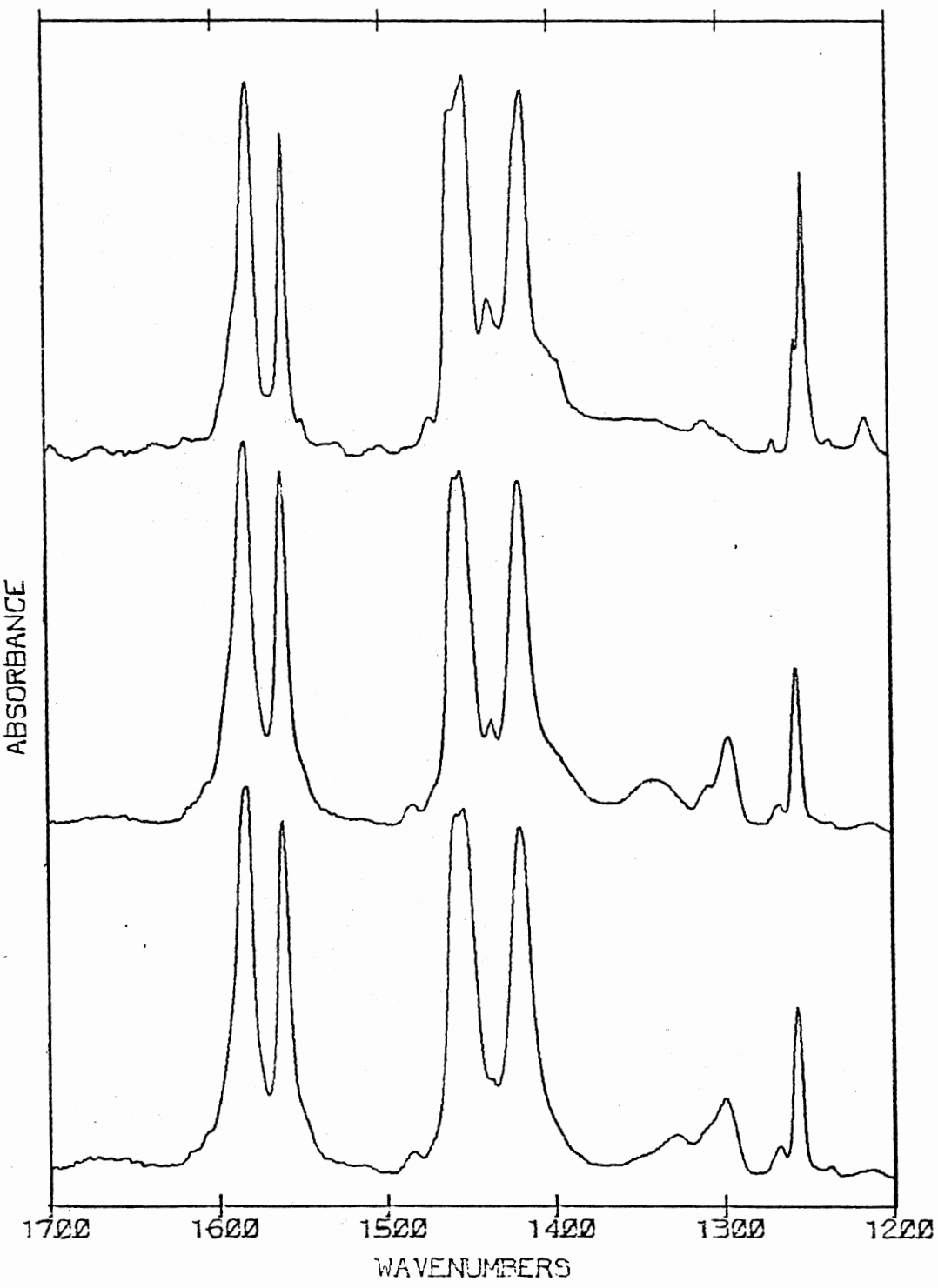

Figure 39. Spectra Showing the Annealing Effect for a Codeposit of Lithium Nitrate and Bipyridine, at 77 K: Lower Curve is the Original Sample at 77 K, and Each Succeeding Upper Curve is the Sample at Higher Temperatures

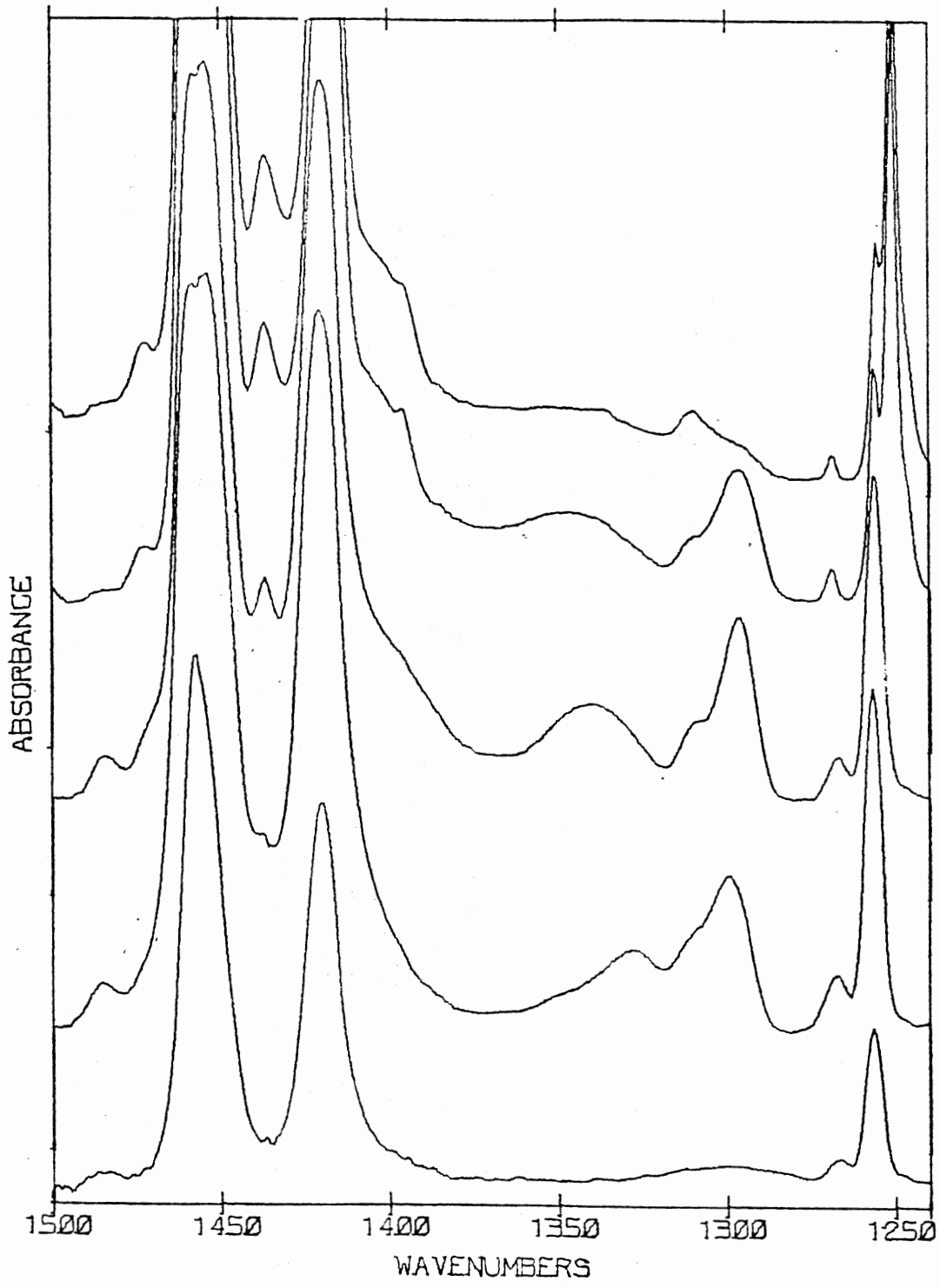

Figure 40. Spectra Showing Greater Detail of the Annealing Effect for a Codeposit of Lithium Nitrate and Bipyridine: Lower Curve is Bipyridine, Second Curve up is Codeposit, both at 77 K, Each Succeeding Upper Curve is the Codeposit at Higher Temperatures

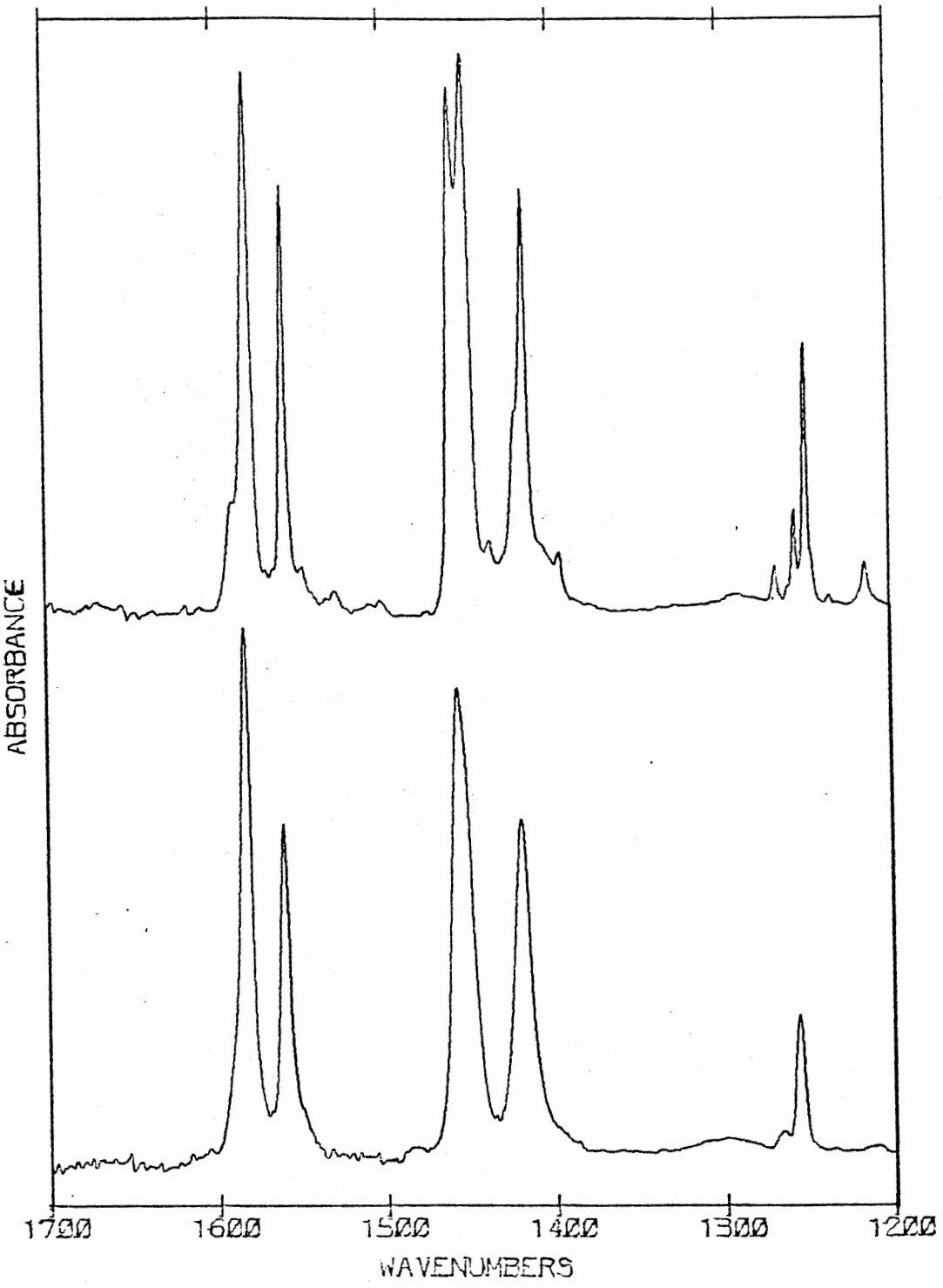

Figure 41. Spectra of "Glassy" Bipyridine at 77 K (Lower Curve), and of a Polycrystalline Film Obtained from Warming the Sample (Upper Curve)

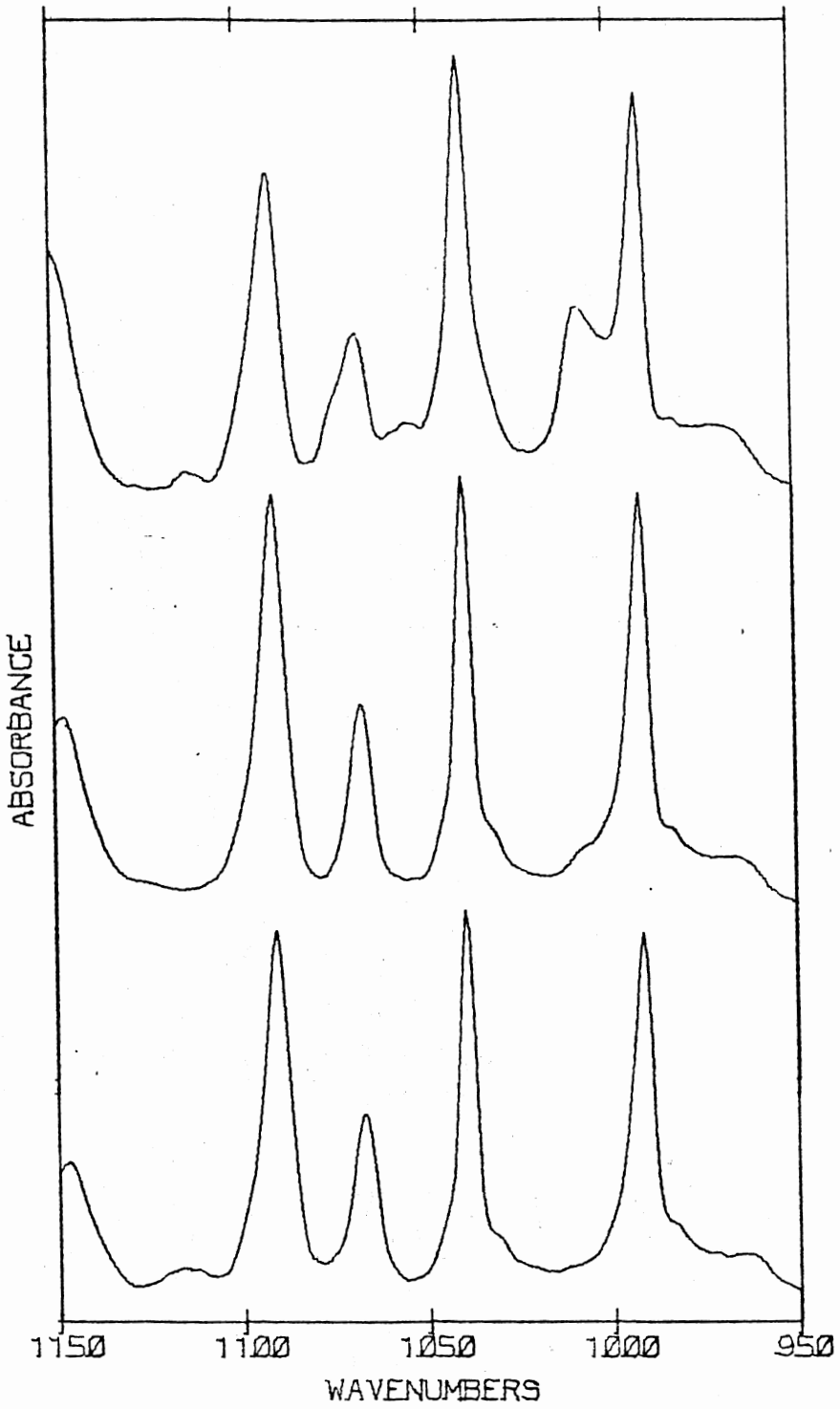

Figure 42. A Selected Region of the Spectra for Bipyridine, and Codeposits of Lithium Nitrate and Bipyridine, at 77 K: The Bottom Curve is of Bipyridine, and Each Succeeding Upper Curve is a Codeposit of Increasing Concentration of Lithium Nitrate

from the argon dilution work of pyridine, and 1,10-phenanthroline, the information obtained from codeposits of lithium nitrate and bipyridine can only be limited. However, some useful information is obtained.

Since it is known that bipyridine(g) has the planes of its aromatic rings at a 30^{o} angle from each other,[50] it might be assumed that, upon codeposition with lithium nitrate, the complex $LiNO_3 \cdot (bipy)_x$ may settle into the matrix with only one half of a bipyridine coordinated. Presumably this is what is seen in Figure 38 (or the second curve up in Figure 40), where the lower frequency ν_3 peak which predominates over all the other lower frequency ν_3 peaks is the one at 1327 cm^{-1} (the values of the higher frequency peaks, 1400-1490 cm^{-1}, can not be determined due to interfering bands of bipyridine). With reference to the interpretation given for the argon dilution work of pyridine and 1,10-phenanthroline, this band corresponds to two bipyridine molecules fully coordinated to an ion pair (which has a monodentate nitrate), plus one bipyridine molecule with only one of it's nitrogens coordinated.

Upon warming the codeposit sample (Figure 40), the first notable change is that the 1327 cm^{-1} absorption is replaced by a band near 1340 cm^{-1}. Given the fact that the bandwidths of bipyridine do not change much during this time, and that this shift occurs before crystallization of the major component of the matrix (bipyridine), it is logical to suspect the shift from 1327 cm^{-1} to 1340 cm^{-1} is due to the rotation and coordination of the unchelated ring of the bipyridine which only half chelated upon deposition.

When first signs of crystallization appear (fourth curve up from the bottom in Figure 40), there appears to be only a broad absorption

near 1347 cm^{-1}, and apparently some of the N_2O_3 has left the lattice (as judged by the diminished peak at 1300 cm^{-1}). Further warming is seen to give a very broad absorption due to nitrate, and allows the N_2O_3 impurity to completely leave the sample (fifth curve up from the bottom in Figure 40). It is interesting to compare the relative energies between the 1327 cm^{-1} to 1340 cm^{-1} shift, and the thermal energy that was necessary for the N_2O_2 to escape the lattice (i.e. a small barrier for a torsional bipyridine motion, previously calculated ab initio for the gas phase to be <38. kJ/mol,[50] vs a larger translation energy necessary for N_2O_3 to escape the lattice).

Though a direct correspondence does not exist, it is natural to compare our results with solution results. Popov has studied the solvation (of what are apparently) ion pairs in various solvents.[51] The solvent used for dissolution of the bipyridine and $LiClO_4$ was nitromethane; nitromethane has a dielectric constant of 35.87, but previous work has implied that ion pairs are formed in the solvent.[52] This implies that the species referred to as $Li(bipyridine)_2^+$ is actually $Li(bipyridine)_2(O_2ClO_2)$, giving a total coordination number of at least five, and possibly six. In light of the different situations in which the complex finds itself in the case of room temperature solution work vs matrix isolation work, the difference in coordinations numbers is not sufficiently different to warrant skepticism.

The Discussion: Bipyridine Bands

As with the other amine analogs, the spectra of bipyridine itself[53] may be expected to undergo modifications when it coordinates

to a lithium nitrate ion pair. So, in as far as arguments from crystalline compounds may be applied to the "glassy" phase, the following is further evidence of coordination:

(a) There are reports of the appearance of a moderately intensive band near 1305 to 1320 cm^{-1} when bipyridine or phenanthroline binds to a transition metal, or rare earth metal, ion (see references 13b, and 54-56 for typical results). However, for the ion of interest, Li^{+}, this "new" band was not reported for the (apparently) mixed crystals of $Li(phen)_xClO_4$,[13b] while no infrared spectrum has been obtained for the compound LiSCN:bipy:H_2O, 1:1:½.[13a]

It is interesting to note, therefore, that a close inspection of the spectra of the annealed codeposits (figures 39 or 40) reveals that a small band appears at 1310 cm^{-1}, in addition to the bands expected in this region due to the nitrate related absorptions. This is most apparent in the spectra of the annealed codeposits, where the 1310 cm^{-1} absorption persists long after the nitrate absorptions have "washed out" into a broad band.

(b) The bands of bipyridine found (in the glassy phase) at 1584 cm^{-1}, 1562 cm^{-1}, 1458 cm^{-1}, and 1420 cm^{-1}, would all be expected to shift upwards by 10 to 20 cm^{-1}, or split, due to interactions with an ion (see references 13b, and 55-59 for typical examples). These shifts were observed, more or less, except for the shift of the 1562 cm^{-1} band (the presence of the 1562 cm^{-1} band shift could not be determined due to the overwhelming bipyridine band at 1584 cm^{-1}).

The 1584 cm^{-1} absorption had a sideband at about 1600 cm^{-1}, which was noticeable even in spectra of samples which had the least amounts of nitrate in them. The 1458 cm^{-1} shifted band was not particularly

noticeable but was apparently present because the original peak could not be subtracted out (without obtaining derivative bands larger than those expected due to the nitrate absorptions) using the spectrum of a "glassy" bipyridine deposit.

The upshift of the 1420 cm^{-1} band was not noticeable due to the overwhelming presence of the 1458 cm^{-1} bipyridine band, as well as the underlying nitrate absorption in the region. The band at 1438 cm^{-1} in the codeposit spectra of Figure 40 appears to be enhanced, and this "enhancement" appears to increase upon annealing the sample. This band is seen in the "glassy" bipyridine spectrum (bottom curve of Figure 41), and the crystalline bipyridine spectrum (top curve of Figure 41), but in neither spectrum is it enhanced to the same degree as in the codeposits.

(c) The bipyridine band which occurs (in the "glassy" phase) at 992 cm^{-1} would be expected to shift upwards by 10 to 30 cm^{-1} upon solvate complex formation (see references 43, 56-58 for typical examples). This was observed as a side band (to the 992 cm^{-1} band) in samples which were less concentrated in nitrate, and as a distinct band (near 1008 cm^{-1}) in samples of higher nitrate concentrations (see Figure 42).

(d) No reliable data was observed for the upshift or splitting of the band at 759 cm^{-1} as was reported for the crystalline compounds of bipyridine (see references 43, 48, 55, 56, and 58 for typical examples). The enhancement of the 742 cm^{-1} band[43] was evident in one sample of higher nitrate concentration, but conflicting results were obtained for other samples.

(e) The band splitting of the 1150 cm^{-1} absorption[55] was not

observed, even in samples of high nitrate concentration.

(f) The "new" band at 1480 to 1500 cm^{-1} in the spectrum of $Cd(bipyridine)_3(halide)_2$, which was proposed to indicate the existence of bipyridine coordinated to a metal through only one of it's nitrogen atoms,[55] was observed at 1488 cm^{-1} only in one sample of very high nitrate concentration. The band in Figure 39 near 1488 cm^{-1} is mostly from bipyridine, as it can be seen in the pure solvent deposit spectrum, Figure 41.

Solvation Spectra, Benzene

The Data

The results from the benzene and lithium nitrate codeposition experimentation are shown in Figure 43. The lower curve is a deposit of pure benzene at 77K, while the top curve is a codeposit of benzene and lithium nitrate at 77K. These two samples, particularly the deposit of pure benzene, are exceptionally dry, as judged by lack of sizable bands attributable to water.[28]

The Discussion: Nitrate Bands

Aside from the small absorption near 1600 cm^{-1} due to water, there are four bands that are in the spectrum for the codeposit that are not in the spectrum for the benzene deposit. Two bands, at 1300 cm^{-1} and near 1840 cm^{-1}, are assigned to a small amount of N_2O_3 (the latter band is not shown, and it's presence is inferred from a broadening of the very intense benzene band in the same location). The remaining two bands unaccounted for are broad absorptions at 1445

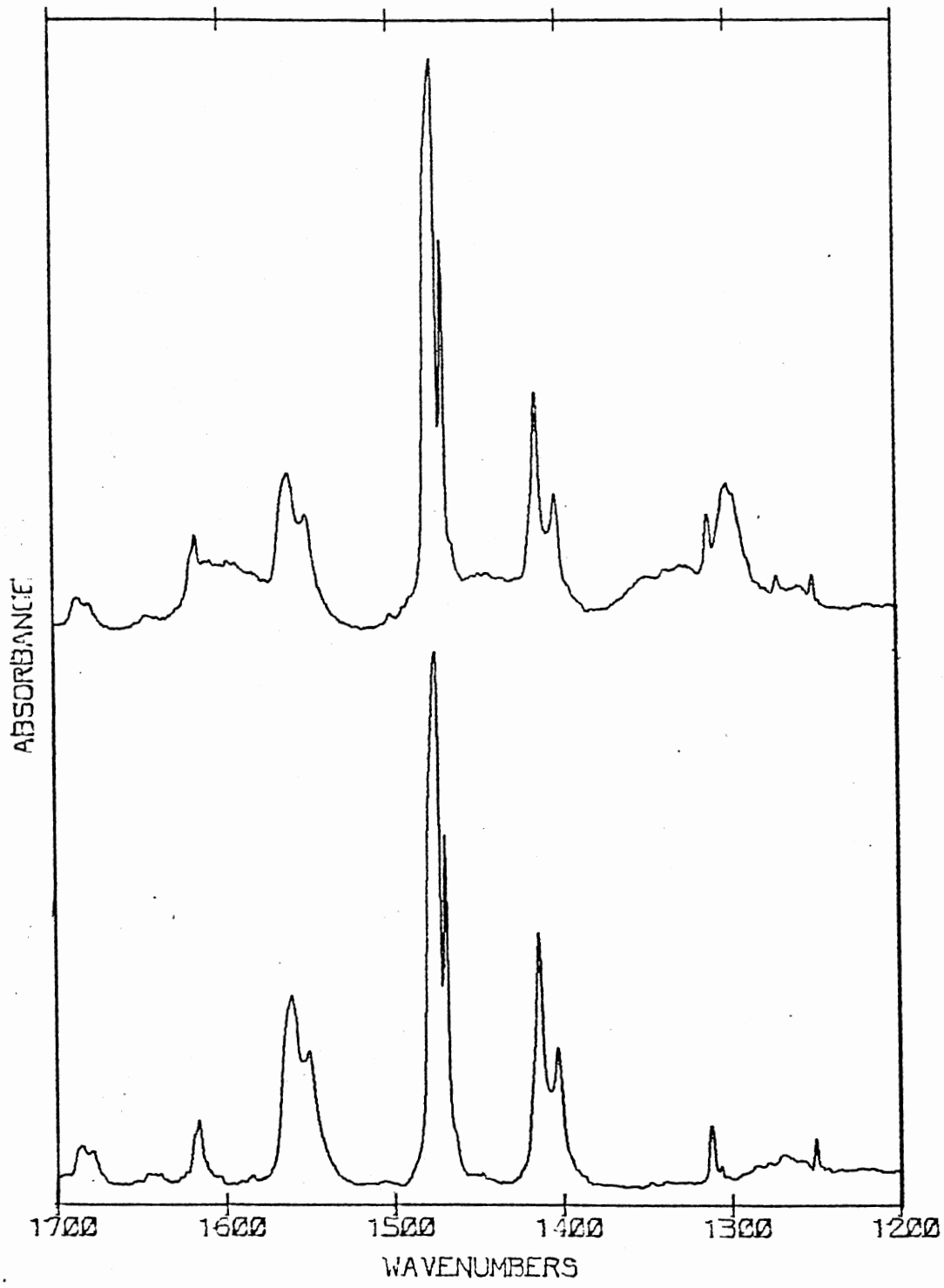

Figure 43. Spectra of Crystalline Benzene (Lower Curve), and of a Codeposit of Benzene and Lithium Nitrate (Upper Curve), at 77 K

cm^{-1} and 1328 cm^{-1} (± 5 cm^{-1}), and these are proposed to be the ν_3 bands of the totally solvated ion pair, $(benzene)_n \cdot LiNO_3$.

It is reported that the sample resulting from quenching benzene vapor to 77K is polycrystalline.[60a,b] As in the case of the annealed codeposits of lithium nitrate and pyridine, it would be premature to speculate on the nature of the solvated ion pair in a polycrystalline sample, though a fully satisfied coordination sphere seems likely.

The Discussion: Benzene Bands

No effort was made to determine possible changes in the benzene spectrum when benzene was codeposited with lithium nitrate.

It should be noted that previous workers have proposed that benzene interacts with argon and xenon strongly enough to radically change it's infrared spectrum.[61a,b] Since the argon dilution work for benzene was not performed, no comments may be made regarding this unusual proposition.

Acid-Base Discussion

It is interesting to investigate the possibility of a correlation between the donor abilities of a solvent molecule (as measured by various means), and the ability of the solvent molecule to decrease the distortion of the nitrate by coordination to the cation of the ion pair. The latter ability may be quantitated by the value represented by $\Delta\nu_3$ ($LiNO_3$ in argon) - $\Delta\nu_3$ ($S \cdot LiNO_3$ in argon). Values of this quantity for various solvents are pyridine (= 28 cm^{-1}), acetonitrile (= 30 cm^{-1}), dimethylformamide (= 42 cm^{-1}), dimethylsulfoxide (= 51

cm^{-1}), and tetrahydrofuran (= 57 cm^{-1}).

The quantitation of the solvent donor ability constitutes a vast literature.[16] In seeking a correlation with $\Delta\nu_3$, perhaps the simplest parameter to try is the enthalpy of reaction of the lithium nitrate ion pair with the above solvents; unfortunately these values are not known. For what correspondence there might be, ICR vapor phase values for ΔH_f of Li^+ reacting with bases gives[14c,d] pyridine (= 184 KJ/mole), acetonitrile (= 180 KJ/mole), and dimethylformamide (= 209 KJ/mole), in fair agreement with the above $\Delta\nu_3$ values of 28 cm^{-1}, 30 cm^{-1}, and 42 cm^{-1}, respectively.

Some information is available on the relative strengths of these bases with respect to each other, in an interaction with $Li^+ClO_4^-$ ion pairs.[51] The chemical shift of the lithium ion (of the $^7LiClO_4$ ion pair) in solutions containing nitromethane, bipyridine, and various solvents, may be used to determine the relative coordinating powers of solvents to $LiClO_4$. It was shown that $LiClO_4$ ion pairs are preferentially solvated by tetrahydrofuran, or dimethylformamide, over bipyridine. This seems reasonable considering that DMF and THF provide larger decreases in $\Delta\nu_3$ values <u>per molecule</u> than pyridine, though their final total solvation $\Delta\nu_3$ values are larger than that of pyridine.

Results of a similar nature, showing relative strengths of bases, could be obtained using the far-IR cage vibrations in mixed solvents,[34] for example, experiments[68] show a preference by $LiClO_4$ for ammonia in solutions of acetonitrile and tetrahydrofuran (note: ΔH_f ($H_3N{\cdot}Li^+(g)$) = 139 KJ/mole,[69] or 164 KJ/mole[14d]). No experiments seem to have been done, however, for pyridine.

Double scale acid-base strength models, while more complicated, have the advantage of yielding more information than single scale models.[16] By far the most successful double scale model is the E and C model.[18a,b] Considering its derivation, and the history of its successful applications, it is not immediately clear that the E and C model is applicable to the interaction between an ion pair and a solvent molecule, because the interaction is expected to be stronger than normally handled by the model.

With the spectroscopic data available (i.e. $\Delta\nu_3$ values for solvates), a little reflection will show that the only analysis using the E and C equation must use the data $\Delta\nu_3$ ($LiNO_3$ in argon) - $\Delta\nu_3$ ($S{\cdot}LiNO_3$ in argon), with the assumption that the latter quantity is proportional to the corresponding ΔH values for $LiNO_3 + S \rightarrow S{\cdot}LiNO_3$ (but see reference 62 also). This assumption is perhaps the weakest link in the reasoning for using the E and C model.

Since $\Delta\nu_3$ is linearly related to the difference in the force constants for coordinated and uncoordinated N-O bonds of the bidentate nitrate,[63] a proportionality between $\Delta\nu_3$ and ΔH certainly seems reasonable. Further, the ΔH_f^o values of $S{\cdot}Li^+$ (derived from mass spectrometric data) mentioned earlier[14c,d] gives credence to this proportionality, if the acids Li^+ and $LiNO_3$ are presumed to be similar.

Indirectly, however, one may argue that there is little useful correlation between ΔH_f^o and $\Delta\nu_3$ by noting that the addition of each solvent molecule to form $(S)_n{\cdot}LiNO_3$ cause a relatively constant incremental decrease from previous $\Delta\nu_3$ values for $(S)_{n-1}LiNO_3$. This is to be compared with the ab initio calculations for ΔH_f^o of $(H_2O)_nLiNO_3$[4a,b] (or ΔH_f^o for $(S)_nLi^+$, references 64-66), in which it is apparent that

the incremental ΔH_f values get smaller as each successive molecule is added. It seems unlikely that $\Delta H_f^o \propto [\Delta\nu_3(LiNO_3 \text{ in argon}) - \Delta\nu_3 (S\cdot LiNO_3 \text{ in argon})]$ for the first solvation step, but that for addition of further solvent molecules $\Delta H_f^o (S_n\cdot LiNO_3) - \Delta H_f^o (S_{n-1}\cdot LiNO_3)$ is not proportional to $\Delta\nu_3 (S_n\cdot LiNO_3) - \Delta\nu_3 (S_{n-1}\cdot LiNO_3)$.

It is no great effort to do E and C calculations, however, so to determine if the bonding and spectroscopic properties of the lithium nitrate ion pair may be described by the E and C equation, the parameters of Table IV were used with a SAS least squares routine (Proc STEPWISE: BACKWARD: NOINT: version 82.B SAS; SAS Institute, SAS circle, P.O. Box 8000, Cary, N.C. 27511-8000) to calculate quasi E and C parameters.

TABLE IV

E AND C ANALYSIS DATA

Substance	E_B [a]	C_B [a]	$\Delta\nu_3 (LiNO_3 \text{ in Ar}) - \Delta\nu_3 (S\cdot LiNO_3 \text{ in Ar})$
Dimethylformamide	1.23	2.48	42
Tetrahydrofuran	.978	4.27	57
Acetonitrile	.886	1.34	30
Dimethylsulfoxide	1.34	2.85	51
Pyridine	1.17	6.4	28

[a] Units of $\sqrt{\text{kcal/mole}}$.

[b] Units of cm^{-1}.

When the data in Table IV is used in the least squares program, the quasi E_A and C_A parameters calculated for $Li^+NO_3^-$ are E_A = 38.7, and C_A = -.678, with R^2 = .927 (Note: these quasi E and C parameters have units of $\sqrt{\text{mole/kcal}}$ cm^{-1}). These E_A and C_A values certainly imply a large amount of electrostatic nature in the acid (which is what was expected), however the correlation coefficient is rather low, and a (significant) negative value for C makes no sense in the context of the model. Therefore the results may indicate that (if the E and C model is applicable) one or more members of the data set may be causing a poor fit.

Inspection of an E and C plot[18a,b] composed of the bases of Table IV shows that pyridine might be the sole offending member. Arbitrarily dropping a member of a small data set to maximize R^2, especially a member differing greatly from other members in C/E value, is risky. However, it could be that factors other than bond strength are operating in the case of pyridine, or that E and C parameters for pyridine are incorrect; therefore, dropping the pyridine values from the data set of Table IV, and analyzing the remaining four solvents, gives E_A = 17.8, C_A = 9.21, and R^2 = .9986 (dropping any of the other four solvents in place of pyridine resulted in a poor fit).

These values give a fit which is reasonably good, and provides a C_A/E_A ratio that can be compared with other ratios determined for complexes.[18a,b] These E_A and C_A values for $LiNO_3$ can be used with the standard E_B and C_B values of bases to determine the $\Delta\nu_3$ of $S \cdot LiNO_3$, even for solvents for which this value has not experimentally been measured. Further, since the E_A and C_A values for $(S)_n \cdot LiNO_3$ are probably larger than the corresponding E_A and C_A values for $(S)_{n+1}LiNO_3$,[62]

one may divide the easily obtained $\Delta\nu_3$ ($LiNO_3$ in argon) - $\Delta\nu_3$ ($LiNO_3$ in 100% aprotic solvent) by the easily calculated $\Delta\nu_3(S\cdot LiNO_3)$ to determine the maximum number of solvent molecules able to coordinate with $LiNO_3$ (note: this is an upper limit to the maximum possible solvation number, and not a calculation of the exact solvation number). Table V summarizes the results of such a calculation.

TABLE V

ESTIMATION OF MAXIMUM SOLVATION NUMBERS OF $LiNO_3$ USING E AND C VALUES

Base	$262-\Delta\nu_3(LiNO_3$ in solvent)		$\Delta\nu_3^{n=1}$(calc'd)[c]	n(calc'd)	n(expt'l)
DMF	179 cm^{-1}	(a)	44.7	4.0	4 (e)
THF	159	(a)	56.7	2.8	3 (e)
ACN	180	(a)	28.1	6.4	5 (e)
DMSO	201	(a)	50.1	4.0	4 (e)
PY	185	(f)	79.8	2.3	6 (f)
NH_3	215	(a)	56.1	3.8	-
Acetone	196	(b)	39.0	5.0	-

[a] Reference 9a.

[b] Reference 12c, 67.

[c] With $LiNO_3$, E = 17.8, C = 9.21; NH_3, E = 1.36, C = 3.46; Acetone, E = .987, C = 2.33; others as reported in Table IV.

[d] $(262-\Delta\nu_3$ ($LiNO_3$ in solvent))$/\Delta\nu_3$ (n=1 calc'd).

[e] Reference 9b.

[f] This work.

To summarize the main points of this section, the following may be noted: (a) The ion pair $LiNO_3$ appears to have shown a strong acidic character in its reactions with Lewis bases. (b) There appears to be an insufficient data base to clearly demonstrate whether the E and C model is useful in this application, though it appears to be so; the necessary linearity between ΔH and $\Delta\nu_3$, which is crucial to the analysis done here, has not been independently demonstrated.

CHAPTER IV

SUMMARY AND CONCLUSIONS

The infrared spectrum for the contact ion pair lithium nitrate (matrix isolated in argon) was observed. Although no major differences were seen in the ion pair bands, comparison of the results with previously published work allowed the assignments of ν_{3a} and ν_{3b} for $(H_2O)_n \cdot LiNO_3$, n = 1-2, as samples in earlier work were apparently contaminated with a small amount of water.

Spectra were also collected for samples of lithium nitrate which had insufficient amounts of argon for complete isolation. Bands appeared which qualitatively substantiate previous work on lithium nitrate aggregates in a CO_2 matrix. These bands, which appeared in the spectrum (to a small extent) even in samples of good isolation, were seen to grow when samples containing the monomer ion pairs were annealed; however, they did not seem to grow to the predominance observed in spectra initially rich in lithium nitrate. It was noticed that higher annealing temperatures were necessary to make these multimer bands grow in samples of monomers than was necessary to make higher-solute peaks appear in mixtures of $LiNO_3$/pyridine/argon, or $LiNO_3/H_2O$/argon. The cause for this lack of mobility is unknown.

The bands for the ν_{3a} and ν_{3b} modes of matrix isolated $(Pyridine)_n \cdot LiNO_3$, n = 1-6, were assigned. The ν_{3a} and ν_{3b} modes for solvates n = 1-4 were easily assigned — later steps, particularly

in the high frequency ν_{3b} region, where peaks were broad, were more difficult to assign. The annealing of samples with low percentage of pyridine allowed excess pyridine to diffuse in the lattice to $(S)_n \cdot LiNO_3$, and this resulted in spectra identical to samples of higher concentration of pyridine.

The spectra of the ν_3 region of the matrix isolated compounds $(\text{phenanthroline})_n LiNO_3$ were somewhat ambiguous, but, in general, supported the assignments of the pyridine complexes. Though some difficulty was experienced with assignments, the spectra were best analyzed in the overall context of the results obtained in the pyridine isolation work, and bipyridine codeposition work.

The spectrum for the bipyridine and lithium nitrate glassy codeposit was similarly interpreted in terms of the matrix isolation work of pyridine and phenanthroline.

The annealing of codeposits of solvents and lithium nitrate gave spectra which were very interesting, but not particularly informative, except to impress one with the complexity of the situation. One definite result is that totally solvated ion pairs can exist (in small amounts) in a crystalline lattice. This was demonstrated not only in the spectra showing the annealing effects for the case of pyridine/lithium nitrate codeposits, but was also demonstrated in the spectrum for the codeposit of lithium nitrate and (crystalline) benzene. As phenanthroline was the only solvent which did not volatilize into the vacuum upon warming, the spectra of its annealed codeposit samples were especially interesting. They indicate that there is, near the crystallization temperature, some unusual ion pair condition, or solvation phenomena, which has yet to be explained.

In the codeposition of the amines with lithium nitrate there was evidence of coordination, as inferred from induced band shifts of the ligand. Like previously reported spectra for complexes with ions, and H-bonded complexes with molecules, these band shifts were manifested in upshifts of existing bands.

Problems with pyridine, or phenanthroline, H-bonding to the nitrate while coordinated (or even while uncoordinated) were not outwardly apparent, though difficulty in assignments of bands to particular solvates would likely be the first place this problem would be noticable. As the data could be fit without excessive speculation, this problem was assumed to be small.

The large number of pyridines which coordinate to the contact ion pair cannot be explained using acid-base models, and appears to imply that factors other than "donicity" can govern the final number of molecules which will eventually coordinate to the ion pair. The E and C analysis of the spectroscopic data was perhaps premature, given that ΔH_f and $\Delta \nu_3$ have not been proven to be correlated. It is not clear whether the (reasonable) results which come from the E and C analysis are real or happenstance.

A few comments on coordination numbers seems to be in order. Investigators have, in the past, gone to great trouble to identify characteristics of species which would identify whether a ligand is "coordinated" to a cation. Qualities such as the capacity for ligand and ion pair to volatilize as a distinct species, the ability to form extractable molecules in solutions, electrochemical molecular weight determinations in solution, observation of X-ray bond distances, calculation of EXAFS σ parameters, and the appearance of vibrational

bands, have been among the more popular methods used.

None of these criteria have proven to be applicable in all cases, of course. Indeed, the data collected so far has succeeded in pointing out that the solvation number is an inexact quantity, determined by the definition of coordination imposed on the system by the experimental probe used. Further, it has become clear that fixed coordination and rigid stereochemistry of alkali ions is not as necessary as might be expected based on the background provided by the better studied aqueous solutions of transition metals. In this vein, it should come as no surprise that the seven coordinate lithium ion implied by this work is not unrealistic.

Lastly, it should be emphasized that the principal use of this type of research is certainly not to promote a new way to determine "the" coordination number. The use of this research is much broader, and best lies in the understanding which may be obtained about the bonding of molecules to molecules via infrared spectroscopy. Through this use we may, in fact, learn what a "coordination number" really is.

BIBLIOGRAPHY

(1) (a) Craddock, S.; Hinchcliffe, A. J. "Matrix Isolation"; Cambridge University Press: New York, 1975. (b) Hallam, H. E., Ed. "Vibrational Spectroscopy of Trapped Species"; John Wiley and Sons: New York, 1973. (C) Barnes, A. J.; Orville-Thomas, W. J.; Muller, A.; Gaufres, R., Eds. "Matrix Isolation Spectroscopy"; D. Reidel Publishing Company: Dordrecht Holland, 1981. (d) Meyer, B. "Low Temperature Spectroscopy"; American Elsevier Publishing Company, Inc.: New York, 1971. (e) Moskovits, M.; Ozin, G. A. "Cryochemistry"; John Wiley and Sons: New York, 1976.

(2) (a) Smith, D.; James, D. W.; Devlin, J. P. J. Phys. Chem. 1972, 54, 4437-4442. (b) Smith, Donald Eugene. "A vibrational study of a series of matrix-isolated nitrates" (Unpub. Ph.D. thesis, Oklahoma State University, 1966).

(3) (a) Pollard, G.; Smyrl, N.; Devlin, J. P. J. Phys. Chem. 1972, 76, 1826-1831. (b) Pollard, Gary Dale. "The vibrational spectra of $LiNO_3$ and KNO_3 in various inert matrices" (Unpub. Ph.D. thesis, Oklahoma State University, 1972).

(4) (a) Moore, J. C.; Devlin, J. P. J. Chem. Phys. 1978, 68, 826-831. (b) Moore, Jesse C. :A theoretical investigation of the distortion of the NO_3^- ion in $LiNO_3$ and $LiNO_3 \cdot nH_2O$" (Unpub. Ph.D. thesis, Oklahoma State University, 1977). (c) Almlof, J.; Ischenko, A. A. Chem. Phys. Lett. 1979, 61, 79-82.

(5) (a) Ogden, J. S. Ber. Bunsenges. Phys. Chem. 1982, 86, 827-837. (b) Beattie, I. A.; Ogden, J. S.; Price, D. D. J. Chem. Soc., Dalton Trans. 1977, 1460-1464. (c) Ogden, J. S. National Bureau of Standards Special Publication 561, 1979, 511-521. (d) Kulikov, V. A.; Ugarov, V. V.; Rambidi, N. G. J. Struct. Chem. 1981, 22, 448-451. (e) Kulikov, V. A.; Ugarov, V. V.; Rambidi; N. G., 1981, 22, 310-311.

(6) (a) Smyrl, N.; Devlin, J. P. J. Phys. Chem. 1973, 77, 3067-3070. (b) Smyrl, Norman Ray. "A vibrational study of a selected series of matrix-isolated alkali metal chlorate and nitrate salts" (Unpub. Ph.D. thesis, Oklahoma State University, 1973).

(7) (a) Ritzhaupt, G.; Devlin, J. P. J. Phys. Chem. 1977, 81, 67-61. (b) Ritzhaupt, G.; Devlin, J. P. J. Phys. Chem. 1975, 79, 2265-2269.

(8) Irish, D. E.; Chang, T. G.; Tang, S. Y.; Petrucci, S. J. Phys. Chem. 1981, 85, 1686-1692.

(9) (a) Toth, J. P.; Thornton, C.; Devlin, J. P. J. Soln. Chem. 1978, 7, 783-794. (b) Toth, J. P.; Ritzhaupt, G.; Devlin, J. P. J. Phys. Chem., 1981, 85, 1387-1391.

(10) Conway, B. E. "Ionic Hydration in Chemistry and Biophysics"; Elsevier/North-Holland Inc.: New York, 1981.

(11) (a) Popovych, O.; Tomkins, R. P. T. "Nonaqueous Solution Chemistry"; John Wiley and Sons: New York, 1981. (b) Amis, E. S.; Hinton, J. F. "Solvent Effects on Chemical Phenomena"; Academic Press: New York, 1973. (c) Bockris, J.; Reddy, A. K. N. "Volume 1 Modern Electrochemistry"; Plenum Press: New York, 1970. (d) Burgess, J. "Metal Ions in Solution"; John Wiley and Sons: New York, 1978.

(12) (a) Perelygin, I. S.; Klimchuk, M. A.; Beloborodova, N. N. Russ. J. Phys. Chem. 1980, 54, 605-606. (b) Perelygin, I. S.; Klimchuk, M. A.; Beloborodova, N. N. Russ. J. Phys. Chem. 1980, 54, 1703-1705. (c) Perelygin, I. S.; Klimchuk, M. A.; Beloborodova, N. N. Russ. J. Inor. Chem. 1981, 26, 27-30.

(13) (a) Vogtle, F.; Muller, M.; Rasshofer, W. Israel J. Chem. 1979, 18, 246-248. (b) Schilt, A. A.; Taylor, R. C. J. Inor. Nucl. Chem. 1959, 9, 211-221, also see (c) Poonia, N. A. Inor. Chim. Acta, 1977, 23, 5-12. (d) Sliwa, W. Heterocycles, 1979, 12, 1207-1237. (e) Tiwari, R. K.; Chandrakumar, C.; Singh, T. P. Zeit. Krist. 1981, 156, 245-246. (f) Jones, P. G.; Klegg, W.; Sheldrick, G. M. Acta Crust. 1980, B36, 160-162. (g) Kapoor, P. N.; Mehrotra, R. C. Coord. Chem. Rev. 1974, 14, 1-27.

(14) (a) Sauer, J.; Deininger, D. J. Phys. Chem. 1982, 86, 1327-1332. (b) Sunner, J.; Nishizawa, K.; Kebarle, P. J. Phys. Chem. 1981, 85, 1814-1820. (c) Staley, R. H.; Beauchamp, J. L. J. Am. Chem. Soc. 1975, 97, 5920-5921. (d) Woodin, Al. L.; Beauchamp, J. L. J. Am. Chem. Soc. 1978, 100, 501-503.

(15) (a) Hammonds, C. N.; Westmoreland, T. D.; Day, M. C. J. Phys. Chem. 1969, 73, 4374-4376. (b) Kolodziejski, W.; Laszlo, R.; Stockis, A. Molecular Physics 1982, 45, 939-947.

(16) Jenson, W. B. "The Lewis Acid-Base Concepts: An Overview"; John Wiley and Sons: New York, 1980.

(17) Gutmann, V. "The Donor-Acceptor Approach to Molecular Interactions"; Plenum Press: New York, 1978.

(18) (a) Drago, R. Coord. Chem. Rev. 1980, 33, 251-277. (b) Drago, R. Pure. Appl. Chem. 1980, 52, 2261-2274.

(19) Scholes, G. In "Supplement to Mellor's Comprehensive Treatise on Inorganic and Theoretical Chemistry"; Briscoe, H. V. A.; Eldridge, A. A.; Dyson, G. M.; Welch, A. J. E., Eds.; John Wiley and Sons: New York, 1961; p. 261.

(20) Burfield, D. R.; Smithers, R. H.; Sui Chai Tan, A. J. Org. Chem. 1981, 46, 629-631.

(21) Nishigaki, S.; Yoshioka, H.; Nakatsu, K. Acta Cryst. 1978, B34, 875-879.

(22) Hart, W. A.; Beumel, Jr., O. R. In "Comprehensive Inorganic Chemistry"; Bailar, Jr., J. C.; Emeléus, H. J., Nyholm, R., Eds.; Pergammon Press Ltd., Oxford, 1973; p. 360.

(23) Swanson, B. I.; Jones, L. H. J. Mol. Spectrosc. 1981, 89, 566-568.

(24) Gmelins Handbuch der Anorganischen Chemie-Lithium; Verlag Chemie, GMBH: Weinheim/Bergstrasse, 1960.

(25) Verrall, R. E., In "Water: A Comprehensive Treatise Volume 3"; Franks, F., Ed.; Plenum Press: New York, 1973.

(26) Kecki, Z.; Sadlej, J.; Sadlej, A. J.; J. Mol. Struct. 1982, 88, 71-78.

(27) Sadlej, J.; Sadlej, A. J. Faraday Discuss. 1977, 64, 112-119.

(28) Bentwood, R. M.; Barnes, A. J.; Orville-Thomas, W. J. J. Mol. Spectrosc. 1980, 84, 391-404; see also Knözinger, E.; Wittenbeck, R. J. J. Am. Chem. Soc. 1983, 105, 2154-2158.

(29) Ault, B. J. Am. Chem. Soc. 1978, 100, 2426-2433.

(30) Büchler, A.; Stauffer, J. L. J. Phys. Chem. 1966, 70, 4092-4094.

(31) Nicolas, M.; Dartyge, E. J. Am. Chem. Soc. 1982, 104, 7403-7406.

(32) Harsányi, L.; Kilár, F. J. Mol. Struct. 1980, 65, 141-152 and references therein.

(33) Castellucci, E.; Sbrana, G.; Verderame, F. D. J. Chem. Phys. 1969, 51, 3762-3770.

(34) (a) Handy, P. R.; Popov, A. I. Spectrochim. Acta 1972, 28A, 1545-1553. (b) Popov, A. I. Pure Appl. Chem. 1975, 41, 275-289. (c) McKinney, W. J.; Popov, A. I. J. Phys. Chem. 1970, 74, 535-537.

(35) Frank, C. W.; Rogers, L. B. Inor. Chem. 1966, 5, 615-622.

(36) Perelygin, I. S. Izv. Vys. Ucheb. Zaved., Khim. i Khim. Tekhnol. 1976, 13, 827-840.

(37) Perelygin, I. S.; Klimchuk, I. S. Russ. J. Phys. Chem. 1976, 50, 1857-1859.

(38) Takahashi, H.; Mamola, K.; Plyler, E. K. J. Mol. Spectrosc. 1966, 21, 217-230.

(39) Maes, G. Bull. Soc. Chim. Belg. 1981, 90, 1093-1107.

(40) Taddei, G.; Castellucci, E.; Verderame, F. D. J. Chem. Phys. 1970, 53, 2407-2411.

(41) König, E.; Madeja, K. Spectrochim. Acta 1967, 23A, 45-54.

(42) Banerjee, A. K.; Prakash, D.; Kejariwal, P.; Roy, S. K. J. Indian Chem. Soc. 1973, L, 691-693.

(43) Sharma, C. L.; De, T. K. Indian J. Chem. 1981, 20A, 618-620.

(44) Layton, A. J.; Myholm, R. S.; Banerjee, A. K.; Fenton, D. E.; Lestas, C. N.; Truter, M. R. J. Chem. Soc. (A) 1970, 1894-1896.

(45) Cheng, C. P.; Plankey, B.; Rund, J. V.; Brown, T. L. J. Am. Chem. Soc. 1977, 99, 8413-8417.

(46) Singh, S. S. Z. Naturforsch. 1969, 24a, 2015-2016.

(47) Jain, S. C.; Rivest, R. Inorg. Chim. Acta, 1970, 4, 291-295.

(48) Fenton, D. E.; Newman, R. J. C. S. Dalten, 1974, 655-657.

(49) Laane, J.; Ohlsen, J. R. in "Progress in Inorganic Chemistry-Volume 27"; Lippard, S. J., Ed.; John Wiley and Sons: New York, 1980, 466-513.

(50) Benedix, R.; Birner, P.; Birnstock, F.; Hennig, H.; Hofmann, H. J. Mol. Struct. 1979, 51, 99-105 and references therein. See also Freundlich, P.; Jakusek, E.; Kolodziej, H. A.; Koll, A.; Pajdowska, M.; Sorriso, S. Zeit. Phys. Chem. Neue. Folge. 1982, Bd131, 161-170.

(51) Schmidt, E.; Hourdakais, A.; Popov, A. Inorg. Chim. Acta 1981, 52, 91-95.

(52) Cahen, Y. M.; Handy, P. R.; Roach, E. T.; Popov, A. I. J. Phys. Chem. 1975, 79, 80-85.

(53) (a) Neto, N.; Muniz-Miranda, M.; Angeloni, L.; Castelluci, E. Spectrochim. Acta 1983, 39A, 97-106 and references therein. (b) Muniz-Miranda, M.; Castellucci, E.; Neto, N.; Sbrana, G. Spectrochim. Acta 1983, 39A, 107-113 and references therein. (c) Castellucci, E.; Angeloni, L.; Neto, N.; Sbrana, G. Chem. Phys. 1979, 42, 365-373.

(54) Sinha, S. P. Spectrochim. Acta 1964, 20, 879-886.

(55) Usatenko, Y. I.; Borishchak, O. A.; Oleinik, T. G. Russ. J. Inor. Chem. 1981, 26, 180-183.

(56) König, E.; Lindner, E. Spectrochim. Acta 1972, 28A, 1393-1403.

(57) Coluccia, S.; Chiorino, A.; Guglielminotti, E.; Morterra, C. J. Chem. Soc. Faraday Trans I 1979, 75, 2188-2198.

(58) König, E.; Madeja, K.; Watson, K. J. J. Am. Chem. Soc. 1968, 90, 1146-1153.

(59) Martin, B.; McWhinnie, W. R.; Waind, G. M. J. Inorg. Nucl. Chem. 1961, 23, 207-223.

(60) (a) Hollenberg, J. L.; Dows, D. A. J. Chem. Phys. 1962, 37, 1300-1307. (b) Yamada, H.; Saheki, M. Bull. Chem. Soc. Jpn. 1983, 56, 35-40.

(61) (a) Rentzepis, P. M.; Douglass, D. C. Nature 1981, 293, 165-166. (b) Le Roy, A.; Dayon, E. C. R. Acad. Sc. Paris 1969, 268B, 48-50.

(62) Drago, R. S.; Long, J. R.; Cosmano, R. Inor. Chem. 1981, 20, 2920-2927.

(63) Hester, R. E.; Grossman, W. E. L. Inor. Chem. 1966, 5, 1308-1312.

(64) Castleman, A. W.; Holland, P. M.; Lindsay, D. M.; Peterson, K. I. J. Am. Chem. Soc. 1978, 100, 6039-6045.

(65) Dzidić, I.; Kebarle, P. J. Phys. Chem. 1970, 74, 1466-1483.

(66) Hirao, K.; Yamabe, S.; Sano, M. J. Phys. Chem. 1982, 86, 2626-2632.

(67) Norwitz, G.; Chasan, D. E. J. Inor. Nucl. Chem. 1969, 31, 2267-2270.

(68) Regis, A.; Corset, J. Can. J. Chem. 1973, 51, 3577-3587.

(69) Castleman, Jr., A. W.; Holland, P. M.; Lindsay, D. M.; Peterson, K. I. J. Am. Chem. Soc. 1978, 100, 6039-6045; see also for related material, Del Bene, J. E.; Frisch, M. J.; Raghavachari, K.; Pople, J. A.; v. R. Scheleyer, P. J. Phys. Chem. 1983, 87, 73-78, and Kolman, P.; Rothenberg, S. 1977, 99, 1333-1342.

VITA

Keith Alan Consani

Candidate for the Degree of

Doctor of Philosophy

Thesis: A MATRIX ISOLATION STUDY OF THE SOLVATION OF LITHIUM NITRATE ION PAIRS WITH BENZENE, PYRIDINE, BIPYRIDINE, AND 1,10-PHENANTHROLINE USING INFRARED SPECTROSCOPY

Major Field: Chemistry

Biographical:

Personal Data: Born in Coffeyville, Kansas, February 25, 1955, the son of Aldo Arthur and Bernice Winifred (Maki) Consani.

Education: Graduated from Leavenworth Senior High School, Leavenworth, Kansas, in May, 1973; attended Washburn University, Topeka, Kansas, in 1974; received Bachelor of Science degree in Chemistry from Kansas State University in 1977; attended Iowa State University from 1977 to 1979; completed requirements for the Doctor of Philosophy degree at Oklahoma State University in July 1983.

Professional Experience: Member of The American Chemical Society and Society of Applied Spectroscopy.